BIOREDUCIBLE POLYMER-MEDIATED GENE THERAPY FOR THE TREATMENT OF ISCHEMIC HEART DISEASE

by

Arlo Nuttall McGinn

A dissertation submitted to the faculty of
The University of Utah
in partial fulfillment of the requirements for the degree of

Doctor of Philosophy

Department of Pharmacology and Toxicology

The University of Utah

May 2013

The University of Utah Graduate School

STATEMENT OF DISSERTATION APPROVAL

The dissertation of **Arlo Nuttall McGinn**

has been approved by the following supervisory committee members:

Sung Wan Kim	, Chair	**11/14/2012** Date Approved
William R. Crowley	, Co-Chair	**11/14/2012** Date Approved
Donald K. Blumenthal	, Member	**11/14/2012** Date Approved
David A. Bull	, Member	**11/14/2012** Date Approved
Philip J. Moos	, Member	**11/14/2012** Date Approved

and by **William R. Crowley**, Chair of the Department of **Pharmacology and Toxicology**

and by Donna M. White, Interim Dean of The Graduate School.

ABSTRACT

Coronary heart disease, especially myocardial infarction, is a serious and deadly disease that remains the number one cause of death in developed nations. While physicians have a wide array of drugs and tools at their disposal to treat myocardial infarction, there is a scarcity of drugs that effectively prevent the pathological remodeling of the left ventricle that occurs after acute infarction and greatly predisposes the patient to the risk of heart failure.

This dissertation focuses on identifying nonviral, bioreducible polymer-based gene therapies to limit infarct expansion, prevent left ventricular remodeling, and retain heart function after myocardial infarction. Bioreducible polymers represent a major advancement in nonviral technology to transfect primary cells, with high efficiency, and low cytotoxicity.

We first examined a combined gene/cell therapy-based strategy by implanting $VEGF_{165}$-transfected primary skeletal myoblasts to the myocardium of infarcted rat hearts. The VEGF-expressing skeletal myoblasts acted as bioreactors, secreting proangiogenic VEGF and inducing new vessel formation in the infarcted hearts. This treatment strategy produced both global and regional improvements in the left ventricle, improving ejection fraction, decreasing cell death, and limiting left ventricular remodeling.

A cationic polymer system utilizing arginine-grafted bioreducible polymer (ABP) was also used to efficiently mediate siRNA knockdown of BNIP3, a hypoxia-inducible

proapoptotic protein. siRNA-mediated BNIP3 knockdown both *in vitro* and *in vivo* protected rat primary cardiomyocytes from hypoxic death. The inhibition of BNIP3 in acutely ischemic rat hearts resulted in improved retention of ejection fraction, decreased infarct formation, decreased cellular remodeling, and decreased left ventricular remodeling.

TABLE OF CONTENTS

LIST OF FIGURES

Figure

LIST OF TABLES

Table

LIST OF ABBREVIATIONS

AAV	adeno-associated virus
ABP	arginine-grafted bioreducible polymer (see also poly(CBA-DAH-R))
ACE	angiotensin converting enzyme
AGENT	angiogenic gene therapy clinical trials
AMD	age-related macular degeneration
ANG-2	angiopoietin-2
ANOVA	analysis of variance
Ang II	angiotensin II
ARC	apoptosis repressor with caspase recruitment domain
ARNT	aryl hydrocarbon receptor nuclear translocator, a.k.a. HIF-1ß
AT	angiotensin receptor
ATP	adenosine triphosphate
BNIP3	BCL2/adenovirus E1B 19 kDa interacting protein 3
bFGF	basic fibroblast growth factor
bPEI	branched polyethyleneimine
BSA	bovine serum albumin
CABG	coronary artery bypass grafting
CBA	cystamine bisacrylamide
CD31	cluster of differentiation 31 (capillary marker)
CSC	cardiac stem cell

cTnT	cardiac troponin-T
CUPID	calcium up-regulation by percutaneous administration of gene therapy in cardiac disease clinical trial
DAB	3-3’ diaminobenzidine
DICOM	digital imaging and communications in medicine image format
DI H2O	deionized water
DMEM	Dubellco’s Modified Eagle’s Medium
DMSO	dimethyl sulfoxide
dsRNA	double-stranded RNA
EF	ejection fraction
ELISA	enzyme-linked immunosorbent assay
EDV	end diastolic volume
EDTA	ethylenediaminetetraacetic acid
EDWT	end diastolic wall thickness
ESV	end systolic volume
ESWT	end systolic wall thickness
EtBR	ethidium bromide
FBS	fetal bovine serum
FDA	U.S. Food and Drug Administration
FGF	fibroblast growth factor
FLASH	MRI fast-low-shot-angle
FOV	MRI field of view
GSH	reduced glutathione
GSSG	oxidized glutathione disulfide

H9C2	secondary rat cardiomyocyte cell line
H&E	hematoxylin and eosin
HIF	hypoxia inducible factor
HIF-1α	hypoxia inducible factor-1α
HIF-1ß	hypoxia inducible factor-1ß
hpf	high-powered field
HRE	hypoxia response element
HRP	horse radish peroxidase
iPSC	induced pluripotent stem cell
LPEI	linear polyethyleneimine
LAD	left anterior descending coronary artery
lPEI	linear polyethyleneimine
Luc	luciferase
LV	left ventricle
MAGIC	myoblast autologous grafting in ischemic cardiomyopathy clinical trial
MeOH	methanol
MI	myocardial infarction
MMP	matrix metalloprotease
MRI	magnetic resonance imaging
MTT	3-(4,5-dimethylthiazol-2-yl)-2,5-diphenyltetrazolium bromide cytotoxicity assay
MWCO	molecular weight cut-off
NEX	MRI number of averages
NIH	National Institutes of Health

NMR	nuclear magnetic resonance
PAGA	poly[α-(4-aminobutyl)-L-glycolic acid)]
PBS	phosphate-buffered saline
PCI	percutaneous coronary intervention
pCMV	cytomegalovirus promoter-containing plasmid
PDGF	platelet-derived growth factor
pDNA	plasmid DNA
PEG	poly(ethylene glycol)
PEI	polyethyleneimine
PHD	prolyl hydroxylase
PHP	poly(4-hydroxy-L-proline ester)
PIGF	placental growth factor
PLL	poly-L-lysine
poly(CBA:DAH)	poly(cystaminebisacrylamide-diaminohexane)
poly(CBA:DAH:R)	poly(cystaminebisacrylamide-diaminohexane-arginine)
pVHL	von Hippel-Lindau tumor suppressor protein
qRT-PCR	quantitative reverse transcriptase PCR
RAS	renin-angiotensin-system
RES	reticuloendothelial system
RLU	relative luminescence units
RNAi	RNA interference
ROS	reactive oxygen species
rPCM	rat primary cardiomyocyte
SCID-X1	x-linked severe combined immunodeficiency

SEM	standard error of the mean
SERCA2a	sarcoplasmic/endoplasmic reticulum calcium ATPase 2
SHP-1	Src homology domain 2 (SH2)-containing tyrosine phosphatase-1
SMA	smooth muscle actin (arteriole marker)
siRNA	small interfering RNA
SS-PAA	disulfide-linked poly(amido amine)
TAE	tris-acetate EDTA
TE	MRI echo time
TFA	trifluoroacetic acid
TLR	toll-like receptor
TNF-α	tumor necrosis factor α
tPA	tissue plasminogen activator
TR	MRI repetition time
TUNEL	terminal deoxynucleotidyl transferase-mediated dUTP nick end labeling assay
UV	ultraviolet
VEGF	vascular endothelial growth factor
W/W	weight to weight ratio of polymer to DNA or siRNA
XIAP	x-linked inhibitor of apoptosis protein

ACKNOWLEDGEMENTS

Completion of this work and project would not have been possible were it not for a number of important and influential people. First and foremost, I would like to thank my professor and mentor, Dr. Sung Wan Kim, for his constant guidance, support, encouragement, and feedback. I would also like to thank my committee co-chair, Dr. William R. Crowley, and all of my committee members, Dr. Donald K. Blumenthal, Dr. Philip J. Moos, and Dr. David A. Bull. Their willingness to meet consistently during my academic career and to offer their support and advice were immensely helpful.

In addition to the support and guidance of my committee members, I would like to extend my thanks to the faculty and staff of the Department of Pharmacology, my class professors, and the Graduate Training Committee. My time here at the University of Utah has been one of intellectual and emotional expansion and I thank all of you for your help in making me who I am now.

My thanks goes out to all of my lab members, past and present, especially Katie Blevins, Stelios Florinas, Mei Ou, and Young Wook Won for your assistance in troubleshooting, brain-storming, and venting. I consider you all friends in addition to valuable coworkers.

To my family and parents, I also extend my thanks for your support, love, and patience throughout this process. And to my wife Megan, I extend the biggest thanks of

all. This would not have been possible were it not for the support, motivation, and encouragement you provided.

This work was supported through the National Institutes of Health, which provided funding through the National Heart, Lung, and Blood Institute grants HL065477 and HL071541.

Chapter 3 is reprinted from *Biomaterials*, 32/3, A.N. McGinn, H.Y. Nam, M. Ou, N. Hu, C.M. Straub, J.W. Yockman, D.A. Bull, S.W. Kim, Bioreducible polymer-transfected skeletal myoblasts for VEGF delivery to acutely ischemic myocardium, 942-949, (2011), with permission from Elsevier.

CHAPTER 1

INTRODUCTION

1.1 General Introduction

Gene therapy is broadly defined as the use of nucleic acids as pharmacological agents at a cellular level to correct genetic abnormalities and dysfunction or to express a protein to treat a disease. Over the past 40 years, the concept of treating or curing disease at its genetic root has moved from mere speculation to a more immediate reality, with thousands of gene therapy clinical trials performed to date [1, 2]. Gene therapy can take many forms, whether it is used to deliver plasmid DNA, small interfering RNA (siRNA), or sense/antisense oligonucleotides and these techniques have all been used in clinical therapies to treat diseases such as muscular dystrophy, cancer, cardiovascular disease, and even HIV [3-6].

However, despite the promise of gene therapy and our increased understanding of the genetic abnormalities that cause disease, the greatest barrier to achieving efficient gene therapy remains the delivery of genetic material to the population of diseased cells [7, 8]. The earliest attempts to overcome the cellular barrier to gene therapy in humans utilized crude and inefficient calcium phosphate systems to chemically transfect bone marrow cells and reinfuse them into the patients [9-11]. More efficient viral systems were not used for gene therapy until several years later and while they are still the predominant vectors used for gene therapy trials today [2], they are not without significant problems

such as immunogenicity, mutagenic potential, toxicity, high expense, and difficulty in manufacture [12, 13].

Nonviral vectors for gene therapy represent a promising alternative to viral vectors for gene delivery as they do not suffer from many of the same limitations [14, 15]. Polymer gene carriers are especially attractive as nonviral vectors because they efficiently protect nucleic acids from degradation, mediate transport across cell membranes, and can be easily modified with shielding agents like polyethylene glycol to increase circulation time and decrease toxicity, or modified with targeting motifs to imbue cell-type specificity to the polymer complex [16, 17].

The work in this dissertation evaluated the application of polymer gene delivery to treat the deleterious effects of pathological left ventricular remodeling after myocardial infarction. Myocardial infarction (MI) is a pathological state characterized by an acute loss of blood supply to the myocardium due to coronary artery occlusion. The obstruction results in decreased oxygen and nutrient delivery to myocardial tissues, causing local tissue death and formation of an infarct. This tissue loss occurs via necrosis, apoptosis, and autophagy and results in a weaker heart that is greatly predisposed to cardiac failure. Significant interest has been shown in developing therapeutic interventions to limit remodeling of the left ventricle (LV), restore heart function, and improve long-term patient prognosis, as the current pharmacological treatments do little to prevent LV remodeling. One technique that has shown potential is antiapoptotic and proangiogenic gene therapy of the LV to restore heart function and limit infarct expansion. While most gene therapy research for treating MI has focused on delivery of recovery factors to ameliorate damage to the myocardium [18-20], current research has suggested that there

are some very promising targets that can help cardiomyocytes survive the hypoxic insult caused by MI, such as targeting proapoptotic factors like BNIP3, a hypoxia-inducible cell death switch that has been shown to be highly upregulated in the myocardium post-MI [21-23].

The work in this dissertation focuses on two therapeutic approaches applying polymer-mediated gene delivery to treat myocardial infarction and tests these approaches in animal models. First, we detail a combined cell therapy/angiogenic strategy where primary rat skeletal myoblasts were transfected *ex vivo* with a $VEGF_{165}$ plasmid and then implanted directly to the infarcted rat myocardium to act as VEGF bioreactors. Second, we detail the design of small interfering RNA (siRNA) towards BNIP3, a proapoptotic protein specifically upregulated by hypoxia and the validation of this target to ameliorate hypoxic cell death after exposure to hypoxia. This *in vitro* validation was then further investigated in a rat model of myocardial ischemia/reperfusion injury.

The multiple approaches to ameliorating the deleterious effects of left ventricle remodeling postmyocardial infarction in this study lead to the dual hypothesis that 1) implantation of $VEGF_{165}$-expressing skeletal myoblasts to infarcted myocardium preserves heart function, increases neoangiogenesis, decreases cardiomyocyte cell death, and increases cardiomyocyte viability, and that 2) reduction of cardiomyocyte BNIP3 levels after myocardial infarction in the short term by siRNA therapy results in decreased hypoxia-induced cell death, increased cell survival, and retention of heart function.

1.2 Study Rationale

The work in this dissertation focuses on identifying polymers with high biocompatibility and low toxicity, identifying and validating gene targets for the

treatment of myocardial infarction, and combining the two components together to successfully treat and limit the negative effects of left ventricular remodeling in animal models of myocardial infarction (Figure 1.1).

The chapter following this brief introduction contains background information and a review of the current literature surrounding myocardial infarction, siRNA and plasmid gene therapy for cardiovascular disease, and polymer gene carriers.

The work in Chapter 3 is unique as it combines polymer-mediated gene therapy with cell therapy to revascularize and repopulate the myocardium after myocardial infarction. This chapter details the *ex vivo* transfection of primary rat skeletal myoblasts with a gene expressing $VEGF_{165}$ and the implantation of these cells in the cardiac wall post-MI. Most angiogenic gene therapy approaches have focused on direct transfection of the endogenous myocardial cell population of cardiomyocytes and fibroblasts. However, these cell populations have proven to be extremely difficult to transfect *in situ*, which results in low expression of transgenes. By transfecting skeletal myoblasts *ex vivo* with an efficient and nontoxic bioreducible polymer, we were able to attain high transfection efficiency, combining the benefit of high angiogenic factor expression and secretion to surrounding tissues with the positive benefit of cell therapy with a myocyte progenitor cell. The implanted cells provide further benefit by repopulating the myocardium and by secreting recovery factors into the myocardial milieu.

The fourth chapter describes the work that was done in determining the polymer gene carriers that would be used in later studies to directly transfect the myocardium with high efficiency and low toxicity. This chapter also details the work performed to evaluate the siRNA target BNIP3 to reduce hypoxia-induced cell death in the infarcted

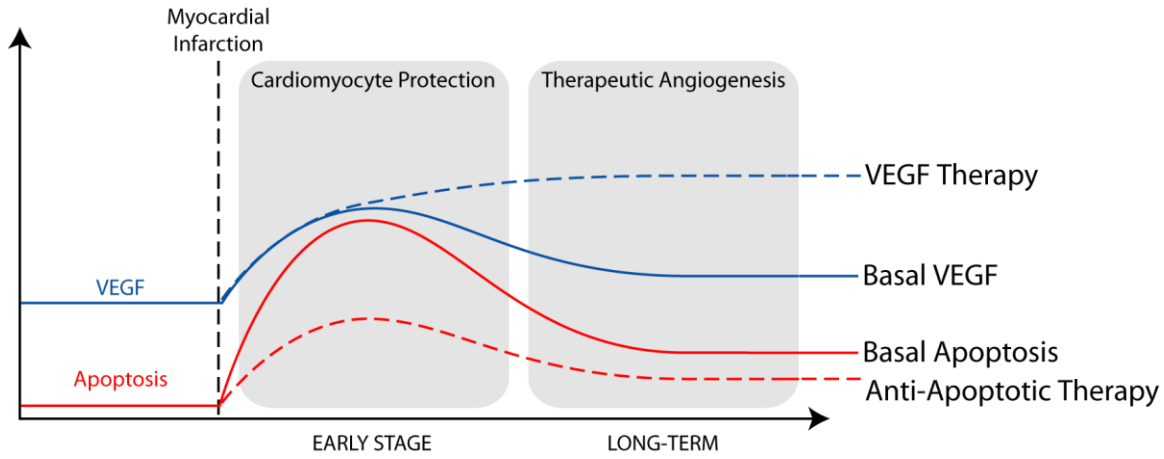

Figure 1.1. Graphical overview of myocardial infarction therapy strategies.

myocardium. An *in vitro* model of hypoxia was used to determine the effects of BNIP3 knockdown on hypoxia survival. To increase the translatability to subsequent *in vivo* studies, primary rat neonatal cardiomyocytes were used.

Chapter 5 applies the work performed in the previous chapter in an *in vivo* rat model of ischemia/reperfusion injury. The transient knockdown of BNIP3 immediately after ischemia/reperfusion injury was achieved by delivering BNIP3 siRNA directly to the myocardium with a novel arginine-conjugated bioreducible polymer. Direct myocardial siRNA gene therapy is easier to achieve than myocardial plasmid gene therapy as siRNA needs only reach the cytoplasm to exert its action, whereas plasmids must penetrate the nucleus in order for expression to occur.

1.3 Specific Aims

In order to test the aforementioned hypotheses, this dissertation was broken up into three separate specific aims.

1.3.1 Specific Aim 1

Determine if intramyocardial implantation of $VEGF_{165}$-transfected skeletal myoblasts after acute myocardial infarction in rats results in retained heart function, decreased infarct size, increased cardiomyocyte viability, and increased capillary and arteriole formation.

We used a rat model of permanent coronary artery occlusion and randomly assigned animals to one of four groups: 1) sham operation control (thoracotomy only), 2) ligation only, 3) implanted skeletal myoblasts alone, and 4) implanted $VEGF_{165}$-expressing skeletal myoblasts. Cardiac function and ventricle geometry were measured four-weeks after surgery by MRI. Histology to determine infarct size and

immunohistochemistry to measure vessel formation, cardiomyocyte viability, and apoptosis were performed on isolated hearts immediately after MRI acquisition.

1.3.2 Specific Aim 2

Characterize the optimal bioreducible polymer carrier to deliver genetic material to cardiomyocytes and determine the protective effects of siRNA-mediated BNIP3 knockdown on hypoxic cardiomyocytes.

Selection of an ideal polymer gene delivery agent for use *in vivo* is a multifaceted process. We identified that a novel poly(amido amine) polymer synthesized by our lab, arginine-grafted poly(cystaminebisacrylamide diaminohexane) (referred to as arginine-grafted bioreducible polymer; ABP), showed the ideal characteristics of high transfection efficiency, low cytotoxicity, and prolonged stability [24, 25]. Cardiomyocytes (especially those from a primary animal source) have long been known to be notoriously difficult to transfect [26, 27]; thus, the identification of the optimal polymer to obtain high transfection efficiencies with minimal toxicity is paramount.

1.3.3 Specific Aim 3

Determine if a reduction of BNIP3 levels in rat cardiomyocytes after acute myocardial ischemia/reperfusion injury results in increased cell survival, decreased apoptosis, and retention of heart function in an *in vivo* rat model.

We used a rat coronary ligation model of myocardial infarction to evaluate the effectiveness of polymer-mediated BNIP3 mRNA knockdown in increasing cardiomyocyte survival and subsequently retaining heart function. Rats were randomly assigned to one of five groups: 1) sham operated control (thoracotomy only), 2) coronary ligation ischemia/reperfusion control, 3) siBNIP3 delivered intramyocardially via

arginine-grafted bioreducible polymer (siBNIP3:ABP), 4) siBNIP3 delivered intramyocardially alone (naked siRNA), and 5) siLuciferase delivered intramyocardially via arginine-grafted bioreducible polymer (siLuc:ABP). Two weeks after surgery, heart function and global and regional ventricle geometry were measured via magnetic resonance imaging (MRI). Additionally, histological and immunohistological analyses were performed on isolated hearts to determine infarct size, cardiomyocyte geometry, cardiomyocyte viability, BNIP3 expression, and degree of apoptosis via TUNEL assay.

1.4 References

[1] T. Friedmann, A brief history of gene therapy, Nat. Genet., 2 (1992) 93-98.

[2] The Journal of Gene Medicine Clinical Trials Database, in: J. Gene Med., John Wiley & Sons, Ltd., 2012.

[3] P.R. Clemens, S. Eghtesad, D.P. Reay, Gene therapy for muscular dystrophy reaches human clinical trial, Ann. Neurol., 66 (2009) 267-270.

[4] R.S. Bora, D. Gupta, T.K. Mukkur, K.S. Saini, RNA interference therapeutics for cancer: challenges and opportunities (review), Mol. Med. Report, 6 (2012) 9-15.

[5] M. Hedman, J. Hartikainen, S. Yla-Herttuala, Progress and prospects: hurdles to cardiovascular gene therapy clinical trials, Gene Ther., 18 (2011) 743-749.

[6] S.J. Zeller, P. Kumar, RNA-based gene therapy for the treatment and prevention of HIV: from bench to bedside, Yale J. Biol. Med., 84 (2011) 301-309.

[7] M. Nishikawa, L. Huang, Nonviral vectors in the new millennium: delivery barriers in gene transfer, Hum. Gene Ther., 12 (2001) 861-870.

[8] D.M. Dykxhoorn, D. Palliser, J. Lieberman, The silent treatment: siRNAs as small molecule drugs, Gene Ther., 13 (2006) 541-552.

[9] N. Wade, Gene therapy pioneer draws Mikadoesque rap, Science, 212 (1981) 1253.

[10] N. Wade, Gene therapy caught in more entanglements, Science, 212 (1981) 24-25.

[11] N. Wade, UCLA gene therapy racked by friendly fire, Science, 210 (1980) 509-511.

[12] R. Tomanin, M. Scarpa, Why do we need new gene therapy viral vectors? Characteristics, limitations and future perspectives of viral vector transduction, Curr. Gene Ther., 4 (2004) 357-372.

[13] H.S. Zhou, D.P. Liu, C.C. Liang, Challenges and strategies: the immune responses in gene therapy, Med. Res. Rev., 24 (2004) 748-761.

[14] J.H. Jeong, S.W. Kim, T.G. Park, Molecular design of functional polymers for gene therapy, Prog. Polym. Sci., 32 (2007) 1239-1274.

[15] T.G. Park, J.H. Jeong, S.W. Kim, Current status of polymeric gene delivery systems, Adv. Drug Deliv. Rev., 58 (2006) 467-486.

[16] S.C. De Smedt, J. Demeester, W.E. Hennink, Cationic polymer based gene delivery systems, Pharm. Res., 17 (2000) 113-126.

[17] D.W. Pack, A.S. Hoffman, S. Pun, P.S. Stayton, Design and development of polymers for gene delivery, Nat. Rev. Drug Discov., 4 (2005) 581-593.

[18] T.A. Khan, F.W. Sellke, R.J. Laham, Gene therapy progress and prospects: therapeutic angiogenesis for limb and myocardial ischemia, Gene Ther., 10 (2003) 285-291.

[19] D.W. Losordo, P.R. Vale, J.F. Symes, C.H. Dunnington, D.D. Esakof, M. Maysky, A.B. Ashare, K. Lathi, J.M. Isner, Gene therapy for myocardial angiogenesis: initial clinical results with direct myocardial injection of phVEGF165 as sole therapy for myocardial ischemia, Circulation, 98 (1998) 2800-2804.

[20] T.K. Rosengart, L.Y. Lee, S.R. Patel, T.A. Sanborn, M. Parikh, G.W. Bergman, R. Hachamovitch, M. Szulc, P.D. Kligfield, P.M. Okin, R.T. Hahn, R.B. Devereux, M.R. Post, N.R. Hackett, T. Foster, T.M. Grasso, M.L. Lesser, O.W. Isom, R.G. Crystal, Angiogenesis gene therapy: phase I assessment of direct intramyocardial administration of an adenovirus vector expressing VEGF121 cDNA to individuals with clinically significant severe coronary artery disease, Circulation, 100 (1999) 468-474.

[21] A. Hamacher-Brady, N.R. Brady, S.E. Logue, M.R. Sayen, M. Jinno, L.A. Kirshenbaum, R.A. Gottlieb, A.B. Gustafsson, Response to myocardial ischemia/reperfusion injury involves Bnip3 and autophagy, Cell Death Differ., 14 (2007) 146-157.

[22] D.A. Kubli, M.N. Quinsay, C. Huang, Y. Lee, A.B. Gustafsson, Bnip3 functions as a mitochondrial sensor of oxidative stress during myocardial ischemia and reperfusion, Am. J. Physiol. Heart Circ. Physiol., 295 (2008) H2025-2031.

[23] T.R. Burton, S.B. Gibson, The role of Bcl-2 family member BNIP3 in cell death and disease: NIPping at the heels of cell death, Cell Death Differ., (2009).

[24] T.I. Kim, M. Ou, M. Lee, S.W. Kim, Arginine-grafted bioreducible poly(disulfide amine) for gene delivery systems, Biomaterials, 30 (2009) 658-664.

[25] S.H. Kim, J.H. Jeong, T.I. Kim, S.W. Kim, D.A. Bull, VEGF siRNA delivery system using arginine-grafted bioreducible poly(disulfide amine), Mol. Pharm., 6 (2009) 718-726.

[26] C. Thiel, M. Nix, Efficient transfection of primary cells relevant for cardiovascular research by nucleofection, Methods Mol. Med., 129 (2006) 255-266.

[27] S. Bauer, S.K. Maier, L. Neyses, A.H. Maass, Optimization of gene transfer into neonatal rat cardiomyocytes and unmasking of cytomegalovirus promoter silencing, DNA Cell Biol., 24 (2005) 381-387.

CHAPTER 2

MYOCARDIAL INFARCTION, GENE THERAPY, AND POLYMER GENE CARRIERS: BACKGROUND AND LITERATURE REVIEW

2.1 Myocardial Infarction

Cardiovascular disease is the most common cause of death in developed nations and accounts for one out of every three deaths in the United States for a total of 811,900 deaths in 2008 [1]. Of the various forms of cardiovascular disease, coronary heart disease is the deadliest, accounting for half of all reported cardiovascular disease-related deaths and 405,300 deaths in 2008 [1]. Myocardial infarction (MI), or heart attack, is a particularly deadly form of heart disease (1 out of 20 deaths, 2008 total of 134,000 deaths [1]) and is characterized by a loss of blood flow to the heart, typically due to coronary artery blockage, resulting in ischemic tissue death. Even when a person survives acute MI, the long-term prognosis is daunting, with an average survival of around six years [1]. The poor prognosis after MI is due to both microscopic cellular and macroscopic geometric damage leading to deterioration in heart function and progression towards heart failure. The deteriorated heart performance is the result of further death of cardiac cells and MI-initiated remodeling of the left ventricle (LV), a process that has been shown to occur immediately after MI and which may continue for the duration of the patient's life [2-4]. The remodeling ultimately results in LV dilation, which has been shown to be a primary determinant of morbidity and mortality [5]. Due to the high

incidence of MI and the limited treatment options in preventing progression to heart failure, many researchers are attempting to develop treatments that will limit LV remodeling and retain heart function.

2.2 Left Ventricular Remodeling

Left ventricular remodeling after myocardial infarction is a complex, progressive, and pathological transformation whereby the ventricle changes shape, size, and composition after MI, leading to decreased function [4, 6]. The heart's capacity to remodel is a necessary adaptive process for normal growth, development, and compensation for exercise stress, but after MI, the process can become maladaptive, decreasing the performance of the heart. Remodeling of the LV has been shown to begin as soon as minutes after a myocardial infarction occurs and can continue for many months and even years [7]. These changes occur due to pathological alterations in the myocardium, including cardiomyocyte apoptosis, cardiomyocyte hypertrophy, fibroblast proliferation, and increased intercellular fibrosis. Slowing or eliminating remodeling is of the utmost clinical value as the degree of remodeling has been shown since the 1970s to correlate highly with poor prognosis, future risk for heart failure, and increased mortality [5, 8, 9].

The process of LV remodeling is regulated by a number of factors, including genetic, mechanical, and hormonal signals [10]. As a result of these multifaceted signals, remodeling occurs at three distinct levels within the heart: at the ventricular level, involving changes in volume, wall thickness, and shape; at the cellular level, involving changes in cell volume, length, number, and cross-sectional area; and at the molecular level, involving changes in gene expression due to neurohormonal signals.

2.2.1 Molecular and Cellular Remodeling

Remodeling begins with activation of an array of paracrine, neuroendocrine, and autocrine factors. These factors are quickly upregulated in response to myocardial injury, mechanical wall stress, alteration in hemodynamics and blood pressure, hypoxia, and increased reactive oxygen species (ROS). Hypotension incident to myocardial infarction activates the renin-angiotensin-system (RAS) [11], increases secretion of natriuretic peptides [12], and increases norepinephrine and other catecholamine production by the adrenal medulla [13, 14]. MI also causes activation of inflammation pathways by triggering a cytokine cascade initiated by tumor necrosis factor alpha (TNF-α) [15]. Dysfunction in the myocardial wall activates angiotensin II type (AT) stretch receptors, inducing hypertrophy through angiotensin II (Ang II) [16]. Hypoxia upregulates a large number of genes with hypoxia inducible factor- (HIF) sensitive hypoxia response elements (HREs) and reperfusion causes a large degree of damage due to rapid increases in reactive oxygen species [17-19]. Collagenases and proteins that degrade the extracellular matrix like matrix metalloproteases (MMPs) are also upregulated, causing degradation of the normal connective tissue and remodeling of the extracellular matrix [20, 21].

2.2.2 Geometric Ventricular Remodeling

Ultimately, the cellular and molecular changes that occur above present as global and regional changes in the LV. Due to the changes in cardiomyocyte numbers, size, and utility, the LV begins to alter in shape and function. The walls of the ventricle begin to thin due to increased fibrosis and cardiomyocyte slippage [22]. Loss of cardiomyocytes via necrosis produces an inflammatory response with fibroblast proliferation and collagen

deposition to replace the dead cells. The remaining cells are embedded and isolated within the fibrotic scar and the rhythmic contraction of the cardiomyocytes begins to suffer as a result [6, 23]. The thinning walls increase the mechanical strain within the heart, causing the ventricle to progressively deform and expand [24]. This expansion leads to increased chamber volume at both systole and diastole with increased LV diameters, especially through the infarct zone and towards the apex of the heart [25]. Due to the serious implications of LV remodeling following MI and its high correlation to heart failure rates, researchers and clinicians are focused on surgical and pharmacological strategies to limit the extent of remodeling that occurs.

2.3 Surgical and Pharmacological Management of Myocardial Infarction

In the event of acute myocardial infarction, the most pressing issue is to eliminate the occlusion, reestablishing blood flow to the myocardium. Rapid restoration of blood flow to the myocardium as measured by time to reperfusion has been consistently demonstrated as the most effect means of increasing patient survival while lessening infarct size [26, 27]. Achieving quick time to reperfusion is a difficult process, however, as there are many steps that must occur rapidly from when a patient first experiences symptoms of an acute MI to when the patient is treated for the condition. A patient suffering an acute MI must first be quickly transported to the hospital, admitted to the emergency department, triaged, and diagnosed, and then finally treated with either thrombolytics or angioplastic percutaneous coronary intervention (PCI) [28]. In complicated cases requiring multivessel replacement, surgical coronary artery bypass grafting (CABG) is performed.

2.3.1 Drugs for Early Reperfusion

Thrombolytic therapy involves the use of fibrinolytic agents to lyse the thrombus/thrombi occluding the coronary arteries. There are three major classes of thrombolytic drugs in use today: the tissue plasminogen activators (tPAs) alteplase, reteplase, and tenecteplase; the streptokinases anistreplase, and natural streptokinase; and urokinase. All three of these drug classes work on the same target within the same clot formation pathway—plasminogen. Plasminogen is the inactive precursor to the active fibrinolytic plasmin and is activated via cleavage of a signal peptide to liberate active plasmin.

The tPAs are all enzyme mimetics of endogenous tPA, which is a proteolytic enzyme released by endothelial cells in response to signals such as hemostasis. The enzyme tPA and its drug analogs function by binding to fibrin where it activates plasminogen that is also bound to the fibrin clot. This localized effect gives the tPA class of fibrinolytics a slight advantage over other fibrinolytic drug classes as it produces more local fibrinolysis with less systemic lytic effect [29]. Alteplase is a recombinant version of the endogenous tPA enzyme but suffers from an extremely short systemic half-life of approximately 5 minutes [30]. Reteplase and tenecteplase are both recombinant mutant forms of tPA with modifications to increase their circulating half-life to 13–16 minutes and 90–130 minutes, respectively [30].

Similar to the tPA class of drugs, streptokinase also acts on plasminogen, but does not possess enzymatic activity to convert plasminogen to plasmin. Instead, it induces a conformational change in plasminogen, which exposes the plasminogen active site, increasing the liberation of plasmin. Since the introduction of the newer tPA class,

streptokinase is not commonly used in a clinical setting as tPAs have been shown to be more effective [31]. Urokinase is not commonly utilized for acute MI as it is not indicated for the condition, being used instead to clear pulmonary emboli.

The use of thrombolytics for acute MI is very time dependent. After approximately 2 hours, fibrin cross-linking within the clot is extensive and the clot is more compact, making lysis more difficult [26, 32]. Thrombolysis of aged clots requires higher fibrinolytic concentrations and is accompanied by increased risk of hemorrhage.

2.3.2 Angioplastic Intervention for Reperfusion

The other common method to restore myocardial blood flow and remove coronary occlusion is primary percutaneous coronary intervention (PCI). PCI involves inserting a guided catheter through a peripheral (usually femoral) artery to gain direct access to the coronary artery blockage. Meta-analyses have consistently shown better long-term outcomes for PCI versus thrombolytic therapy, reducing short-term mortality, reinfarction, stroke, and long-term death [33].

PCI was first used for revascularization in the 1970s by inserting a catheter with a balloon tip through the vasculature and through the coronary blockage then expanding the balloon to expand the artery, restoring blood flow [34]. While percutaneous balloon angioplasty revolutionized the way coronary artery diseases were treated, the effectiveness of the procedure was limited due to side effects such as thrombus formation and rapid coronary artery reocclusion. To improve upon balloon angioplasty, other devices were developed that removed the plaque blockage or physically left a device such as a stent to hold the vessel open. Bare metal stents were introduced in 1986 [35] and were further improved in 2003 by coating bare metal stents with a drug-eluting polymer

to form drug-eluting stents [36, 37]. The drug-eluting stents release pharmacological agents to limit neointimal hyperplasia, a process where the damage to the endothelial wall causes continued growth and division of endothelial and smooth muscle cells into the intimal space of the vessel, eventually restricting blood flow and occluding the vessel [38, 39]. Current drug-eluting stents contain antiproliferative agents such as sirolimus and paclitaxel. Early trials showed excellent prevention of restenosis, with 0% restenosis using a sirolimus-eluting stent versus 26.6% restenosis with a bare metal stent at 6 months [40]. Similarly, some of the early trials with paclitaxel-eluting stents showed the same 0% 6-month restenosis rate versus a 10% restenosis rate with standard stents [41].

While the short-term success of drug-eluting stents is extremely high, long-term use of the devices is accompanied by risks that are not seen in patients who receive bare metal stents. Some of these complications include late and very-late thrombosis [42, 43], hypersensitivity immune response [44, 45], delayed healing [46], and endothelial dysfunction [47]. Recently conducted meta-analyses of trials using drug-eluting stents confirms that their use is not without unique risks, but shows that the benefits are still in favor of using the newer stents over bare metal stents [48, 49].

Next generation drug-eluting stents are already in development and are currently being tested in humans. Improvements include new biodegradable polymers with enhanced biocompatibility that do not induce as serious an inflammatory response as the current nonbiodegradable polymers [50], updated antiproliferative drugs, and polymer-free drug-eluting stents [51, 52].

2.3.3 Pharmacological Management Post-MI

Patients managing the after-effects of myocardial infarction can be placed on a variety of pharmacological agents designed to lessen the risk factors for heart failure. These drugs positively affect the heart by either increasing the contractile force of remaining cardiomyocytes or by reducing the workload on the heart. These drugs include angiotensin-converting enzyme (ACE) inhibitors, ß-blockers, diuretics, angiotensin receptor blockers, aldosterone antagonists, hydralazine and isosorbide dinitrate, and digitalis glycosides.

The use of inotropic agents in heart failure is usually managed with care as most inotropic agents (with the exception of digitalis glycosides) have shown increased mortality rates in heart failure patients [53, 54]. However, while the use of inotropes may shorten the patient's lifespan, the quality of life of patients on these drugs is dramatically improved. Inotropic agents such as digoxin, phosphodiesterase inhibitors (milrinone), and ß-receptor agonists (dopamine and dobutamine) exert their positive hemodynamic effects by increasing cardiac output while reducing, to a lesser degree, neurohormonal activation.

Angiotensin receptor blockers and ACE inhibitors are some of the most common drugs used post-MI and have demonstrated their ability to both slow, stabilize, and even mildly reverse pathological remodeling [55]. Due to neurohormonal activation after MI, the sympathetic nervous system and RAS are activated, leading to high levels of angiotensin, aldosterone, and norepinephrine in the myocardium. Increased myocardial levels of norepinephrine are especially problematic as norepinephrine is proapoptotic to the myocardium [56, 57]. Large multicenter trials have demonstrated increased survival, retention of function, fewer hospitalizations, and retained heart geometry in MI patients

receiving ACE inhibitors [58-61]. Efficient inhibition of the RAS using angiotensin-receptor blockers has also been shown to provide a survival benefit and limit remodeling [62, 63].

ß-blockers are used to counteract the effects of sympathetic nervous system activation and are well known to reduce remodeling and limit progression to heart failure. The beneficial mechanism of these drugs comes from negative chronotropic effects on heart rate, resulting in reduced intramyocardial neurohormone levels, decreased oxygen demand, and decreased infarct expansion [64]. Clinical studies have repeatedly demonstrated this benefit with long-term and short-term improvement seen in infarct expansion, LV ejection fraction, and myocardial dysfunction [65-67].

Aldosterone antagonism is hypothesized to produce beneficial effects in post-MI patients through inhibition of myocardial fibrosis [68, 69]. Studies evaluating aldosterone antagonists in combination with angiotensin receptor blockers showed improvement in LV mass, end diastolic/systolic volumes, and ejection fraction [70].

Patients who have undergone some form of PCI receive prophylactic treatment to prevent recurrence of atherosclerosis and thrombosis. Most guidelines recommend dual antiplatelet therapy with life-time, low-dose aspirin, and thienopyridine prescribed for one year. Statin drugs are also prescribed to help reduce serum cholesterol levels, ß-blockers are used to decrease cardiac workload and arrhythmias, and lifestyle management changes are recommended to lower the risk for recurrence.

The current first-line therapies of angiotensin and ß receptor blockade, and ACE inhibition, have clearly been demonstrated to aid in patient outcome and limit remodeling; however, pathological remodeling still continues in most patients. Because

of this, novel targets and treatment strategies such as antiapoptosis, antiinflammation, matrixmetalloprotease inhibition, cell-based, and proangiogenic therapies are currently being evaluated to prevent remodeling and increase LV function and patient survival.

2.3.4 Decreasing Infarct Size at Primary Intervention

Several strategies to reduce infarct size by limiting the extent of injury caused by reperfusion are actively being investigated. Some success has been observed in trials using adjuvant adenosine to limit infarct size by reducing free radical formation and neutrophil accumulation. The AMISTAD I trial found that administration of adenosine reduced anterior infarct size by 33% but had no effect on inferior infarctions [71]. Further investigation in the AMISTAD II trial found a nonsignificant trend towards smaller infarct sizes with low-dose adenosine but significantly smaller infarct sizes with high doses [72].

Some progress has been made in using therapeutic hypothermia to reduce the degree of reperfusion injury. Therapeutic hypothermia requires lowering the temperature of the heart either locally or by cooling the whole body to approximately 33 °C. This approach has demonstrated cardioprotective capabilities in animal models [73, 74] and in human studies [75]. However, it suffers from several limitations, including uncontrollable shivering, decreased drug metabolism, and the prolonged period required to achieve adequate cooling (approximately 1 hour) [76].

2.4 Gene Therapy for Recovery of Myocardial Function

Significant gains have been made in recent years in pharmacological therapies of the infarcted myocardium. While these gains have improved post-MI life expectancy and helped limit progression to heart failure, the therapeutic regimens are mainly focused on

decreasing the burden on the injured heart. In order to more fully treat the infarcted heart, therapies are actively being sought that can regenerate functional myocardium or prevent the loss of cardiomyocytes caused at the time of injury and afterwards. Gene therapy is one technique that is being investigated as a method for protecting the myocardium and preventing the loss of cardiomyocytes.

To date, there have been over 1,800 gene therapy clinical trials performed in humans [77]. Successful gene transfer in the cardiovascular system was first seen as long ago as 1989 [78]. Since that time, the popularity of cardiovascular diseases as a target for gene therapy has continued with cardiovascular diseases second only to cancer in popularity for gene therapy indications. Of all the almost 2,000 gene therapy clinical trials performed to this point, 155 or 8.4% of all trials have been indicated for the treatment of cardiovascular diseases [77].

While many gene targets have been investigated as potential strategies to treat cardiovascular disease in animal models, thus far, the overwhelming majority of human trials have utilized angiogenic factors to treat the disease [79]. The only other target evaluated in humans is sarcoplasmic/endoplasmic reticulum calcium ATPase 2 (SERCA2a). This target was recently evaluated in the Calcium Up-Regulation by Percutaneous Administration of Gene Therapy in Cardiac Disease (CUPID) trial and showed functional improvement after treatment with an adeno-associated virus 1 AAV1-SERCA2a vector [80, 81].

In addition to the angiogenic targets used in human clinical trials, a wider array of targets have been evaluated in animal models and shown to prevent left ventricular remodeling. Other gene therapy approaches include targeting extra-cellular matrix

degradation, via TGF-ßR [82], decorin [83], and integrin-linked kinase expression [84]. Other strategies utilize gene transfer to minimize cell death and include targeting antiapoptosis or prosurvival factors after ischemia/reperfusion injury. These targets include soluble Fas [85], heme oxygenase-1 [86], targets such as midkine growth factor [87], Bcl-2 [88], and the TNF-α receptor-1 [89]. Additionally, previous work in our laboratory has investigated VEGF expression in a plasmid under control of a hypoxia-specific RTP-801 promoter [90-92], using a novel cholesterol-conjugated cationic polymer and a terplex system composed of DNA, low density lipoprotein, and stearyl-poly-L-lysine [92].

In addition to plasmid-based approaches, several groups have utilized gene therapy to deliver siRNA to the myocardium to lower mRNA levels of deleterious proteins. Some of the siRNA targets investigated include PHD2 [93-95], SHP-1 [96], ALOX5 [97], and PTP-1B [98]. While these groups have mainly focused on the delivery of prosurvival, protective, and general antiapoptotic genes, no one has been able to demonstrate the utility of a system to protect from more specific hypoxia-induced apoptosis.

2.5 Tissue Oxygen Levels and Hypoxia Response

Cellular response to oxygen is a complex and tightly regulated process, mediated by a myriad of proteins (Figure 2.1). One important protein for regulating tissue O_2 response is the transcription factor hypoxia inducible factor-1 (HIF-1). HIF-1 is a heterodimeric protein consisting of a HIF-1α and HIF-1ß subunit (HIF-1ß is also known as the aryl hydrocarbon receptor nuclear translocator, ARNT). While HIF-1ß is constitutively expressed and remains localized within the nucleus regardless of O_2 levels

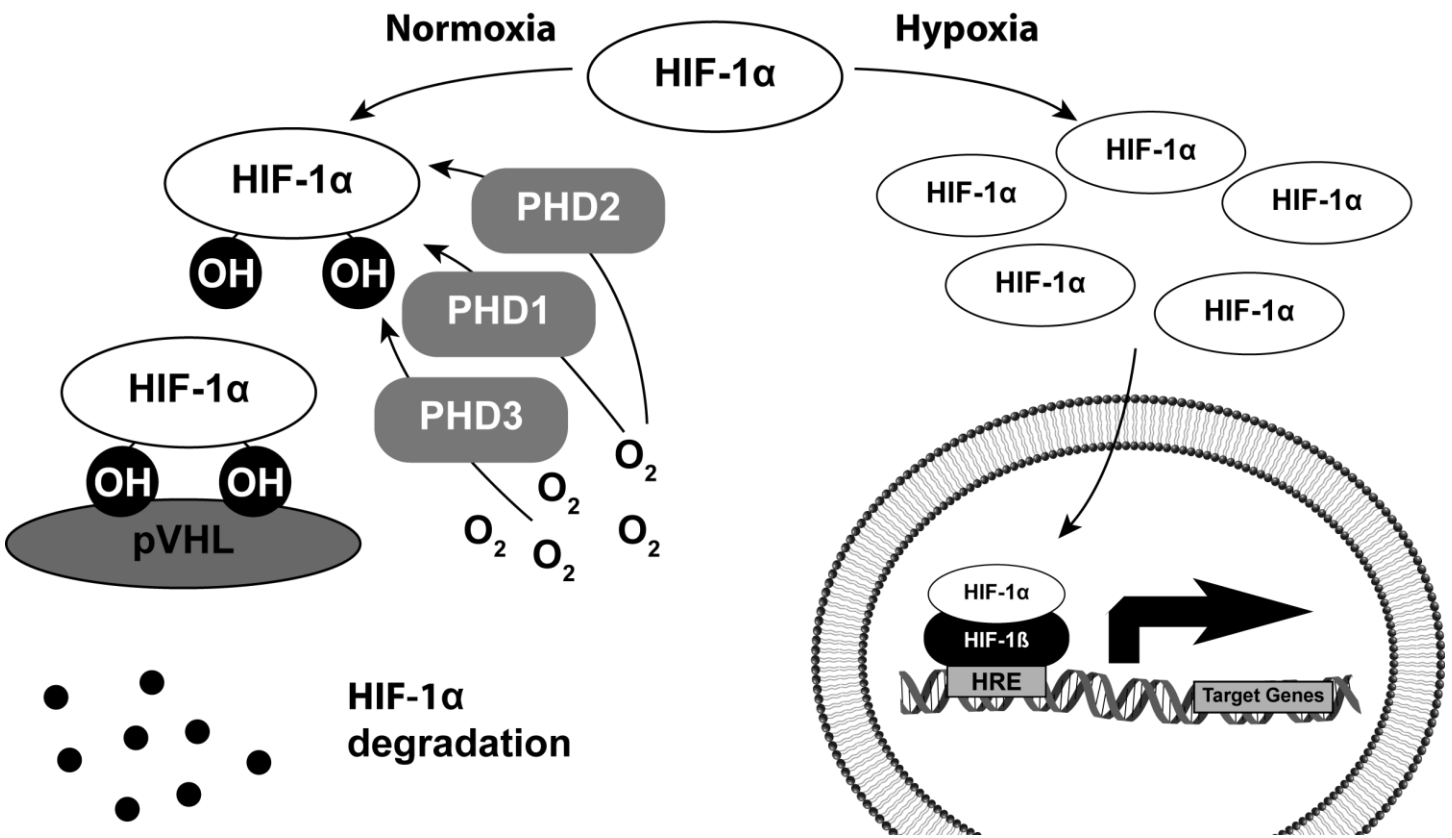

Figure 2.1. The cellular oxygen response mediated through HIF-1α.

[99-101], HIF-1α levels are kept low under normoxic conditions via posttranslational, oxygen-dependent degradation [102]. During normoxia, the 402/564 prolyl residues of HIF-1α are hydroxylated by the oxygen-dependent prolyl hydroxylases (PHD1, PHD2, and PHD3) [103]. The enzymatic activity of these hydroxylases is dependent on both iron and molecular O_2 availability. After HIF-1α has been hydroxylated, it binds to the von Hippel-Lindau tumor suppressor protein (pVHL) [104]. Ubiquitination of HIF-1α is mediated by the pVHL complex, targeting HIF-1α for proteasomal degradation. Under hypoxic conditions, the PHDs lack the molecular O_2 necessary for their enzymatic action, resulting in decreased HIF-1α degradation. HIF-1α then translocates to the nucleus where it is free to heterodimerize with HIF-1ß to form the active transcription factor HIF-1. This transcription factor induces the upregulation of genes containing hypoxia response elements (HREs) in their promoters, allowing for genetic adaptation to decreased oxygen levels [105]. While the primary physiological response to lowered O_2 levels is an adaptive and prosurvival response, if normal levels of O_2 are not restored, the cell will ultimately undergo apoptosis, autophagy, or necrosis.

2.6 The Proapoptotic Protein BNIP3

The myocardium has historically been found to be highly resistant to apoptosis with an average observed apoptotic rate of 1 in 100,000 cardiomyocytes [106]. This low level of observed apoptosis is thought to be at least partially due to high myocardial expression levels of caspase inhibitors such as the apoptosis repressor with caspase recruitment domain (ARC) and X-linked inhibitor of apoptosis protein (XIAP) [107]. In diseased hearts, however, the rate of apoptosis has been shown to dramatically increase over 200-fold for both ischemic cardiomyopathies and idiopathic dilated

cardiomyopathies [106]. While cardiomyocytes are capable of spontaneous regeneration after myocardial infarction, the degree to which they regenerate is insufficient to compensate for the increased rate of cell loss [108, 109]. With the balance of cell death and regeneration tipped towards cell death, the heart gradually loses more and more cardiomyocytes and progresses in a path towards heart failure.

Apoptosis and cell death following acute myocardial infarction has been shown to be readily detectable in humans especially within a one-week time frame after MI. Studies have shown that apoptosis peaks within the first few days, decreasing rapidly after four days to a much lower level [110].

An important cellular mediator of hypoxia-inducible cell death is Bcl-2/adenovirus E1B nineteen-kilodalton interacting protein 3 (BNIP3). BNIP3 is an HRE-containing proapoptotic protein belonging to the Bcl-2 family and is one of the most highly upregulated proteins in response to hypoxia [111-113]. Human BNIP3 is a 194-amino acid protein with several domains that dictate its structure. BNIP3 has a transmembrane domain at residues 164–184, which allows it to insert into the mitochondrial membrane and homodimerize with other BNIP3 proteins in the membrane to form an ion channel [114, 115]. BNIP3 also has a Bcl-2 homology domain 3 (BH3) at residues 104–119, which allows it to bind with the antiapoptotic Bcl-2 [116]. Finally, BNIP3 also has an evolutionarily conserved cysteine residue at amino acid 64, which is thought to increase BNIP3 stability under conditions of oxidative stress [117]. Under oxidative conditions such as after MI when high levels of ROS are present in the myocardium, the cytosolic compartment switches from a reductive environment to an oxidative environment. When this occurs, disulfide bonds become more favorable and

stable. The BNIP3 cysteine, which is located on the cytosolic side of the protein when it inserts into the mitochondrial membrane, forms a stabilizing disulfide bonds with its homodimer, increasing its activity and depolarizing the mitochondrial membrane [117].

While BNIP3 has been studied extensively, the exact mechanisms by which it brings about cell death are not yet completely understood. However, it has been shown that cells where BNIP3 is upregulated can undergo one of at least three pathways that can lead to death: apoptosis, autophagy, or necrosis (Figure 2.2). As BNIP3 plays such a pivotal role in the regulation of the hypoxia death response, it is a prime candidate for gene therapy to selectively disable hypoxia-inducible cell death [118].

2.6.1 BNIP3-Regulated Apoptosis

It is postulated that BNIP3 induces cell death through localization to the mitochondrial membrane and depolarizing the membrane [114]. In some cell types, the localization of BNIP3 to the mitochondria causes cytochrome c release, initiating the caspase cascade and committing the cell to apoptosis [119]. However, in other cells such as neurons, BNIP3 induces endonuclease G release from the mitochondria but does not cause cytochrome c release, causing caspase-independent cell death [120].

2.6.2 BNIP3-Regulated Autophagy

Autophagy is a catabolic cellular process by which proteins and subcellular organelles are compartmentalized, and broken down by lysosomal degradation. In the heart and other tissues, autophagy is a normal process allowing cells to eliminate damaged proteins and organelles while scavenging many of the nutrients contained in the digested structures. Unlike apoptosis and necrosis, however, initiation of autophagy does

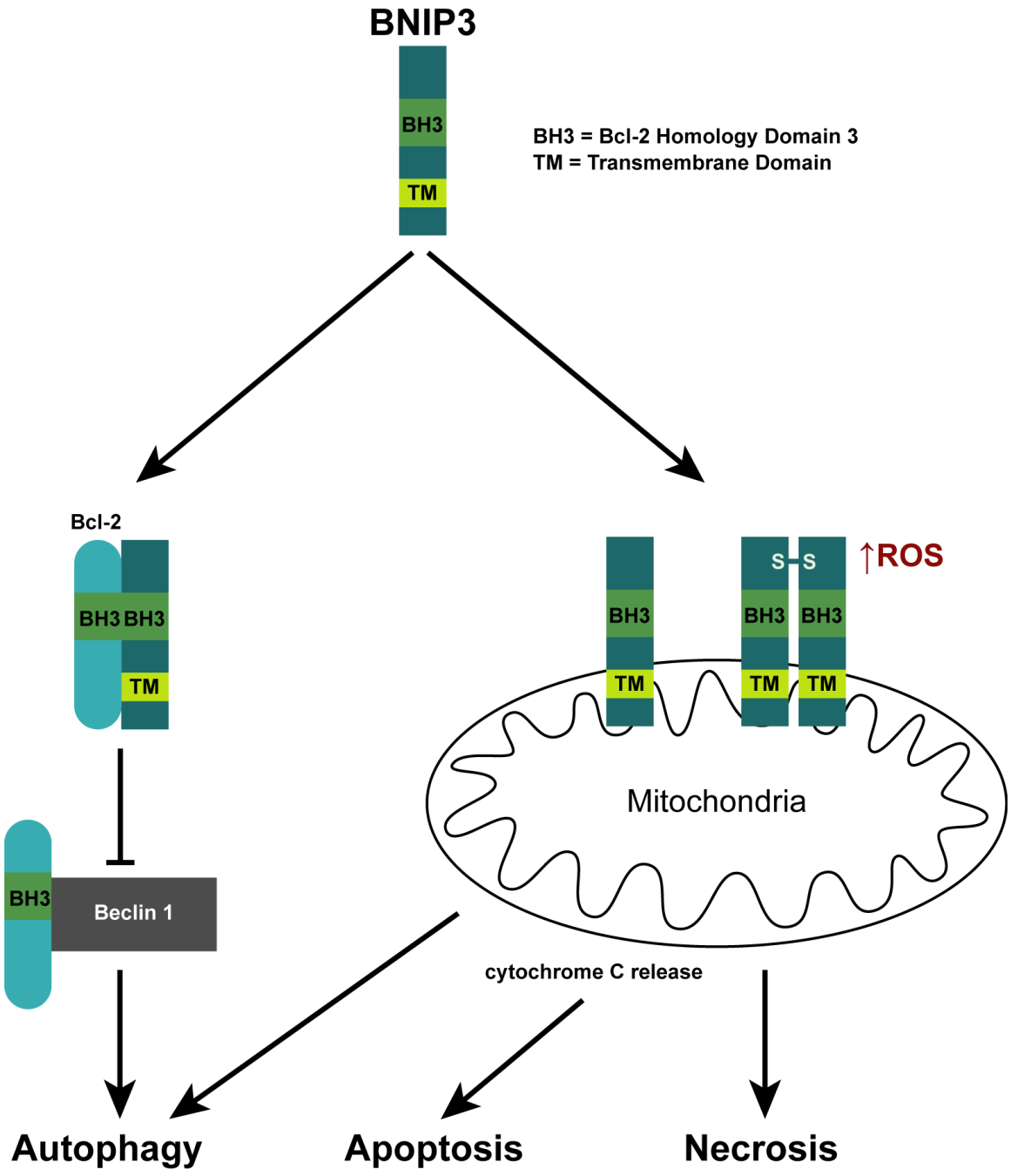

Figure 2.2. BNIP3-regulated death pathways. Adapted from [115]

not necessarily end in cell death. Autophagy is a normal cellular process that is observed in some healthy cell types [121-123]. The process allows for recycling of dysfunctional organelles, and defective cytoplasmic proteins without committing the cell to a death fate. In some animal models of repetitive ischemia/reperfusion, cardiac injury autophagy has been observed as a precursor to eventual apoptosis, with autophagic cell death occurring at a later time than apoptotic cells [124]. This observation would suggest a protective mechanism, giving cardiomyocytes extra time to acclimate to the disturbed oxygen and nutrient status post-ischemia/reperfusion and to attempt to avoid apoptosis by removing damaged intracellular structures.

The autophagic role of BNIP3 and its related family member Nix/BNIP3L in cardiomyocytes has received a great deal of attention over the past years. The role of BNIP3 in inducing autophagy is thought to be due to its interaction with the antiapoptotic Bcl-2. This antiapoptotic protein plays a role in sequestering beclin-1, a protein which is known to induce autophagy. Since BNIP3 has a BH3 domain through which it can bind Bcl-2, BNIP3 can act as a competitive inhibitor of Bcl-2 for beclin. In periods of high BNIP3 expression such as hypoxia, BNIP3 displaces beclin by binding to Bcl-2, causing beclin to initiate autophagy [125, 126].

2.6.3 BNIP3-Regulated Necrosis

Unlike the death pathways listed above which are energy- and ATP-dependent, necrosis is a passive process. Necrosis usually occurs as a result of overwhelming injury, which causes cellular swelling, dysregulation of organelle function, and ultimately leads to rupture of the cell membrane. This rupture rapidly releases cellular contents to the extracellular environment, damaging neighboring cells and causing inflammation.

BNIP3 has been shown to play a role in the necrosis of neurons [127, 128], tumor cells [129-131], and cardiomyocytes [117, 132]. BNIP3-mediated necrosis is thought to occur through interactions at the mitochondrial membrane similar to its site of action for inducing autophagy and apoptosis. However, over-activation of BNIP3 at the mitochondrial membrane is thought to rapidly push the cell to a necrotic as opposed to autophagic fate. In addition to the conserved transmembrane and BH3 domain, BNIP3 also has a conserved cysteine residue at position 64 located on the cytosolic side where BNIP3 inserts into the mitochondrial membrane [117]. When the cytoplasmic compartment shifts from a predominantly reductive environment to a predominantly oxidative environment under oxidative stress situations such as is experienced during reperfusion injury in cardiomyocytes, this cysteine residue forms a disulfide bond with the cysteine residue on another BNIP3 protein forming a covalent homodimer [116, 117]. This increase in activity on the mitochondrial membrane is thought to push the cell towards a necrotic as opposed to autophagic cell death [133].

2.7 RNA Interference and siRNA

RNA interference (RNAi) refers to the endogenous cellular pathway by which double-stranded RNA (dsRNA) is processed into small interfering RNA (siRNA) that can target mRNA transcripts for gene silencing.

The RNAi phenomenon was originally observed by Guo and colleagues in 1995. While performing gene function studies in *C. elegans*, they detected a sense strand sequence as the complementary antisense sequence for repressing gene expression [134]. This observation was further investigated by Fire *et al.* in 1998 and they published a seminal paper demonstrating that introduction of double-stranded RNA sequences

produced a more potent and specific interference effect than either the sense or antisense strand alone [135]. This discovery initiated a period of rapid research further elucidating the mechanism and potential impact of RNAi. A summary of many important publications highlighting the discovery and development of RNAi can be seen in Table 2.1.

Using siRNA to target a specific protein is particularly attractive because of the ability of siRNA to knockdown one target while essentially sparing all other proteins. Careful design of siRNA constructs is performed by using algorithms that optimize siRNA efficiency, analyzing selected constructs for lack of shared homology to other proteins by utilizing NCBI Blast searches, and by screening several siRNA constructs to determine the sequence with the highest knockdown efficiency and fewest off-target effects. Additionally, published sequences that have been shown to effect efficient knockdown of the target can be used [136-138].

Many researchers use siRNA as a laboratory tool for the analysis of gene function and to easily and rapidly decrease specific protein levels. However, many people have also been looking at siRNA as a potential therapeutic. While siRNA possess many attributes that make them ideal candidates for therapeutics, there are inherent issues with employing siRNA *in vivo*. Nucleotides have extremely short extracellular half-lives (seconds to minutes in the circulation [139]). Also, their large size (average 13.5 kDa), charged phosphodiester backbone, and hydrophilicity impede their ability to cross cell membranes. Therefore, a delivery vehicle is needed to protect the nucleotides from degradation and aid in gaining access to the cellular compartment.

Table 2.1. Seminal Publications in the History of RNAi Discovery

Year	Author	Organism	Discovery	Reference
1995	Guo *et al.*	*C. elegans*	RNA sense strand interferes with gene expression	[134]
1998	Fire *et al.*	*C. elegans*	Double-stranded RNA reduces gene expression more potently than sense or antisense strands alone	[135]
2000	Zamore *et al.*	*D. melanogaster*	Dicer protein processes double-stranded RNA to 21–23 nt fragments	[140]
2001	Elbashir *et al.*	Mammals	First observation of RNAi in mammalian cells	[141]
2002	Paddison *et al.*	Mammals	RNAi through expressed short hairpin RNA (shRNA)	[142]
2004	Acuity Pharmaceuticals	*H. sapiens*	First human Phase I clinical trial using siRNA	
2010	Davis *et al.*	*H. sapiens*	Targeted systemic polymer nanoparticle siRNA delivery demonstrated dose-dependent target accumulation	[143]

2.7.1 siRNA Therapy and Clinical Trials

Over forty clinical trials utilizing siRNA or shRNA have been performed or are in progress (Table 2.2). While many of these trials are still early-stage (Phase I and II), at least one trial is in late-stage Phase III trials. Despite the large number of clinical trials, no candidates have yet gained FDA approval.

The first clinical trials investigating RNAi were performed with naked, unmodified siRNA and were delivered either by local injection to the therapeutic site or via inhalation to the lungs. Even when the first trials began, the limitations of poor siRNA bioavailability were understood. Therefore, ocular diseases with a separated physiological compartment that allowed easy access and protection from rapid degradation in the circulation were used. However, the knockdown even in these isolated compartments has not been very high and while some benefit was observed in early trials targeting age-related macular degeneration (AMD), it has been hypothesized that the observed benefit may be from activation of toll-like receptors (TLRs) and not target knockdown [146, 147].

While the clinical success of siRNA over the past decade has been disappointing, there is still hope for its therapeutic potential. A better understanding of the limitations of siRNA therapy, including off-target effects, short effect duration, low efficacy, and TLR activation has led to marked overall improvements over the years. New siRNA technologies, including improved siRNA chemical modifications to increase availability and decrease degradability, and development of efficient viral and nonviral delivery systems to increase siRNA delivery to target cells, are currently being investigated in clinical trials with more promising results [145, 148].

Table 2.2. Current siRNA and shRNA Clinical Trials

Drug	Target	Delivery Vehicle	Disease	Company/Sponsor	Phase	Status	Clinicaltrials.gov Identifier	Start Date
Cancers								
Bcr-Abl siRNA	Bcr-Abl	Anionic liposome	CML	U of Duisburg	I	Completed	N/A	2010
FANG vaccine	furin/ TGFß1 TGFß2	Autologous *ex vivo* electroporated GMCSF cells	Solid cancers	Gradalis, Inc.	I	Recruiting	NCT01061840	Dec ’09
			Advanced cancer	Gradalis, Inc.	I	Recruiting	NCT01505153	Feb ’12
			Melanoma	Gradalis, Inc.	II	Recruiting	NCT01453361	Oct ’11
			Ovarian cancer	Gradalis, Inc.	II	Recruiting	NCT01551745	Mar ’12
			Ovarian cancer	Gradalis, Inc.	II	Recruiting	NCT01309230	Feb ’11
			Colon cancer	Gradalis, Inc.	II	Recruiting	NCT01505166	Mar ’12
siRNA-transfected dendritic cells	LMP2 LMP7 MECL1	*Ex vivo* transfected dendritic cells	Melanoma	Duke University	I	Recruiting	NCT00672542	Jan ’08
TKM-080301	PLK1	Liposome (cationic and fusogenic lipids with PEG)	Cancer	Tekmira	I	Recruiting	NCT01262235	Dec ’10
			Primary/secondary liver cancer	NCI	I	Completed	NCT01437007	Aug ’11
ALN-VSP02	KSP VEGF	Liposome (mixture of cationic and fusogenic lipids with PEG)	Liver cancer	Alnylam	I	Completed	NCT00882180	Mar ’09
			Solid tumors	Alnylam	I	Ongoing	NCT01158079	Jul ’10
Atu027	PKN3	lipoplex	Solid tumors	Silence Therapeutics	I	Recruiting	NCT00938574	Jun ’09
CALAA-01	RRM2	cyclodextrin and PEG nanoparticle with transferrin-targeting	Solid tumors	Calando	I	Ongoing	NCT00689065	May ’08
siG12D LODER	KRASG12D	LODER biodegradable polymer matrix	Pancreatic cancer	Silenseed	0/I	Recruiting	NCT01188785	Jan ’11
			Pancreatic cancer	Silenseed	II	Not yet open	NCT01676259	Sep ’12
CEQ508	ß-catenin	shRNA in *E. coli*	Colon cancer	Marina	I	On-hold	N/A	2010
siRNA-EphA2-DOPC	EphA2	Neutral DOPC liposome	Advanced cancers	MD Anderson	I	Not yet open	NCT01591356	Nov ’12

Table 2.2. Continued.

Drug	Target	Delivery Vehicle	Disease	Company/Sponsor	Phase	Status	Clinicaltrials.gov Identifier	Start Date
Ocular disorders								
Bevasiranib	VEGF	Naked siRNA	Wet AMD	Opko Health	I	Completed	NCT00722384	Aug ’04
					II	Completed	NCT00259753	Jul ’05
					III	Terminated	NCT00499590	Aug ’07
					III	Withdrawn	NCT00557791	Nov ’09
			Diabetic macular edema	Opko Health	II	Completed	NCT00306904	Jan ’06
AGN211745 (Sirna-027)	VEGF-R1	Naked siRNA	AMD	Allergan/Sirna	I/II	Competed	NCT00363714	Nov ’04
			AMD	Allergan	II	Terminated	NCT00395057	Jan ’07
PF-04523655	RTP-801	Naked siRNA	Wet AMD	Quark/Pfizer	I	Completed	NCT00725686	Feb ’07
			Diabetic retinopathy	Quark/Pfizer	II	Terminated	NCT00701181	Jun ’08
			Wet AMD	Quark/Pfizer	II	Completed	NCT00713518	Nov ’09
			Diabetic macular edema, retinopathy, choroidal neovascularization	Quark	II	Recruiting	NCT01445899	Feb ’12
QPI-1007	Caspase-2	Naked siRNA	Nonarteritic anterior ischemic optic neuropathy (NAION)	Quark	I	Ongoing	NCT01064505	Feb ’10
SYL040012	Adrenergic receptor ß2	Naked siRNA	Glaucoma, ocular hypertension	Sylentis	I	Completed	NCT00990743	Sep ’09
					I/II	Recruiting	NCT01227291	Oct ’10
SYL1001	TrpV1	Naked siRNA	Dry eye, ocular pain	Sylentis	I	Completed	NCT01438281	Jul ’11
Inhaled formulations								
ExcellairTM	Syk kinase	Unknown	Asthma	ZaBeCor	II	Unknown	N/A	2009
ALN-RSV01	RSV nucleocapsid	Naked siRNA	RSV infection	Alnylam	II	Completed	NCT00496821	Jul ’07
					II	Completed	NCT00658086	Apr ’08
					IIb	Completed	NCT01065935	Feb ’10

Table 2.2. Continued.

Drug	Target	Delivery Vehicle	Disease	Company/Sponsor	Phase	Status	Clinicaltrials.gov Identifier	Start Date
Miscellaneous disorders								
PRO-040201	ApoB	Liposome (mixture of cationic and fusogenic lipids with PEG)	Hypercholest-erolemia	Tekmira	I	Terminated	NCT00927459	Jun ’09
ALN-TTR01	TTR	Liposome (mixture of cationic and fusogenic lipids with PEG)	Transthyretin-mediated amyloidosis	Alnylam	I	Completed	NCT01148953	Jun ’10
I5NP	P53	Naked siRNA	AKI after cardiovascular surgery	Quark	I	Completed	NCT00554359	Aug ’07
			AKI after cardiovascular surgery	Quark	I	Terminated	NCT00683553	May ’08
			Delayed graft function in kidney transplantation	Quark	I/II	Recruiting	NCT00802347	Dec ’08
TD101	Keratin 6aN171K mutant mRNA	Naked siRNA	Pachyonychia congenital	Transderm	Ib	Completed	NCT00716014	Jan ’08
pHIV7-shI-TAR-CCR5RZ treated CD4 cells	HIV Tat/rev, TAR, CCR5	*Ex vivo* lentiviral-transfected autologous T-cells	HIV	City of Hope	0	Teminated	NCT01153646	Apr ’10

CML = chronic myelogenous leukemia; GMCSF = granulocyte macrophage colony stimulating factor; LMP = low molecular mass protein; MECL1 = multicatalytic endopeptidase complex subunit 1; PLK1 = polo-like kinase 1; NCI = National Cancer Institute; KSP = kinesin spindle protein; VEGF = vascular endothelial growth factor; PEG = polyethylene glycol; PKN3 = protein kinase N3; RRM2 = ribonucleotide reductase subunit M2; VEGF-R1 = VEGF receptor 1; TrpV1 = capsaicin receptor; Syk = spleen tyrosine kinase; RSV = respiratory syncytial virus; ApoB = apolipoprotein B; TTR = transthyretin; p53 = tumor protein 53; AKI = acute kidney injury; HIV = human immunodeficiency virus; TAR = HIV trans-activation response element;CCR5 = CC chemokine receptor type 5. All data from www.clinicaltrials.gov, press releases, corporate websites, Vaishnaw *et al.* [144], and Burnett *et al.* [145].

2.8 Gene Delivery and Carriers

Naked DNA and RNA alone are highly inefficient drugs. In order for them to be successfully utilized in research or clinical settings, a carrier must be used or chemical modifications made to overcome the many barriers that prevent uptake of genetic material. In order to successfully introduce genetic material in the form of DNA or RNA to a cell, there are several barriers that must be surmounted. These barriers include: 1) rapid degradation in the circulation or extracellular space; 2) nonselective delivery to nontarget cells; 3) crossing the cell membrane; 4) escape from degradative compartments (i.e., the endosome and lysosome); 5) dissociation of cargo from the carrier; and 6) in the case of DNA, successful nuclear localization of the gene [149, 150].

Several methods for gene delivery which overcome these obstacles are currently available, but most techniques can generally be classified within two classes—viral and nonviral [151-154]. As their name implies, viral methods utilize viruses that have been attenuated to be nonreplicating and nonpathogenic and have been loaded with a gene for delivery. While viral gene vectors have evolved over millions, if not billions, of years to efficiently overcome the above-listed hurdles to transduce cellular organisms, they create safety concerns due to their immunogenicity and the potential for insertional mutagenesis.

In order to circumvent these problems and generate delivery systems that can efficiently and selectively deliver genetic material to target tissues, a great deal of research has been done on developing nonviral methods for gene therapy. Nonviral methods consist of physical methods of transfection and the use of synthetic chemicals—

most commonly cationic lipids and polymers. A comparison of the most common viral and nonviral delivery vectors can be seen in Table 2.3.

2.8.1 Viral Gene Delivery

Viral methods are extremely efficient, but their clinical usefulness is hampered by several major restrictions. Viral delivery is limited by problems with potential insertional mutagenesis [157, 158], difficulty and high expense incurred in large-scale manufacturing and quality control [159, 160], limited DNA cargo capacity, and immunogenicity. In 1999, an 18-year-old patient enrolled in an adenoviral gene therapy clinical trial for ornithine transcarbamylase deficiency experienced a fatal systemic inflammatory response against the adenoviral vector [161]. Later in 2000, a French group reported successful treatment of a group of children suffering from X-linked severe combined immunodeficiency (SCID-X1). However, in 2002, it was reported that two of the ten children in the trial had developed a form of leukemia [162]. Further analysis of the children led to the discovery that the retrovirus vector had integrated near a proto-oncogene promoter, causing the development of leukemia [163].

2.8.1.1 Adenoviral Gene Therapy

Adenoviruses were one of the first viral vector types used for gene therapy applications. Adenoviruses are a nonenveloped, double-stranded DNA-type virus with an approximately 36 kb genome encoding over 50 polypeptides. The adenovirus has a capacity of approximately 8.5 kb for foreign DNA, which is sufficient to accommodate most therapeutic genes. Some of the benefits of adenovirus vectors include their high efficiency, stability, nonintegrative nature, ability to infect both dividing and quiescent cells, and the lack of viral sequences in the progeny of dividing cells [164, 165].

Table 2.3. Relative Comparison of Gene Transfer Methods

	Vector	Gene Transfer Efficiency	Immunogenicity	Duration of Expression	Loading Capacity	Ease of Manufacturing	Safety Concerns
Viral	Adenovirus	++++	++++	+++	++	+	
	Lentivirus	+++	+++	+++	++	+	HIV origins
	Retrovirus	++++	++	++++	++	+	Insertional mutagenesis
	Adeno-associated virus	++++	++	+++	+	+	Insertional mutagenesis
Nonviral	Naked	+	++	+	++++	++++	
	Liposome	++	++	++	++++	+++	
	Polymer	++	+	++	++++	++++	

References [155, 156].

However, most humans have been exposed to several adenoviral serotypes and have formed antibodies against the virus. As a result, when adenovirus vectors are administered to humans, almost 90% of the virus is eliminated within 24 hours. In addition to the rapid immune system clearance of adenoviral vectors, the capsid coat on the vectors has been known to stimulate acute and dangerous immune responses [161, 166, 167]. The last disadvantage of using adenoviral vectors is the short duration of gene expression achieved in transfected cells. Typical expression times for adenoviral-transfected cells are between 1–8 weeks [168, 169].

2.8.1.2 Retroviral Gene Therapy

Retroviruses are small RNA viruses (7–11 kb genome) that replicate via a DNA intermediate and were also some of the first viral constructs applied towards gene therapy [170]. While the total genome is much smaller than the adenovirus genome, due to the simplistic nature of the virus, a roughly 8 kb therapeutic gene can be delivered without compromising the function of the virus [171]. The major benefit of retrovirus use is its ability to effect long-term, stable expression of therapeutic genes due to host chromosome integration.

Limitations of the use of retroviral vectors include: relatively low transfection efficiency compared to other viruses, low viral stability, the inability to transduce nondividing cell types, and of course the risk of insertional mutagenesis [172].

2.8.1.3 Adeno-associated Viral Gene Therapy

The adeno-associated viruses (AAV) are human parvoviruses that normally require the help of another virus such as adenovirus to infect cells. They possess a small 4.7 kb genome of single-stranded DNA, which is converted to double-stranded DNA

after infection. The AAV can chromosomally integrate but shows less potential for insertional mutagenesis due to its preferential insertion to a specific site on the human chromosome 19 [173, 174]. The AAV family is one of the most actively investigated viral vectors currently due to the multiple advantages of the system. AAV vectors produce long-term expression, can efficiently transduce a wide variety of host cells with tissue-specific targeting capabilities, are a nonpathogenic virus, and they evoke a minimal immune response [175-177].

Several of the major limitations of AAV vectors include their small transgene packaging capacity, the still present risk of insertional mutagenesis, and difficulty in producing high viral titers sufficient for clinical trials and large-scale manufacturing [178, 179].

2.8.1.4 Other Viruses

Other viruses that are commonly used for gene therapy include the lentiviruses, and the herpes simplex viruses. Lentivirus vectors are useful for their ability to transfect nondividing cell populations and maintain stable gene expression for extended periods [180]. Vectors based on herpes simplex contain a large genome of 152 kb of double-stranded RNA, allowing for the insertion of large single transgenes or even multiple therapeutic sequences.

Less common viral vectors include plus-strand RNA viruses such as Sindbis virus, hepatitis A, and polio. These viruses are more commonly investigated for viral immunization strategies since they produce high, yet transient, gene expression to evoke an immune response against the transduced cells.

2.8.2 Nonviral Delivery Systems

The nonviral delivery systems consist of methods such as injection of naked DNA [181]; delivery by gene gun [182]; by electroporation [183]; by ultrasound [184]; and by transfer to the highly perfused organs by hydrodynamic delivery [185, 186]. While these methods are capable of inserting genetic material into cells, they are neither practical nor efficient delivery systems. To overcome the limitations of the physical approaches above, chemicals such as lipids and polymers are used as quasi-viral mimetics. These chemicals allow for DNA protection from nuclease activity, relatively efficient uptake by cells, and tissue specificity when conjugated with a targeting motif.

2.8.2.1 Naked Polynucleotide Delivery

Some of the first methods used to transfer genetic materials to living tissue utilized unmodified DNA. Delivery of naked nucleotides without the assistance of any physical system is extremely inefficient due to the hydrophilic nature of DNA, its high molecular weight, and its negatively charged phosphate backbone. Thus, the dense negative charges are repulsed by the negatively charged cell membrane. However, delivery of naked nucleic acids has seen some clinical application in closed organ systems such as the eye, treating age-related macular degeneration (AMD) [187, 188].

2.8.2.2 Electroporation Gene Delivery

Electroporation uses an electric field to temporarily increase permeability through the cell membrane. The electric pulses generated by this technique generate transient pores that allow polynucleotides to pass through. This technique has been used to effect gene transfer both *in vitro* and *in vivo* since 1982, and 1991, respectively [189, 190]. To perform *in vivo* electroporation, the DNA is injected first to the target area then an

electric field with varied pulse duration, and voltage is applied from two electrodes. This technique can achieve transfection efficiencies similar to those seen from viruses [191], but is best suited to models where localized gene transfer is desirable, the target is accessible by electrodes, and where electric pulses will not disrupt normal organ function (e.g., the heart).

2.8.2.3 Ultrasound Gene Delivery

Ultrasound-mediated delivery of polynucleotides functions in a similar manner to electroporation, but uses sound waves instead of electrical pulses to induce cell membrane permeability [192]. Recent advances have combined ultrasound gene therapy with microbubbles to increase transfer efficiencies [193]. The technique employs gas-filled microbubbles stabilized with lipids, polymers, or proteins which stabilize the bubbles to allow for systemic administration. The target site is then exposed to ultrasound and when the microbubbles pass through the sonic cone, they oscillate, and cavitate, releasing their cargo at a high velocity and disrupting cell membranes. Ultrasonic gene delivery systems are more versatile and practical than their electroporation counterparts, but still require a solid tissue target site that is accessible via probe [194].

2.8.2.4 Hydrodynamic Gene Delivery

Hydrodynamic gene transfer was first reported *in vivo* in 1999 [185]. Gene transfer by this method is achieved by injecting a very large volume of a DNA-containing solution into the tail vein of small rodents. The process of injecting a large volume (usually 8–12% of body weight) over a short period of time (3–5 seconds) causes the endothelial lining of the cardiovascular system to leak, allowing the DNA to penetrate into the tissue [195]. Hydrodynamic gene transfer allows for fast and easy transfection of

highly perfused organs such as the liver, kidney, lungs, and heart, but is limited to rodent models. The process of scaling this technique up to the volumes required to achieve the same effect in humans is not feasible. However, advances using catheters to perform local hydrodynamic gene transfer have been made, allowing for this technique to be used in large animals [196].

2.8.2.5 Gene Gun Delivery

Finally, the last physical nonviral gene delivery method commonly utilized is gene transfer via gene gun. The gene gun system was first developed and used to transfect plants in 1987 [197]. Genetic material is coated onto metal particles such as gold, silver, or tungsten and the particles are delivered at a high velocity, powered by a compressed gas such as helium, into the target. This technique has been successfully used to deliver DNA to dermis, muscle, and tumor tissues and has even been used in five clinical trials on gene therapy to date [77].

2.8.3 Lipid-mediated Gene Delivery

Transfer of genetic material using lipids was first accomplished in 1987 by Felgner *et al.* [198]. Of the nonviral methods, transfection using cationic lipids (i.e., lipofection) is the most popular and extensively studied, with thousands of publications examining hundreds of distinct variations of the basic shared lipid structure [199]. Cationic lipids used for gene delivery share three common features: a positively charged head group, a hydrophobic tail, and a linker region that joins the two regions together (Figure 2.3).

Cationic lipids function by condensing polynucleotides through electrostatic interaction between the positively charged lipid head and the negatively charged

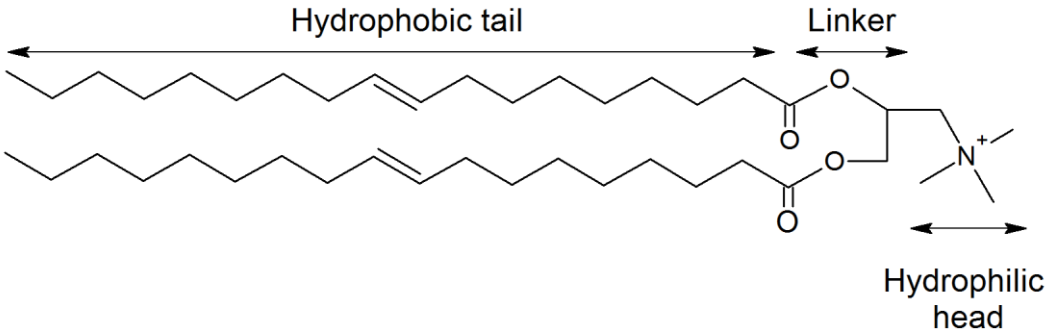

Figure 2.3. The three domains of cationic lipids used in gene delivery: a hydrophobic tail and a hydrophilic head, joined by a linker. The above structure is that of 1,2-dioleoyloxy-3-trimethylammonium propane (DOTAP), a commonly used cationic lipid for gene delivery.

phosphodiester backbone of the DNA or RNA. The resultant tightly bound complex is termed a lipoplex and serves to protect the genetic cargo while aiding in cell penetration. Transfection efficiency and toxicity depend on a myriad of customizable factors, such as the composition of each of the hydrophilic and hydrophobic portions, and the DNA/lipid ratio.

The most effective lipoplex formulations typically have a residual positive charge on the complex. This allows for association with cell membranes through interaction with the negatively charged membrane surface and causes the lipoplex to be endocytosed by the cell. In order to escape the endosomal compartment, it is hypothesized that the cationic lipids interact with anionic phospholipids in the wall of the endosome, facilitating concurrent disruption of the endosomal wall and dissociation of the polynucleotides from the lipids, releasing the cargo to the cell interior [200].

Cationic lipoplexes are the most commonly used nonviral chemical transfection system in human trials. To date, they have been used in 111 clinical trials, composing 5.9% of all gene therapy trials completed [77]. Limitations of cationic lipids for human therapy include the immune response they can elicit, acute toxicity, and the short duration of expression they mediate. Since cationic lipid lipoplexes form relatively loose complexes with DNA [201] with some externally exposed cargo [202], the patient's immune system can recognize unmethylated CpG sequences from the plasmid DNA and mount a TLR9-mediated immune response increasing cytokine production [203]. Conjugation of polyethylene glycol (PEG) to cationic lipids has been shown to reduce both acute toxicity and ameliorate the immune response, but reduces transfection efficiency [204].

2.8.4 Polymer Gene Delivery

The other nonviral chemical method utilizes cationic polymers to mediate transfection and protect polynucleotides. Polycations are a particularly useful class of polymer for gene therapy. Similar to cationic lipids, these polymers form complexes with genetic material through electrostatic interactions between positively charged groups (usually amines) on the polymer and negatively charged phosphates on the nucleic acid backbone.

These polymer:DNA complexes (termed polyplexes) mediate gene delivery primarily through bulk endocytosis into the cell; however, targeting moieties can be attached to increase cell specificity by receptor-mediated endocytosis. Once inside the endosomal compartment, most polyplexes employ an entirely different escape mechanism from the lipoplex escape mechanism, termed the "proton sponge effect" described below. An overview of polyplex entry mechanisms, endosomal escape, and DNA expression or siRNA knockdown can be seen in Figure 2.4.

2.8.4.1 Polyethyleneimine Gene Delivery

The polycation polyethyleneimine (PEI) was first shown to effect transfection of cells in 1995 by Boussif *et al*. [205] and is still used as a comparative benchmark in many experiments today. As a polymer, PEI demonstrated the unique ability to avoid lysosomal degradation by escaping from the endosome within cells. PEI can be synthesized as both a linear or branched polycationic polymer with primary, secondary, and tertiary amine groups in the ratio 1:2:1. The array of amine groups with their varying pK_a values gives the polymer the ability to buffer over a wide range of pH values. At the physiological blood pH of 7.4, the amine groups in PEI are approximately 20% protonated, but when

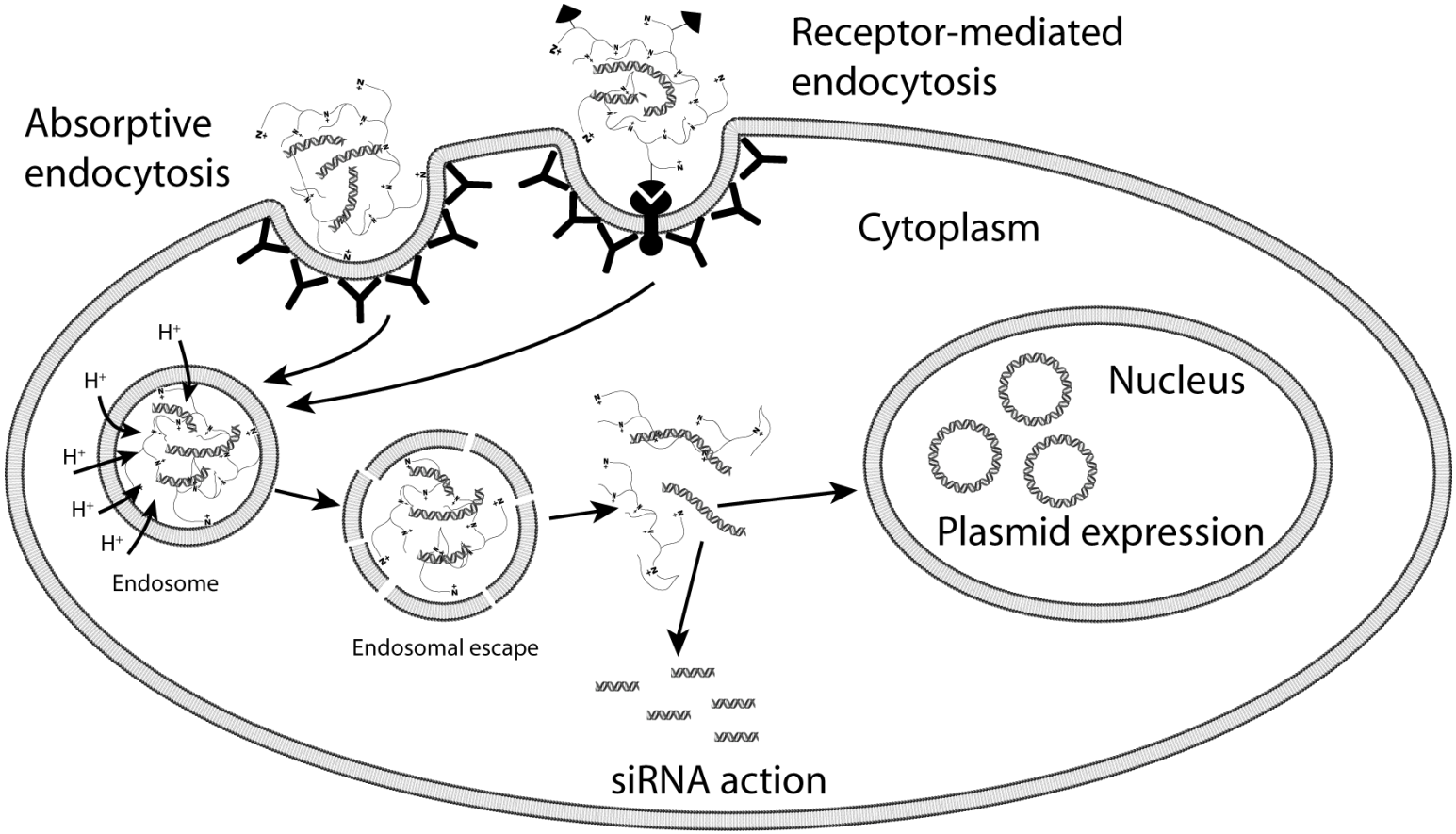

Figure 2.4. Overview of polyplex internalization, endosomal escape, DNA expression, and siRNA-mediated knockdown.

lowered to pH 5, such as that seen in the endosome, the degree of protonation more than doubles to 45% [206]. The "proton sponge effect" postulates that as protons are pumped into the endosome to lower the pH and aid in degradation, PEI and other cationic polymers buffer against the change, causing more protons and chloride counterions to be pumped in to lower the pH. Due to the much higher ionic strength within the endosome, water diffuses across the endosomal membrane via osmosis, causing the endosome to swell and rupture [206, 207]. The high concentration of counterions and the increased internal polymer electrostatic repulsions caused by the protonated amines is thought to help decomplex the polymer from the DNA/RNA cargo, releasing it to the cytoplasm [208, 209].

PEI comes in two common forms: branched and linear (Figure 2.5). Branched PEI (bPEI) is the most commonly used form for gene delivery due to its higher amine density and its wider buffering range. While the positive charge imbued by the amine groups is necessary for its DNA/RNA-complexation and endosomal-escaping functions, it also contributes to a high degree of toxicity seen when using PEI *in vivo*. The charged nature of the polymer leads to interaction with serum proteins, causing aggregation, and leads to unfavorable cell membrane destabilization [210]. Additionally, a great deal of PEI toxicity is due to its nondegradable nature [211].

Strategies to improve upon PEI transfection efficiencies while decreasing cellular toxicity include: synthesis of a novel acid-labile PEI (Figure 2.6) [212], conjugation with PEG to reduce toxicity [213], and linking low-molecular PEI via degradable or reducible bonds [214, 215]. Early work performed in our lab investigated conjugation of low-molecular weight PEI, which has traditionally demonstrated improved toxicity compared

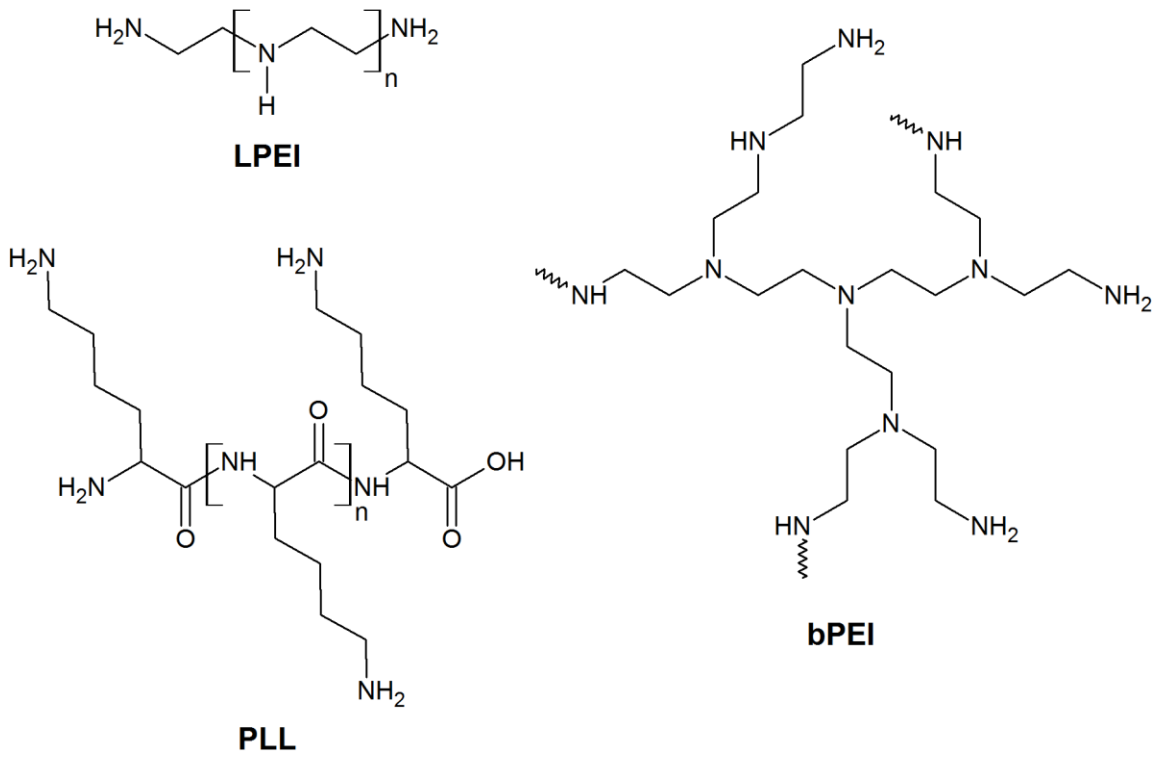

Figure 2.5. The chemical structures of the prototypical cationic polymers linear polyethyleneimine (LPEI), branched PEI (bPEI), and poly-L-lysine (PLL).

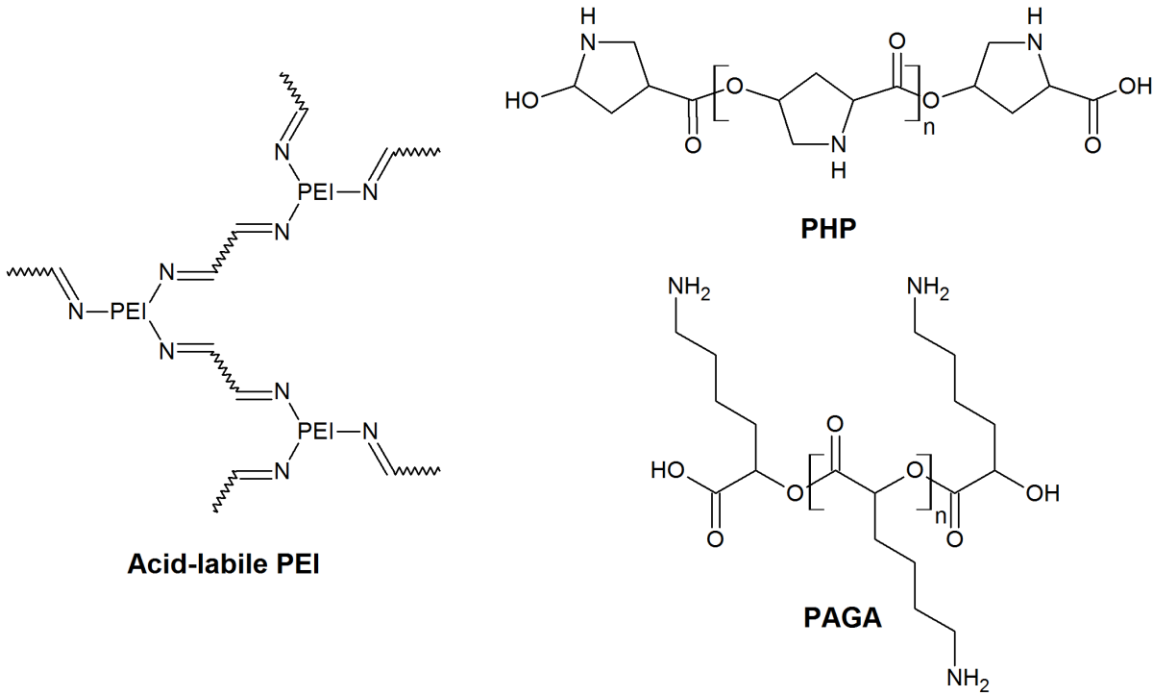

Figure 2.6. Chemical structures of the degradable cationic polymers acid-labile polyethyleneimine (PEI), poly(4-hydroxyl-L-proline ester) (PHP), and poly[α-(4-aminobutyl)-L-glycolic acid] (PAGA). Adapted from Kim *et al.* [212].

to high molecular weight but severely decreased transfection efficiency, with cholesterol to form a water-soluble lipoprotein [216].

2.8.4.2 Poly-L-Lysine Gene Delivery

Another common cationic polymer used for gene delivery is poly-L-lysine (PLL) (Figure 2.5). PLL acts as a cationic gene carrier due to its large number of ε-amino groups, allowing for electrostatic condensation and complexation of polynucleotides. This polymer was one of the first cationic polymers observed to demonstrate gene transfection capabilities [217]. However, its transfection efficiency is highly variable between cell types, and typically is not as high as that seen with other cationic polymers like PEI. Additionally, because the amine groups on PLL have much higher pK_a values than other cationic polymers, it does not efficiently escape the endosomal compartment. To increase transfection efficiency with PLL, chloroquine (an endosomolytic agent) is often delivered with PLL [218, 219]. Unfortunately, the addition of chloroquine increases toxicity and is not feasible for *in vivo* applications.

2.8.4.3 Degradable Polymers for Gene Delivery

One of the major limitations of the early generation of cationic polymers was their nondegradability. Once the polymer carrier has penetrated and delivered its nucleic acid cargo inside of a cell, the inability of the cell to clear the polymer carrier results in delayed toxicity (7–9 hours after transfection) [211, 220]. To overcome this limitation in the early cationic polymers, carriers with degradable linkers were developed to allow the cell to break down the high molecular weight polymers into smaller fragments, aiding in their clearance and reducing their toxicity. Some of the major chemical moieties used to

allow for degradation of polymers include: hydrolyzable ester linkages, acid-labile imine linkers, and bioreducible disulfide linkages.

The first degradable polymer developed for gene delivery was the polyester agent poly(4-hydroxy-L-proline ester) (PHP) (Figure 2.6). The polymer is degradable due the incorporation of hydrolyzable ester bonds as the monomer linker groups. The rate of hydrolysis of PHP is enhanced by the presence of the amine groups and the polymer is readily degradable, hydrolyzing in less than 24 hours [221]. Another early biodegradable polymer for gene delivery, poly[α-(4-aminobutyl)-L-glycolic acid] (PAGA) (Figure 2.6), was developed in this lab and was shown to a safe and nontoxic alternative to polymers such as PLL [222].

While polymers incorporating ester or other hydrolyzable bonds reduce delayed toxicity due to intracellular accumulation of polycation carriers and their resultant disruption of cellular function, the nonspecific nature of hydrolyzable bond degradation leads to limited circulatory and extracellular *in vivo* half-lives. In order to develop polymers with the ideal characteristics of resistance to degradation in the extracellular space, but which degrade inside the cell, releasing their cargo and allowing for clearance, polycationic polymers with reducible disulfide bonds were developed.

2.8.4.4 Bioreducible Polymers for Gene Delivery

Disulfide bonds are an attractive linker for polymeric gene carriers due to their stability in extracellular environments, but their susceptibility to reduction in the intracellular, particularly cytoplasmic, space through thiol-disulfide exchange [223, 224]. Many proteins, especially those which are secreted, form disulfide bonds between

cysteine residues as a way to lend stability to the protein, aid in protein folding, and maintain the folded structure.

Exposed disulfide bonds are particularly susceptible to reduction in the cytoplasm due to the high concentration of the thiol-containing molecule glutathione. The cytoplasm is a highly reductive environment, owing to a high concentration of glutathione (0.5–10 mM intracellular versus 15 μM extracellular) [225-227], and because the cytoplasm maintains a ratio of reduced glutathione/oxidized glutathione disulfide (GSH/GSSG) of up to 100/1 [228]. The reduced glutathione pool is maintained through the action of the NADH-dependent flavoenzyme glutathione reductase to convert GSSG back to the reduced GSH form to maintain the reductive gradient. Glutathione stores are also maintained by synthesis of new glutathione from glutamate, cysteine, and glycine by γ-glutamylsynthetase followed by glutathione synthetase. When GSH levels are high, glutathione reduces disulfide bonds via thiol-disulfide exchange. In this reaction, the thiolate anion on GSH attacks a sulfur atom contained in a disulfide bond. The primary disulfide bond is broken and a new disulfide bond between glutathione and the attacked sulfur group is formed [223].

Due to the large difference between intracellular and extracellular glutathione levels, disulfide bonds have proven to be excellent linkers in gene delivery polymers, imbuing stability in the circulation and extracellular milieu while rapidly degrading once the polymer is internalized to the cytoplasm. This results in increased transfection efficiencies, with decreased toxicity and cellular accumulation.

The first disulfide-containing polymer used for gene delivery was a disulfide-linked PEI [229]. Gosselin *et al.* found that their disulfide-crosslinked PEI significantly

increased transfection efficiency in Chinese hamster ovary cells compared to the nonreducible parent low molecular weight PEI. The levels of transfection were almost equivalent to that seen with 25 kDa bPEI. Other groups investigated different disulfide cross-linkers to form bioreducible PEI and also found transfection efficiencies similar to 25 kDa bPEI with decreased or very similar cytotoxicities [215, 230].

Other classes of bioreducible polymers beyond disulfide-linked PEI have also been synthesized and include disulfide poly(amido amine)s (SS-PAAs), and poly(ß-amino ester)s (Figure 2.7). SS-PAAs employ Michael addition-type reactions between primary amines and cystamine bisacrylamide. Some of the first polymers synthesized from this family demonstrated that they can condense nucleic acids to positively charged and nano-sized polyplexes (+20 mV ζ-potential and <200 nm, respectively) [231, 232]. These SS-PAAs also demonstrated greater buffering capabilities than even the amine-rich PEI polymers, aiding in escape from the endosomal compartment via the proton sponge effect. SS-PAAs are also capable of highly efficient transfection even in the presence of serum with little cytotoxicity even at high polymer:nucleic acid weight ratios [232]. Finally, many SS-PAAs contain pendant amine groups that are amenable to modification, allowing grafting of targeting moieties to the polymer.

2.8.5 Targeted Polymer Gene Carriers

In order to enhance the efficiency and especially specificity of polymer gene carriers for target cells, targeting groups can be attached to the carrier. Nontargeting polymer gene carriers interact nonspecifically with cells through interaction with negatively charged surface molecules like glycosaminoglycans and enter the cell via adsorptive endocytosis [233, 234]. Also, when given systemically, charged polyplexes

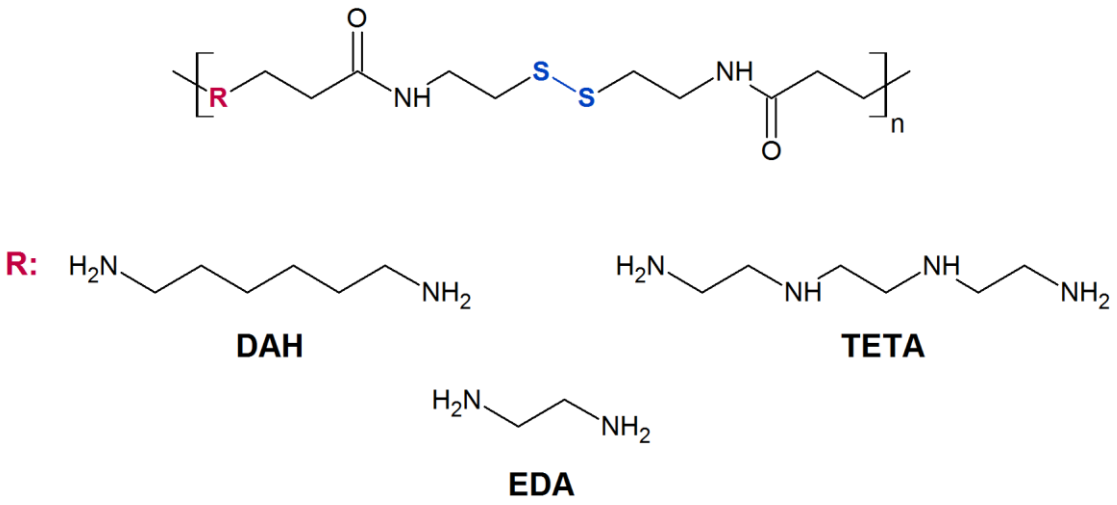

Figure 2.7. Bioreducible poly(amido amines) based on cystamine bisacrylamide. DAH = diaminohexane, TETA = triethylenetetramine, EDA = ethylene diamine

are bound by serum proteins, resulting in rapid clearance by the reticuloendothelial system (RES) [235]. Conjugation of shielding moieties such as PEG have been shown to increase circulatory half-life, but decrease transfection efficiency by interfering with cell surface interaction, and do not increase target cell specificity [236, 237].

To allow polyplexes to selectively transfect specific cell types, a variety of functional groups and targeting moieties can be conjugated to the polymer, including peptides, sugars, antibodies/antibody fragments, and proteins [238]. The specific interaction of these targeting groups with cell membrane components leads to receptor-mediated endocytosis, allowing polyplex entry to the cell [239]. By combining targeting ligand polymer conjugation to increase target cell uptake with PEG shielding to reduce nonspecific cellular interactions, polymers with high tissue specificity and transfection efficiency can be synthesized.

2.9 Cell Therapy for Cardiovascular Disease

With the surge of interest in stem cells as a therapeutic strategy in the late 1990s, it was not long before attempts were made to apply stem cell therapy to MI. Since the loss of viable tissue in the ischemic region after myocardial infarction has long been known to decrease the functionality of the myocardium, the potential for stem cells to repopulate the heart and form contractile cardiomyocytes was quickly investigated [240, 241].

A variety of cell sources have been used in studies of cell therapy for ischemic heart disease, but they can be classified as allogeneic (from another donor) or autologous (from the patient). The earliest studies evaluating stem cells for cardiac repair used allogeneic stem cells such as embryonic stem cells, which were also one of the first stem

cell populations discovered. As the research around stem cell classes advanced, more populations of stem cells were discovered and evaluated for cardiac repair (Table 2.4).

2.9.1 Mesenchymal Stem Cells

Adult mesenchymal stem cells are most commonly derived from bone marrow or adipose tissue. In the area of cardiac cell therapy, however, bone marrow-derived mesenchymal stem cells have been the most thoroughly investigated. Mesenchymal stem cells are multipotent in nature, differentiating to cardiomyocytes, adipocytes, osteoblasts, chondrocytes, and many other cell types, though not as many as pluripotent stem cells [243, 244].

One of the reasons for the intense interest of using mesenchymal and other bone marrow-derived stem cells for cardiac therapy is the ease of obtaining the cells from bone marrow aspirates. Stem cells can rapidly be isolated from bone marrow and quickly expanded to a sufficient number to allow for autologous donation. Though autologous therapy is relatively simple with this stem cell lineage, mesenchymal stem cells are less immunogenic than other cell types, making allogeneic cell therapy a possibility [245]. Allogeneic therapy eliminates or greatly reduces the delay necessary when autologous cells are isolated, expanded, and prepared for implantation.

Mesenchymal stem cells, while capable of differentiating to cardiomyocytes, appear to do so only at a very low rate when injected *in vivo* [245, 246]. While this limits the repopulation of the myocardium with functional cardiomyocytes, implanted mesenchymal stem cells have been shown to have a positive effect on resident cells through the secretion of paracrine growth factors [243, 247].

Table 2.4 Cell Types Investigated for Cardiac Repair

Allogenic Stem Cells	Autologous Stem Cells
Embryonic stem cells	Cardiac stem cells
Fetal cardiomyocytes	Adipose-derived stem cells
Human umbilical cord-derived stem cells	Skeletal myoblasts
	Bone marrow-derived stem cells
	Mononuclear/CD34+ fraction
	Mesenchymal stem cells
	Endothelial progenitor cells
	Multipotent adult progenitor cells
	Induced pluripotent stem cells

Adapted from Mozid *et al.* [242].

2.9.2 Cardiac Stem Cells

The heart has long been viewed as a static organ, with little to no cardiomyocyte turnover. Recently, however, this view has been disproven with the discovery of resident populations of cardiac stem cells (CSCs) within the myocardium [248]. While these cells make up less than 2% of the total cells within the myocardium, they have been shown to contribute to the growth of new cardiomyocytes [249, 250] and coronary vessels [249], especially during pathological states [248, 251]. Importantly, these resident stem cells have demonstrated they play a role in regeneration of cardiomyocytes and vascular cells after myocardial infarction [249].

Despite their low population levels within the myocardium, CSCs can be harvested from patients, proliferated *ex vivo*, and used for autologous implantation [252]. At least two clinical trials evaluating CSCs in human patients suffering from ischemic cardiomyopathy [253] and MI [254] have been completed with encouraging results. Cells were delivered by intracoronary infusion and in both trials provided improvement in infarct size and LV function.

While CSCs have shown promising results thus far, because the field is still nascent, they are still one of the least studied stem cells for cardiac repair. Little is known about their long-term fate in the heart and if the positive results seen in short-term studies will vary over to the long term.

2.9.3 Embryonic Stem Cells

Human embryonic stem cells were first isolated in 1998 and are a pluripotent stem cell capable of differentiating into almost all cell lineages [255]. Importantly for use in cardiac cell therapy, embryonic stem cells have been shown to differentiate into

contracting cardiomyocytes [256, 257]. The use of embryonic stem cells is still the source of passionate ethical debate due to their source with the resulting regulatory restrictions limiting their adoption.

While embryonic stem cells have often been considered the gold standard source for stem cell therapy, their use is not without limitations. Since embryonic stem cells are derived from allogenic sources, they can trigger immunogenicity in the recipient [258]. Additionally, embryonic stem cells have shown predisposition to form teratomas when they are injected *in vivo* [259]. Finally, while embryonic stem cells are known to differentiate to cardiomyocytes, there is some debate whether the stem cells implant with sufficient structural and electromechanical efficiency to contribute to functional recovery of the myocardium [260].

2.9.4 Skeletal Myoblasts

Skeletal myoblasts are not true stem cells as they are limited in their ability to differentiate past a myocyte fate. They are derived from skeletal muscle satellite cells that normally are located under the basal membrane in a quiescent state [261]. When injury occurs, the satellite cells mobilize, proliferate, and fuse to existing muscle cells in order to regenerate muscle tissue. Skeletal myoblasts are satellite cells that are in the process of proliferating but have not yet fused with skeletal myocytes.

Skeletal myoblasts were one of the first cell populations considered for cardiac repair because of several clinically attractive attributes they possess. Some of these attributes that make them an ideal cell source for cardiac cell therapy include: a high resistance to hypoxia [262]; ease of isolation [242, 263]; rapid expansion capabilities (a small biopsy can provide over one billion cells in a 2–3 week time period and the process

can be automated) [264]; and finally, since they are easily derived from an autologous origin, they do not provoke an immune response [265]. Additionally, the limited differentiation capabilities of skeletal myoblasts may be considered a limitation as they do not directly transdifferentiate to cardiomyocytes [266], but it is also a benefit since there is no risk of teratoma formation.

Even though skeletal myoblasts do not directly differentiate to cardiomyocytes, experimental studies in both small and large animal studies have shown they can be successfully implanted to ischemic hearts to provide functional left ventricular benefit [267-272].

Early uncontrolled human trials evaluating the therapeutic benefit of skeletal myoblast implantation in chronic heart failure patients showed promising results in the form of improved global and regional contractility, and cell viability [273-276]. However, subsequent expanded and controlled human clinical trials have produced more mixed results. The myoblast autologous grafting in ischemic cardiomyopathy (MAGIC) trial was a multicenter, controlled, randomized, and double-blinded Phase II trial evaluating autologous skeletal myoblasts. Cells were expanded *ex vivo* for 3 weeks then implanted intramyocardially to the ischemic border zone during bypass surgery. Unfortunately, in this trial, there was no significant improvement in the primary endpoints of global and regional LV function [277]. The longest trial of the impact of skeletal myoblast implantation for cardiac repair comes from Dib *et al.* In a nonrandomized, uncontrolled Phase I trial, patients showed improvements in LV ejection fraction and myocardial viability with no observed adverse consequences of skeletal myoblast therapy 4 years after implantation [278, 279]. Additionally, histological

analysis of implanted skeletal myoblasts in humans has shown that the cells form striated myotubes in the scar area and engraft in-line with endogenous cardiomyocytes [278, 280].

There was initially some concern as implantation of skeletal myoblasts to the heart was reported to increase the risk of arrhythmias [273, 275, 279, 280]. However, the MAGIC trial did not observe any significant increase in arrhythmias in patients receiving skeletal myoblasts but did note a trend toward significance [277]. In response to the proarrythmogenic concerns of skeletal myoblasts, Chachques *et al.* hypothesized that the arrythmogenicity of the cells was due to an inflammatory and antigenic response against the fetal bovine serum used to expand the isolated cells. In a study to test this hypothesis, isolated cells were expanded using serum derived from the donor. This study detected no incidence of arrhythmias over a 1–2 year period [281].

Our lab has demonstrated previously that primary skeletal myoblasts transfected with a human isoform of $VEGF_{165}$ express and secrete high levels of VEGF for up to one week [282] and that these cells promote angiogenesis *in vivo* as reported in Chapter 3 of this dissertation [283].

2.9.5 Induced Pluripotent Stem Cells

In light of the recent awarding of the 2012 Nobel Prize in Physiology or Medicine jointly to John B. Gurdon and Shinya Yamanaka for the discovery that differentiated cells can be reprogrammed to become pluripotent stem cells [284, 285], a brief overview of recent advances applying this technology to MI is warranted. Induced pluripotent stem cells (iPSCs) are still most commonly derived from a fibroblast cell source, which can be harvested from an autologous skin biopsy. Once dedifferentiated to a pluripotent state,

iPSCs can be differentiated to a cardiomyocyte fate [286, 287]. Murine and porcine studies have shown that iPSCs administered to the heart improve cardiac function and attenuate LV remodeling [288, 289].

While the investigation of iPSC use for myocardial repair is still in its infant stages, they have great potential for cardiovascular applications. iPSCs can be generated from donor biopsies and have excellent differentiation capabilities. However, limitations include rapid teratoma formation and the time required (over 30 days) to generate replicating iPSCs from fibroblasts.

2.10 Therapeutic Angiogenesis

Therapeutic angiogenesis refers to the treatment strategy of establishing new vasculature to cells and tissues that are not adequately served by the circulatory system [290]. Over the years, more clinical success in blocking angiogenesis in the cases of cancer and ocular diseases have been achieved, but a great deal of research is being performed investigating the potential benefit of establishing blood supply to ischemic tissue. The formation of new vessels, whether arterial or venous in nature, is a complex physiological process and is mediated by several large families of proteins that promote directed vessel growth and vessel maturation. Some of the major families with therapeutic applications include the VEGF, PDGF, and FGF families.

2.10.1 VEGF

The most popular family of angiogenic factors for establishing new blood vessels is the vascular endothelial growth factor (VEGF) family. The mammalian VEGF family consists of 7 factors, VEGF-A, -B, -C, -D, -E, -F, and placental growth factor (PIGF). All members of the VEGF family produce their action by interacting with the tyrosine kinase

receptors VEGFR-1/Flt1, VEGFR-2/Flk1/KDR, and VEGFR-3/Flt2. These receptors are found in high abundance on the surface of endothelial cells. VEGF-A is the most active family member and stimulates vessel growth by signaling through VEGFR-2 [291]. VEGF-A is known to be one of the most important angiogenic forms of VEGF and VEGF-A deficiency on even one allele is embryonically lethal, showing severely abnormal blood vessel development [292]. VEGF-A has five isoforms containing 121, 145, 165, 189, or 206 amino acids. Of the five isoforms, $VEGF_{165}$ is the most promising candidate for therapeutic use due to its ability to create the necessary growth factor gradients needed for efficient and functional vessel growth, and because it is 100× more potent than $VEGF_{121}$ [293].

$VEGF_{165}$ acts through interaction with the VEGFR-1 and VEGFR-2 receptors to stimulate endothelial cell growth and vessel sprouting. Endothelial tip cells sense the levels of VEGF-A and rapidly guide capillary migration towards the source of VEGF-A expression [294].

2.10.2 Other Angiogenic Factors

Two additional proangiogenic factors investigated for therapeutic vessel growth are platelet-derived growth factor (PDGF), and fibroblast growth factor (FGF). The PDGF family plays an important role in angiogenesis but aids more in the maturation of vessels, allowing them to function properly than in their initial formation [295]. The PDGF growth factors help recruit pericytes to budding and growing vessels [296, 297]. Without proper pericyte recruitment, the formed vessels are immature, leaky, display a high degree of tortuosity, decreased perfusion, and do not always remain viable after angiogenic therapy has ceased [298, 299]. Due to the important role PDGF plays in

producing highly functional vessels, PDGF therapy is often paired with VEGF therapy, combining the potency of VEGF at stimulating rapid vessel formation, with PDGF to convert the newly formed vessels into stable and mature vessels [300, 301].

FGF is another family of angiogenic proteins with 23 members and similar function as the VEGF family. The FGF proteins promote angiogenesis by interacting with 4 unique cell membrane-bound tyrosine kinase receptors [302]. Unlike VEGF, FGF receptors are expressed on many different cell types, including smooth muscle cells and fibroblasts, and can act on these cells causing them to secrete additional angiogenic factors [303]. Heart studies have shown that FGF signaling induces hedgehog, angiopoietin-2 (ANG-2), and VEGF-B release, and aids in supporting long-term vascular integrity [304]. Initial testing of FGF in the Angiogenic Gene Therapy (AGENT1) trial showed improved exercise tolerability in patients after 4 weeks [305]. However, the followup study in the AGENT 3/4 trial was prematurely interrupted as the study was not going to be able to reach the primary end point [306].

2.11 References

[1] V.L. Roger, A.S. Go, D.M. Lloyd-Jones, E.J. Benjamin, J.D. Berry, W.B. Borden, D.M. Bravata, S. Dai, E.S. Ford, C.S. Fox, H.J. Fullerton, C. Gillespie, S.M. Hailpern, J.A. Heit, V.J. Howard, B.M. Kissela, S.J. Kittner, D.T. Lackland, J.H. Lichtman, L.D. Lisabeth, D.M. Makuc, G.M. Marcus, A. Marelli, D.B. Matchar, C.S. Moy, D. Mozaffarian, M.E. Mussolino, G. Nichol, N.P. Paynter, E.Z. Soliman, P.D. Sorlie, N. Sotoodehnia, T.N. Turan, S.S. Virani, N.D. Wong, D. Woo, M.B. Turner, Heart disease and stroke statistics--2012 update: a report from the American Heart Association, Circulation, 125 (2012) e2-e220.

[2] E. Palojoki, A. Saraste, A. Eriksson, K. Pulkki, M. Kallajoki, L.M. Voipio-Pulkki, I. Tikkanen, Cardiomyocyte apoptosis and ventricular remodeling after myocardial infarction in rats, Am. J. Physiol. Heart Circ. Physiol., 280 (2001) H2726-2731.

[3] S.R. Tiyyagura, S.P. Pinney, Left ventricular remodeling after myocardial infarction: past, present, and future, Mt. Sinai J. Med., 73 (2006) 840-851.

[4] R.G. McKay, M.A. Pfeffer, R.C. Pasternak, J.E. Markis, P.C. Come, S. Nakao, J.D. Alderman, J.J. Ferguson, R.D. Safian, W. Grossman, Left ventricular remodeling after myocardial infarction: a corollary to infarct expansion, Circulation, 74 (1986) 693-702.

[5] H.D. White, R.M. Norris, M.A. Brown, P.W. Brandt, R.M. Whitlock, C.J. Wild, Left ventricular end-systolic volume as the major determinant of survival after recovery from myocardial infarction, Circulation, 76 (1987) 44-51.

[6] B.I. Jugdutt, Ischemia/Infarction, Heart Fail. Clin., 8 (2012) 43-51.

[7] J.A. Erlebacher, J.L. Weiss, M.L. Weisfeldt, B.H. Bulkley, Early dilation of the infarcted segment in acute transmural myocardial infarction: role of infarct expansion in acute left ventricular enlargement, J. Am. Coll. Cardiol., 4 (1984) 201-208.

[8] D.L. Mann, Mechanisms and models in heart failure: A combinatorial approach, Circulation, 100 (1999) 999-1008.

[9] L.W. Eaton, J.L. Weiss, B.H. Bulkley, J.B. Garrison, M.L. Weisfeldt, Regional cardiac dilatation after acute myocardial infarction: recognition by two-dimensional echocardiography, N. Engl. J. Med., 300 (1979) 57-62.

[10] J.L. Rouleau, J. de Champlain, M. Klein, D. Bichet, L. Moyé, M. Packer, G.R. Dagenais, B. Sussex, J.M. Arnold, F. Sestier, J.O. Parker, P. McEwan, V. Bernstein, T.E. Cuddy, G. Lamas, S.S. Gottlieb, J. McCans, C. Nadeau, F. Delage, P. Hamm, M.A. Pfeffer, Activation of neurohumoral systems in postinfarction left ventricular dysfunction, J. Am. Coll. Cardiol., 22 (1993) 390-398.

[11] M.G. Sutton, N. Sharpe, Left ventricular remodeling after myocardial infarction: pathophysiology and therapy, Circulation, 101 (2000) 2981-2988.

[12] A.M. Richards, M.G. Nicholls, T.G. Yandle, C. Frampton, E.A. Espiner, J.G. Turner, R.C. Buttimore, J.G. Lainchbury, J.M. Elliott, H. Ikram, I.G. Crozier, D.W. Smyth, Plasma N-terminal pro-brain natriuretic peptide and adrenomedullin: new neurohormonal predictors of left ventricular function and prognosis after myocardial infarction, Circulation, 97 (1998) 1921-1929.

[13] R.A. Little, K.N. Frayn, P.E. Randall, H.B. Stoner, C. Morton, D.W. Yates, G.S. Laing, Plasma catecholamines in the acute phase of the response to myocardial infarction, Arch. Emerg. Med., 3 (1986) 20-27.

[14] C. Hall, Interaction and modulation of neurohormones on left ventricular remodeling, in: M.G. Sutton (Ed.) Left Ventricular Remodelling After Acute Myocardial Infarction, Sciene Press Ltd, London, 1996, pp. 89-99.

[15] N.G. Frangogiannis, C.W. Smith, M.L. Entman, The inflammatory response in myocardial infarction, Cardiovasc. Res., 53 (2002) 31-47.

[16] J. Sadoshima, S. Izumo, The cellular and molecular response of cardiac myocytes to mechanical stress, Annu. Rev. Physiol., 59 (1997) 551-571.

[17] D.M. Yellon, D.J. Hausenloy, Myocardial reperfusion injury, N. Engl. J. Med., 357 (2007) 1121-1135.

[18] P. Saikumar, Z. Dong, J.M. Weinberg, M.A. Venkatachalam, Mechanisms of cell death in hypoxia/reoxygenation injury, Oncogene, 17 (1998) 3341-3349.

[19] B.J. Zimmerman, D.N. Granger, Reperfusion injury, Surg. Clin. North Am., 72 (1992) 65-83.

[20] F.G. Spinale, Myocardial matrix remodeling and the matrix metalloproteinases: influence on cardiac form and function, Physiol. Rev., 87 (2007) 1285-1342.

[21] M.L. Lindsey, MMP induction and inhibition in myocardial infarction, Heart Fail. Rev., 9 (2004) 7-19.

[22] G. Olivetti, J.M. Capasso, E.H. Sonnenblick, P. Anversa, Side-to-side slippage of myocytes participates in ventricular wall remodeling acutely after myocardial infarction in rats, Circ. Res., 67 (1990) 23-34.

[23] P. Whittaker, D.R. Boughner, R.A. Kloner, Role of collagen in acute myocardial infarct expansion, Circulation, 84 (1991) 2123-2134.

[24] M.A. Pfeffer, Left ventricular remodeling after acute myocardial infarction, Annu. Rev. Med., 46 (1995) 455-466.

[25] G.F. Mitchell, G.A. Lamas, D.E. Vaughan, M.A. Pfeffer, Left ventricular remodeling in the year after first anterior myocardial infarction: a quantitative analysis of

contractile segment lengths and ventricular shape, J. Am. Coll. Cardiol., 19 (1992) 1136-1144.

[26] Indications for fibrinolytic therapy in suspected acute myocardial infarction: collaborative overview of early mortality and major morbidity results from all randomised trials of more than 1000 patients. Fibrinolytic Therapy Trialists' (FTT) Collaborative Group, Lancet, 343 (1994) 311-322.

[27] B.R. Brodie, T.D. Stuckey, T.C. Wall, G. Kissling, C.J. Hansen, D.B. Muncy, R.A. Weintraub, T.A. Kelly, Importance of time to reperfusion for 30-day and late survival and recovery of left ventricular function after primary angioplasty for acute myocardial infarction, J. Am. Coll. Cardiol., 32 (1998) 1312-1319.

[28] A. Barbagelata, E.R. Perna, P. Clemmensen, B.F. Uretsky, J.P. Canella, R.M. Califf, C.B. Granger, G.L. Adams, R. Merla, Y. Birnbaum, Time to reperfusion in acute myocardial infarction. It is time to reduce it!, J. Electrocardiol., 40 (2007) 257-264.

[29] H.R. Lijnen, D. Collen, Fibrinolysis and the control of hemostasis, in: G. Stamatoyannopoulos, P.W. Majerus, R.M. Permutter, H. Varmus (Eds.) The Molecular Basis of Blood Diseases, W.B. Saunders Co., Philadelphia, 2001, pp. 740-763.

[30] C.F. Lacy, L.L. Armstrong, M.P. Goldman, L.L. Lance, A. American Pharmaceutical, Drug information handbook, 2003-2004, Lexi-Comp ; American Pharmaceutical Association, Hudson, Ohio; [Washington, D.C.], 2003.

[31] The effects of tissue plasminogen activator, streptokinase, or both on coronary-artery patency, ventricular function, and survival after acute myocardial infarction. The GUSTO Angiographic Investigators, N. Engl. J. Med., 329 (1993) 1615-1622.

[32] E. Boersma, A.C. Maas, J.W. Deckers, M.L. Simoons, Early thrombolytic treatment in acute myocardial infarction: reappraisal of the golden hour, Lancet, 348 (1996) 771-775.

[33] E.C. Keeley, J.A. Boura, C.L. Grines, Primary angioplasty versus intravenous thrombolytic therapy for acute myocardial infarction: a quantitative review of 23 randomised trials, Lancet, 361 (2003) 13-20.

[34] A. Gruntzig, Transluminal dilatation of coronary-artery stenosis, Lancet, 1 (1978) 263.

[35] U. Sigwart, J. Puel, V. Mirkovitch, F. Joffre, L. Kappenberger, Intravascular stents to prevent occlusion and restenosis after transluminal angioplasty, N. Engl. J. Med., 316 (1987) 701-706.

[36] J.E. Sousa, M.A. Costa, A.C. Abizaid, B.J. Rensing, A.S. Abizaid, L.F. Tanajura, K. Kozuma, G. Van Langenhove, A.G. Sousa, R. Falotico, J. Jaeger, J.J. Popma, P.W. Serruys, Sustained suppression of neointimal proliferation by sirolimus-eluting stents:

one-year angiographic and intravascular ultrasound follow-up, Circulation, 104 (2001) 2007-2011.

[37] M. Degertekin, P.W. Serruys, D.P. Foley, K. Tanabe, E. Regar, J. Vos, P.C. Smits, W.J. van der Giessen, M. van den Brand, P. de Feyter, J.J. Popma, Persistent inhibition of neointimal hyperplasia after sirolimus-eluting stent implantation: long-term (up to 2 years) clinical, angiographic, and intravascular ultrasound follow-up, Circulation, 106 (2002) 1610-1613.

[38] P.W. Serruys, P. de Jaegere, F. Kiemeneij, C. Macaya, W. Rutsch, G. Heyndrickx, H. Emanuelsson, J. Marco, V. Legrand, P. Materne, et al., A comparison of balloon-expandable-stent implantation with balloon angioplasty in patients with coronary artery disease. Benestent Study Group, N. Engl. J. Med., 331 (1994) 489-495.

[39] D.L. Fischman, M.B. Leon, D.S. Baim, R.A. Schatz, M.P. Savage, I. Penn, K. Detre, L. Veltri, D. Ricci, M. Nobuyoshi, et al., A randomized comparison of coronary-stent placement and balloon angioplasty in the treatment of coronary artery disease. Stent Restenosis Study Investigators, N. Engl. J. Med., 331 (1994) 496-501.

[40] M.C. Morice, P.W. Serruys, J.E. Sousa, J. Fajadet, E. Ban Hayashi, M. Perin, A. Colombo, G. Schuler, P. Barragan, G. Guagliumi, F. Molnar, R. Falotico, A randomized comparison of a sirolimus-eluting stent with a standard stent for coronary revascularization, N. Engl. J. Med., 346 (2002) 1773-1780.

[41] E. Grube, S. Silber, K.E. Hauptmann, R. Mueller, L. Buellesfeld, U. Gerckens, M.E. Russell, TAXUS I: six- and twelve-month results from a randomized, double-blind trial on a slow-release paclitaxel-eluting stent for de novo coronary lesions, Circulation, 107 (2003) 38-42.

[42] F. Feres, J.R. Costa, Jr., A. Abizaid, Very late thrombosis after drug-eluting stents, Catheter. Cardiovasc. Interv., 68 (2006) 83-88.

[43] E.P. McFadden, E. Stabile, E. Regar, E. Cheneau, A.T. Ong, T. Kinnaird, W.O. Suddath, N.J. Weissman, R. Torguson, K.M. Kent, A.D. Pichard, L.F. Satler, R. Waksman, P.W. Serruys, Late thrombosis in drug-eluting coronary stents after discontinuation of antiplatelet therapy, Lancet, 364 (2004) 1519-1521.

[44] J.R. Nebeker, R. Virmani, C.L. Bennett, J.M. Hoffman, M.H. Samore, J. Alvarez, C.J. Davidson, J.M. McKoy, D.W. Raisch, B.K. Whisenant, P.R. Yarnold, S.M. Belknap, D.P. West, J.E. Gage, R.E. Morse, G. Gligoric, L. Davidson, M.D. Feldman, Hypersensitivity cases associated with drug-eluting coronary stents: a review of available cases from the Research on Adverse Drug Events and Reports (RADAR) project, J. Am. Coll. Cardiol., 47 (2006) 175-181.

[45] B. Azarbal, J.W. Currier, Allergic reactions after the implantation of drug-eluting stents: is it the pill or the polymer?, J. Am. Coll. Cardiol., 47 (2006) 182-183.

[46] M. Joner, A.V. Finn, A. Farb, E.K. Mont, F.D. Kolodgie, E. Ladich, R. Kutys, K. Skorija, H.K. Gold, R. Virmani, Pathology of drug-eluting stents in humans: delayed healing and late thrombotic risk, J. Am. Coll. Cardiol., 48 (2006) 193-202.

[47] S.H. Hofma, W.J. van der Giessen, B.M. van Dalen, P.A. Lemos, E.P. McFadden, G. Sianos, J.M. Ligthart, D. van Essen, P.J. de Feyter, P.W. Serruys, Indication of long-term endothelial dysfunction after sirolimus-eluting stent implantation, Eur. Heart J., 27 (2006) 166-170.

[48] G. De Luca, M.T. Dirksen, C. Spaulding, H. Kelbaek, M. Schalij, L. Thuesen, B. van der Hoeven, M.A. Vink, C. Kaiser, C. Musto, T. Chechi, G. Spaziani, L.S. Diaz de la Llera, V. Pasceri, E. Di Lorenzo, R. Violini, G. Cortese, H. Suryapranata, G.W. Stone, Drug-eluting vs bare-metal stents in primary angioplasty: a pooled patient-level meta-analysis of randomized trials, Arch. Intern. Med., 172 (2012) 611-621; discussion 621-612.

[49] E.L. Wallace, A. Abdel-Latif, R. Charnigo, D.J. Moliterno, B. Brodie, R. Matnani, K.M. Ziada, Meta-analysis of long-term outcomes for drug-eluting stents versus bare-metal stents in primary percutaneous coronary interventions for ST-segment elevation myocardial infarction, Am. J. Cardiol., 109 (2012) 932-940.

[50] R.A. Costa, A.J. Lansky, A. Abizaid, R. Mueller, Y. Tsuchiya, K. Mori, E. Cristea, M.B. Leon, J.E. Sousa, T. Schmidt, K.E. Hauptmann, E. Grube, Angiographic results of the first human experience with the Biolimus A9 drug-eluting stent for de novo coronary lesions, Am. J. Cardiol., 98 (2006) 443-446.

[51] J.R. Costa, Jr., A. Abizaid, R. Costa, F. Feres, L.F. Tanajura, L.A. Mattos, R. Staico, D. Siqueira, A.G. Sousa, R. Bonan, J.E. Sousa, Preliminary results of the hydroxyapatite nonpolymer-based sirolimus-eluting stent for the treatment of single de novo coronary lesions a first-in-human analysis of a third-generation drug-eluting stent system, JACC Cardiovasc. Interv., 1 (2008) 545-551.

[52] R.A. Byrne, J. Mehilli, R. Iijima, S. Schulz, J. Pache, M. Seyfarth, A. Schomig, A. Kastrati, A polymer-free dual drug-eluting stent in patients with coronary artery disease: a randomized trial vs. polymer-based drug-eluting stents, Eur. Heart J., 30 (2009) 923-931.

[53] M. Packer, J.R. Carver, R.J. Rodeheffer, R.J. Ivanhoe, R. DiBianco, S.M. Zeldis, G.H. Hendrix, W.J. Bommer, U. Elkayam, M.L. Kukin, et al., Effect of oral milrinone on mortality in severe chronic heart failure. The PROMISE Study Research Group, N. Engl. J. Med., 325 (1991) 1468-1475.

[54] J.N. Cohn, S.O. Goldstein, B.H. Greenberg, B.H. Lorell, R.C. Bourge, B.E. Jaski, S.O. Gottlieb, F. McGrew, 3rd, D.L. DeMets, B.G. White, A dose-dependent increase in mortality with vesnarinone among patients with severe heart failure. Vesnarinone Trial Investigators, N. Engl. J. Med., 339 (1998) 1810-1816.

[55] H. Nakashima, K. Kumagai, Reverse-remodeling effects of angiotensin II type 1 receptor blocker in a canine atrial fibrillation model, Circ. J., 71 (2007) 1977-1982.

[56] E. Iwai-Kanai, K. Hasegawa, M. Araki, T. Kakita, T. Morimoto, S. Sasayama, alpha- and beta-adrenergic pathways differentially regulate cell type-specific apoptosis in rat cardiac myocytes, Circulation, 100 (1999) 305-311.

[57] Y.C. Fu, C.S. Chi, S.C. Yin, B. Hwang, Y.T. Chiu, S.L. Hsu, Norepinephrine induces apoptosis in neonatal rat cardiomyocytes through a reactive oxygen species-TNF alpha-caspase signaling pathway, Cardiovasc. Res., 62 (2004) 558-567.

[58] Effect of enalapril on survival in patients with reduced left ventricular ejection fractions and congestive heart failure. The SOLVD Investigators, N. Engl. J. Med., 325 (1991) 293-302.

[59] M.A. Konstam, M.F. Rousseau, M.W. Kronenberg, J.E. Udelson, J. Melin, D. Stewart, N. Dolan, T.R. Edens, S. Ahn, D. Kinan, et al., Effects of the angiotensin converting enzyme inhibitor enalapril on the long-term progression of left ventricular dysfunction in patients with heart failure. SOLVD Investigators, Circulation, 86 (1992) 431-438.

[60] M.A. Pfeffer, E. Braunwald, L.A. Moye, L. Basta, E.J. Brown, Jr., T.E. Cuddy, B.R. Davis, E.M. Geltman, S. Goldman, G.C. Flaker, et al., Effect of captopril on mortality and morbidity in patients with left ventricular dysfunction after myocardial infarction. Results of the survival and ventricular enlargement trial. The SAVE Investigators, N. Engl. J. Med., 327 (1992) 669-677.

[61] Effect of ramipril on mortality and morbidity of survivors of acute myocardial infarction with clinical evidence of heart failure. The Acute Infarction Ramipril Efficacy (AIRE) Study Investigators, Lancet, 342 (1993) 821-828.

[62] A.P. Maggioni, I. Anand, S.O. Gottlieb, R. Latini, G. Tognoni, J.N. Cohn, Effects of valsartan on morbidity and mortality in patients with heart failure not receiving angiotensin-converting enzyme inhibitors, J. Am. Coll. Cardiol., 40 (2002) 1414-1421.

[63] C.B. Granger, J.J. McMurray, S. Yusuf, P. Held, E.L. Michelson, B. Olofsson, J. Ostergren, M.A. Pfeffer, K. Swedberg, Effects of candesartan in patients with chronic heart failure and reduced left-ventricular systolic function intolerant to angiotensin-converting-enzyme inhibitors: the CHARM-Alternative trial, Lancet, 362 (2003) 772-776.

[64] N. Sharpe, Pharmacologic effects on cardiac remodeling, Curr. Heart Fail. Rep., 1 (2004) 9-13.

[65] R.N. Doughty, G.A. Whalley, H.A. Walsh, G.D. Gamble, J. Lopez-Sendon, N. Sharpe, Effects of carvedilol on left ventricular remodeling after acute myocardial infarction: the CAPRICORN Echo Substudy, Circulation, 109 (2004) 201-206.

[66] S.A. Hall, C.G. Cigarroa, L. Marcoux, R.C. Risser, P.A. Grayburn, E.J. Eichhorn, Time course of improvement in left ventricular function, mass and geometry in patients with congestive heart failure treated with beta-adrenergic blockade, J. Am. Coll. Cardiol., 25 (1995) 1154-1161.

[67] B.A. Groenning, J.C. Nilsson, L. Sondergaard, T. Fritz-Hansen, H.B. Larsson, P.R. Hildebrandt, Antiremodeling effects on the left ventricle during beta-blockade with metoprolol in the treatment of chronic heart failure, J. Am. Coll. Cardiol., 36 (2000) 2072-2080.

[68] K.T. Weber, Aldosterone in congestive heart failure, N. Engl. J. Med., 345 (2001) 1689-1697.

[69] J.N. Cohn, Myocardial structural effects of aldosterone receptor antagonism in heart failure, J. Am. Coll. Cardiol., 50 (2007) 597-599.

[70] A.K. Chan, J.E. Sanderson, T. Wang, W. Lam, G. Yip, M. Wang, Y.Y. Lam, Y. Zhang, L. Yeung, E.B. Wu, W.W. Chan, J.T. Wong, N. So, C.M. Yu, Aldosterone receptor antagonism induces reverse remodeling when added to angiotensin receptor blockade in chronic heart failure, J. Am. Coll. Cardiol., 50 (2007) 591-596.

[71] K.W. Mahaffey, J.A. Puma, N.A. Barbagelata, M.F. DiCarli, M.A. Leesar, K.F. Browne, P.R. Eisenberg, R. Bolli, A.C. Casas, V. Molina-Viamonte, C. Orlandi, R. Blevins, R.J. Gibbons, R.M. Califf, C.B. Granger, Adenosine as an adjunct to thrombolytic therapy for acute myocardial infarction: results of a multicenter, randomized, placebo-controlled trial: the Acute Myocardial Infarction STudy of ADenosine (AMISTAD) trial, J. Am. Coll. Cardiol., 34 (1999) 1711-1720.

[72] A.M. Ross, R.J. Gibbons, G.W. Stone, R.A. Kloner, R.W. Alexander, A randomized, double-blinded, placebo-controlled multicenter trial of adenosine as an adjunct to reperfusion in the treatment of acute myocardial infarction (AMISTAD-II), J. Am. Coll. Cardiol., 45 (2005) 1775-1780.

[73] T. Miki, G.S. Liu, M.V. Cohen, J.M. Downey, Mild hypothermia reduces infarct size in the beating rabbit heart: a practical intervention for acute myocardial infarction?, Basic Res. Cardiol., 93 (1998) 372-383.

[74] M.W. Dae, D.W. Gao, D.I. Sessler, K. Chair, C.A. Stillson, Effect of endovascular cooling on myocardial temperature, infarct size, and cardiac output in human-sized pigs, Am. J. Physiol. Heart Circ. Physiol., 282 (2002) H1584-1591.

[75] S.R. Dixon, R.J. Whitbourn, M.W. Dae, E. Grube, W. Sherman, G.L. Schaer, J.S. Jenkins, D.S. Baim, R.J. Gibbons, R.E. Kuntz, J.J. Popma, T.T. Nguyen, W.W. O'Neill, Induction of mild systemic hypothermia with endovascular cooling during primary percutaneous coronary intervention for acute myocardial infarction, J. Am. Coll. Cardiol., 40 (2002) 1928-1934.

[76] K.H. Polderman, I. Herold, Therapeutic hypothermia and controlled normothermia in the intensive care unit: practical considerations, side effects, and cooling methods, Crit. Care Med., 37 (2009) 1101-1120.

[77] The Journal of Gene Medicine Clinical Trials Database, in: J. Gene Med., John Wiley & Sons, Ltd., 2012.

[78] E.G. Nabel, G. Plautz, F.M. Boyce, J.C. Stanley, G.J. Nabel, Recombinant gene expression in vivo within endothelial cells of the arterial wall, Science, 244 (1989) 1342-1344.

[79] R. Hinkel, T. Trenkwalder, C. Kupatt, Gene therapy for ischemic heart disease, Expert Opin. Biol. Ther., 11 (2011) 723-737.

[80] M. Jessup, B. Greenberg, D. Mancini, T. Cappola, D.F. Pauly, B. Jaski, A. Yaroshinsky, K.M. Zsebo, H. Dittrich, R.J. Hajjar, Calcium Upregulation by Percutaneous Administration of Gene Therapy in Cardiac Disease (CUPID): a phase 2 trial of intracoronary gene therapy of sarcoplasmic reticulum Ca2+-ATPase in patients with advanced heart failure, Circulation, 124 (2011) 304-313.

[81] B.E. Jaski, M.L. Jessup, D.M. Mancini, T.P. Cappola, D.F. Pauly, B. Greenberg, K. Borow, H. Dittrich, K.M. Zsebo, R.J. Hajjar, Calcium upregulation by percutaneous administration of gene therapy in cardiac disease (CUPID Trial), a first-in-human phase 1/2 clinical trial, J. Card. Fail., 15 (2009) 171-181.

[82] H. Okada, G. Takemura, K. Kosai, Y. Li, T. Takahashi, M. Esaki, K. Yuge, S. Miyata, R. Maruyama, A. Mikami, S. Minatoguchi, T. Fujiwara, H. Fujiwara, Postinfarction gene therapy against transforming growth factor-beta signal modulates infarct tissue dynamics and attenuates left ventricular remodeling and heart failure, Circulation, 111 (2005) 2430-2437.

[83] L. Li, H. Okada, G. Takemura, K. Kosai, H. Kanamori, M. Esaki, T. Takahashi, K. Goto, A. Tsujimoto, R. Maruyama, I. Kawamura, T. Kawaguchi, T. Takeyama, T. Fujiwara, H. Fujiwara, S. Minatoguchi, Postinfarction gene therapy with adenoviral vector expressing decorin mitigates cardiac remodeling and dysfunction, Am. J. Physiol. Heart Circ. Physiol., 297 (2009) H1504-1513.

[84] L. Ding, L. Dong, X. Chen, L. Zhang, X. Xu, A. Ferro, B. Xu, Increased expression of integrin-linked kinase attenuates left ventricular remodeling and improves cardiac function after myocardial infarction, Circulation, 120 (2009) 764-773.

[85] H. Okada, G. Takemura, K. Kosai, A. Tsujimoto, M. Esaki, T. Takahashi, S. Nagano, H. Kanamori, S. Miyata, Y. Li, T. Ohno, R. Maruyama, A. Ogino, L. Li, M. Nakagawa, K. Nagashima, T. Fujiwara, H. Fujiwara, S. Minatoguchi, Combined therapy with cardioprotective cytokine administration and antiapoptotic gene transfer in postinfarction heart failure, Am. J. Physiol. Heart Circ. Physiol., 296 (2009) H616-626.

[86] Y.L. Tang, Y. Tang, Y.C. Zhang, K. Qian, L. Shen, M.I. Phillips, Protection from ischemic heart injury by a vigilant heme oxygenase-1 plasmid system, Hypertension, 43 (2004) 746-751.

[87] A. Sumida, M. Horiba, H. Ishiguro, H. Takenaka, N. Ueda, H. Ooboshi, T. Opthof, K. Kadomatsu, I. Kodama, Midkine Gene Transfer after Myocardial Infarction in Rats Prevents Remodeling and Ameliorates Cardiac Dysfunction, Cardiovasc. Res., (2009).

[88] Z. Chen, C.C. Chua, Y.S. Ho, R.C. Hamdy, B.H. Chua, Overexpression of Bcl-2 attenuates apoptosis and protects against myocardial I/R injury in transgenic mice, Am. J. Physiol. Heart Circ. Physiol., 280 (2001) H2313-2320.

[89] M. Sugano, M. Koyanagi, K. Tsuchida, T. Hata, N. Makino, In vivo gene transfer of soluble TNF-alpha receptor 1 alleviates myocardial infarction, FASEB J., 16 (2002) 1421-1422.

[90] J.W. Yockman, A. Kastenmeier, H.M. Erickson, J.G. Brumbach, M.G. Whitten, A. Albanil, D.Y. Li, S.W. Kim, D.A. Bull, Novel polymer carriers and gene constructs for treatment of myocardial ischemia and infarction, J. Control. Release, (2008).

[91] M. Lee, J. Rentz, M. Bikram, S. Han, D.A. Bull, S.W. Kim, Hypoxia-inducible VEGF gene delivery to ischemic myocardium using water-soluble lipopolymer, Gene Ther., 10 (2003) 1535-1542.

[92] D.A. Bull, S.H. Bailey, J.J. Rentz, J.S. Zebrack, M. Lee, S.E. Litwin, S.W. Kim, Effect of Terplex/VEGF-165 gene therapy on left ventricular function and structure following myocardial infarction: VEGF gene therapy for myocardial infarction, J. Control. Release, 93 (2003) 175-181.

[93] R. Natarajan, F.N. Salloum, B.J. Fisher, R.C. Kukreja, A.A. Fowler, 3rd, Hypoxia inducible factor-1 activation by prolyl 4-hydroxylase-2 gene silencing attenuates myocardial ischemia reperfusion injury, Circ. Res., 98 (2006) 133-140.

[94] R. Natarajan, F.N. Salloum, B.J. Fisher, E.D. Ownby, R.C. Kukreja, A.A. Fowler, 3rd, Activation of hypoxia-inducible factor-1 via prolyl-4 hydoxylase-2 gene silencing attenuates acute inflammatory responses in postischemic myocardium, Am. J. Physiol. Heart Circ. Physiol., 293 (2007) H1571-1580.

[95] R. Natarajan, F.N. Salloum, B.J. Fisher, L. Smithson, J. Almenara, A.A. Fowler, 3rd, Prolyl hydroxylase inhibition attenuates post-ischemic cardiac injury via induction of endoplasmic reticulum stress genes, Vascul. Pharmacol., 51 (2009) 110-118.

[96] M. Sugano, K. Tsuchida, T. Hata, N. Makino, RNA interference targeting SHP-1 attenuates myocardial infarction in rats, FASEB J., 19 (2005) 2054-2056.

[97] O.O. Lisovyy, V.E. Dosenko, V.S. Nagibin, L.V. Tumanovska, M.O. Korol, O.V. Surova, O.O. Moibenko, Cardioprotective effect of 5-lipoxygenase gene (ALOX5) silencing in ischemia-reperfusion, Acta Biochim. Pol., 56 (2009) 687-694.

[98] H. Song, Z. Zhang, L. Wang, Small interference RNA against PTP-1B reduces hypoxia/reoxygenation induced apoptosis of rat cardiomyocytes, Apoptosis, 13 (2008) 383-393.

[99] L.E. Huang, Z. Arany, D.M. Livingston, H.F. Bunn, Activation of hypoxia-inducible transcription factor depends primarily upon redox-sensitive stabilization of its alpha subunit, J. Biol. Chem., 271 (1996) 32253-32259.

[100] P.J. Kallio, I. Pongratz, K. Gradin, J. McGuire, L. Poellinger, Activation of hypoxia-inducible factor 1alpha: posttranscriptional regulation and conformational change by recruitment of the Arnt transcription factor, Proc. Natl. Acad. Sci. U. S. A., 94 (1997) 5667-5672.

[101] H. Li, H.P. Ko, J.P. Whitlock, Induction of phosphoglycerate kinase 1 gene expression by hypoxia. Roles of Arnt and HIF1alpha, J. Biol. Chem., 271 (1996) 21262-21267.

[102] L.E. Huang, J. Gu, M. Schau, H.F. Bunn, Regulation of hypoxia-inducible factor 1alpha is mediated by an O2-dependent degradation domain via the ubiquitin-proteasome pathway, Proc. Natl. Acad. Sci. U. S. A., 95 (1998) 7987-7992.

[103] Q. Ke, M. Costa, Hypoxia-inducible factor-1 (HIF-1), Mol. Pharmacol., 70 (2006) 1469-1480.

[104] Y. Yuan, G. Hilliard, T. Ferguson, D.E. Millhorn, Cobalt inhibits the interaction between hypoxia-inducible factor-alpha and von Hippel-Lindau protein by direct binding to hypoxia-inducible factor-alpha, J. Biol. Chem., 278 (2003) 15911-15916.

[105] G.L. Semenza, G.L. Wang, A nuclear factor induced by hypoxia via de novo protein synthesis binds to the human erythropoietin gene enhancer at a site required for transcriptional activation, Mol. Cell. Biol., 12 (1992) 5447-5454.

[106] G. Olivetti, R. Abbi, F. Quaini, J. Kajstura, W. Cheng, J.A. Nitahara, E. Quaini, C. Di Loreto, C.A. Beltrami, S. Krajewski, J.C. Reed, P. Anversa, Apoptosis in the failing human heart, N. Engl. J. Med., 336 (1997) 1131-1141.

[107] H.Y. Chang, H. Nishitoh, X. Yang, H. Ichijo, D. Baltimore, Activation of apoptosis signal-regulating kinase 1 (ASK1) by the adapter protein Daxx, Science, 281 (1998) 1860-1863.

[108] M. Rota, M.E. Padin-Iruegas, Y. Misao, A. De Angelis, S. Maestroni, J. Ferreira-Martins, E. Fiumana, R. Rastaldo, M.L. Arcarese, T.S. Mitchell, A. Boni, R. Bolli, K. Urbanek, T. Hosoda, P. Anversa, A. Leri, J. Kajstura, Local activation or implantation of cardiac progenitor cells rescues scarred infarcted myocardium improving cardiac function, Circ. Res., 103 (2008) 107-116.

[109] O. Bergmann, R.D. Bhardwaj, S. Bernard, S. Zdunek, F. Barnabe-Heider, S. Walsh, J. Zupicich, K. Alkass, B.A. Buchholz, H. Druid, S. Jovinge, J. Frisen, Evidence for cardiomyocyte renewal in humans, Science, 324 (2009) 98-102.

[110] P.W. Thimister, L. Hofstra, I.H. Liem, H.H. Boersma, G. Kemerink, C.P. Reutelingsperger, G.A. Heidendal, In vivo detection of cell death in the area at risk in acute myocardial infarction, J. Nucl. Med., 44 (2003) 391-396.

[111] S. Kothari, J. Cizeau, E. McMillan-Ward, S.J. Israels, M. Bailes, K. Ens, L.A. Kirshenbaum, S.B. Gibson, BNIP3 plays a role in hypoxic cell death in human epithelial cells that is inhibited by growth factors EGF and IGF, Oncogene, 22 (2003) 4734-4744.

[112] R.K. Bruick, Expression of the gene encoding the proapoptotic Nip3 protein is induced by hypoxia, Proc. Natl. Acad. Sci. U. S. A., 97 (2000) 9082-9087.

[113] K. Guo, G. Searfoss, D. Krolikowski, M. Pagnoni, C. Franks, K. Clark, K.T. Yu, M. Jaye, Y. Ivashchenko, Hypoxia induces the expression of the pro-apoptotic gene BNIP3, Cell Death Differ., 8 (2001) 367-376.

[114] E.V. Bocharov, Y.E. Pustovalova, K.V. Pavlov, P.E. Volynsky, M.V. Goncharuk, Y.S. Ermolyuk, D.V. Karpunin, A.A. Schulga, M.P. Kirpichnikov, R.G. Efremov, I.V. Maslennikov, A.S. Arseniev, Unique dimeric structure of BNip3 transmembrane domain suggests membrane permeabilization as a cell death trigger, J. Biol. Chem., 282 (2007) 16256-16266.

[115] T.R. Burton, S.B. Gibson, The role of Bcl-2 family member BNIP3 in cell death and disease: NIPping at the heels of cell death, Cell Death Differ., (2009).

[116] G. Chinnadurai, S. Vijayalingam, S.B. Gibson, BNIP3 subfamily BH3-only proteins: mitochondrial stress sensors in normal and pathological functions, Oncogene, 27 Suppl 1 (2008) S114-127.

[117] D.A. Kubli, M.N. Quinsay, C. Huang, Y. Lee, A.B. Gustafsson, Bnip3 functions as a mitochondrial sensor of oxidative stress during myocardial ischemia and reperfusion, Am. J. Physiol. Heart Circ. Physiol., 295 (2008) H2025-2031.

[118] G.W. Dorn, 2nd, L.A. Kirshenbaum, Cardiac reanimation: targeting cardiomyocyte death by BNIP3 and NIX/BNIP3L, Oncogene, 27 (2008) S158-S167.

[119] K.M. Regula, K. Ens, L.A. Kirshenbaum, Inducible expression of BNIP3 provokes mitochondrial defects and hypoxia-mediated cell death of ventricular myocytes, Circ. Res., 91 (2002) 226-231.

[120] L. Zhang, L. Li, H. Liu, K. Prabhakaran, X. Zhang, J.L. Borowitz, G.E. Isom, HIF-1alpha activation by a redox-sensitive pathway mediates cyanide-induced BNIP3 upregulation and mitochondrial-dependent cell death, Free Radic. Biol. Med., 43 (2007) 117-127.

[121] M. Ogata, S. Hino, A. Saito, K. Morikawa, S. Kondo, S. Kanemoto, T. Murakami, M. Taniguchi, I. Tanii, K. Yoshinaga, S. Shiosaka, J.A. Hammarback, F. Urano, K. Imaizumi, Autophagy is activated for cell survival after endoplasmic reticulum stress, Mol. Cell. Biol., 26 (2006) 9220-9231.

[122] T. Shintani, D.J. Klionsky, Autophagy in health and disease: a double-edged sword, Science, 306 (2004) 990-995.

[123] S. Rodriguez-Enriquez, L. He, J.J. Lemasters, Role of mitochondrial permeability transition pores in mitochondrial autophagy, Int. J. Biochem. Cell Biol., 36 (2004) 2463-2472.

[124] L. Yan, D.E. Vatner, S.J. Kim, H. Ge, M. Masurekar, W.H. Massover, G. Yang, Y. Matsui, J. Sadoshima, S.F. Vatner, Autophagy in chronically ischemic myocardium, Proc. Natl. Acad. Sci. U. S. A., 102 (2005) 13807-13812.

[125] N.M. Mazure, J. Pouyssegur, Atypical BH3-domains of BNIP3 and BNIP3L lead to autophagy in hypoxia, Autophagy, 5 (2009) 868-869.

[126] Y. Aviv, J. Shaw, H. Gang, L.A. Kirshenbaum, Regulation of autophagy in the heart: "you only live twice", Antioxid. Redox. Signal., 14 (2011) 2245-2250.

[127] B.B. Cho, L.H. Toledo-Pereyra, Caspase-independent programmed cell death following ischemic stroke, J. Invest. Surg., 21 (2008) 141-147.

[128] R. Chavez-Valdez, L.J. Martin, D.L. Flock, F.J. Northington, Necrostatin-1 attenuates mitochondrial dysfunction in neurons and astrocytes following neonatal hypoxia-ischemia, Neuroscience, 219 (2012) 192-203.

[129] J.Y. Kim, Y.J. Kim, S. Lee, J.H. Park, BNip3 is a mediator of TNF-induced necrotic cell death, Apoptosis, 16 (2011) 114-126.

[130] H.M. Sowter, M. Ferguson, C. Pym, P. Watson, S.B. Fox, C. Han, A.L. Harris, Expression of the cell death genes BNip3 and NIX in ductal carcinoma in situ of the breast; correlation of BNip3 levels with necrosis and grade, J. Pathol., 201 (2003) 573-580.

[131] H.M. Sowter, P.J. Ratcliffe, P. Watson, A.H. Greenberg, A.L. Harris, HIF-1-dependent regulation of hypoxic induction of the cell death factors BNIP3 and NIX in human tumors, Cancer Res., 61 (2001) 6669-6673.

[132] C. Vande Velde, J. Cizeau, D. Dubik, J. Alimonti, T. Brown, S. Israels, R. Hakem, A.H. Greenberg, BNIP3 and genetic control of necrosis-like cell death through the mitochondrial permeability transition pore, Mol. Cell. Biol., 20 (2000) 5454-5468.

[133] G.W. Dorn, 2nd, Mitochondrial pruning by Nix and BNip3: an essential function for cardiac-expressed death factors, J Cardiovasc. Transl. Res., 3 (2010) 374-383.

[134] S. Guo, K.J. Kemphues, par-1, a gene required for establishing polarity in C. elegans embryos, encodes a putative Ser/Thr kinase that is asymmetrically distributed, Cell, 81 (1995) 611-620.

[135] A. Fire, S. Xu, M.K. Montgomery, S.A. Kostas, S.E. Driver, C.C. Mello, Potent and specific genetic interference by double-stranded RNA in Caenorhabditis elegans, Nature, 391 (1998) 806-811.

[136] R.H. Medema, Optimizing RNA interference for application in mammalian cells, Biochem. J., 380 (2004) 593-603.

[137] A. Reynolds, D. Leake, Q. Boese, S. Scaringe, W.S. Marshall, A. Khvorova, Rational siRNA design for RNA interference, Nat. Biotechnol., 22 (2004) 326-330.

[138] T. Tuschl, The siRNA User Guide, (2004).

[139] J. Soutschek, A. Akinc, B. Bramlage, K. Charisse, R. Constien, M. Donoghue, S. Elbashir, A. Geick, P. Hadwiger, J. Harborth, M. John, V. Kesavan, G. Lavine, R.K. Pandey, T. Racie, K.G. Rajeev, I. Rohl, I. Toudjarska, G. Wang, S. Wuschko, D. Bumcrot, V. Koteliansky, S. Limmer, M. Manoharan, H.P. Vornlocher, Therapeutic silencing of an endogenous gene by systemic administration of modified siRNAs, Nature, 432 (2004) 173-178.

[140] P.D. Zamore, T. Tuschl, P.A. Sharp, D.P. Bartel, RNAi: double-stranded RNA directs the ATP-dependent cleavage of mRNA at 21 to 23 nucleotide intervals, Cell, 101 (2000) 25-33.

[141] S.M. Elbashir, J. Harborth, W. Lendeckel, A. Yalcin, K. Weber, T. Tuschl, Duplexes of 21-nucleotide RNAs mediate RNA interference in cultured mammalian cells, Nature, 411 (2001) 494-498.

[142] P.J. Paddison, A.A. Caudy, E. Bernstein, G.J. Hannon, D.S. Conklin, Short hairpin RNAs (shRNAs) induce sequence-specific silencing in mammalian cells, Genes Dev., 16 (2002) 948-958.

[143] M.E. Davis, J.E. Zuckerman, C.H. Choi, D. Seligson, A. Tolcher, C.A. Alabi, Y. Yen, J.D. Heidel, A. Ribas, Evidence of RNAi in humans from systemically administered siRNA via targeted nanoparticles, Nature, 464 (2010) 1067-1070.

[144] A.K. Vaishnaw, J. Gollob, C. Gamba-Vitalo, R. Hutabarat, D. Sah, R. Meyers, T. de Fougerolles, J. Maraganore, A status report on RNAi therapeutics, Silence, 1 (2010) 14.

[145] J.C. Burnett, J.J. Rossi, K. Tiemann, Current progress of siRNA/shRNA therapeutics in clinical trials, Biotechnol. J., 6 (2011) 1130-1146.

[146] M.E. Kleinman, K. Yamada, A. Takeda, V. Chandrasekaran, M. Nozaki, J.Z. Baffi, R.J. Albuquerque, S. Yamasaki, M. Itaya, Y. Pan, B. Appukuttan, D. Gibbs, Z. Yang, K.

Kariko, B.K. Ambati, T.A. Wilgus, L.A. DiPietro, E. Sakurai, K. Zhang, J.R. Smith, E.W. Taylor, J. Ambati, Sequence- and target-independent angiogenesis suppression by siRNA via TLR3, Nature, 452 (2008) 591-597.

[147] W.G. Cho, R.J. Albuquerque, M.E. Kleinman, V. Tarallo, A. Greco, M. Nozaki, M.G. Green, J.Z. Baffi, B.K. Ambati, M. De Falco, J.S. Alexander, A. Brunetti, S. De Falco, J. Ambati, Small interfering RNA-induced TLR3 activation inhibits blood and lymphatic vessel growth, Proc. Natl. Acad. Sci. U. S. A., 106 (2009) 7137-7142.

[148] J.C. Burnett, J.J. Rossi, RNA-based therapeutics: current progress and future prospects, Chem. Biol., 19 (2012) 60-71.

[149] S.D. Li, L. Huang, Gene therapy progress and prospects: non-viral gene therapy by systemic delivery, Gene Ther., 13 (2006) 1313-1319.

[150] D. Schaffert, E. Wagner, Gene therapy progress and prospects: synthetic polymer-based systems, Gene Ther., 15 (2008) 1131-1138.

[151] Y. Chen, H. Yu, Advanced biomedical techniques for gene delivery, Recent Pat. Biomed. Eng., 5 (2012) 23-28.

[152] M.D. Brown, A.G. Schatzlein, I.F. Uchegbu, Gene delivery with synthetic (non viral) carriers, Int. J. Pharm., 229 (2001) 1-21.

[153] P. Osten, V. Grinevich, A. Cetin, Viral vectors: a wide range of choices and high levels of service, Handb. Exp. Pharmacol., (2007) 177-202.

[154] W.T. Godbey, A.G. Mikos, Recent progress in gene delivery using non-viral transfer complexes, J. Control. Release, 72 (2001) 115-125.

[155] A.J. Phillips, The challenge of gene therapy and DNA delivery, J. Pharm. Pharmacol., 53 (2001) 1169-1174.

[156] N.B. Wasala, J.H. Shin, D. Duan, The evolution of heart gene delivery vectors, J. Gene Med., 13 (2011) 557-565.

[157] G. Romano, I.R. Marino, F. Pentimalli, V. Adamo, A. Giordano, Insertional mutagenesis and development of malignancies induced by integrating gene delivery systems: implications for the design of safer gene-based interventions in patients, Drug News Perspect., 22 (2009) 185-196.

[158] C. Baum, Insertional mutagenesis in gene therapy and stem cell biology, Curr. Opin. Hematol., 14 (2007) 337-342.

[159] M. Lusky, Good manufacturing practice production of adenoviral vectors for clinical trials, Hum. Gene Ther., 16 (2005) 281-291.

[160] J.F. Wright, Manufacturing and characterizing AAV-based vectors for use in clinical studies, Gene Ther., 15 (2008) 840-848.

[161] S.E. Raper, N. Chirmule, F.S. Lee, N.A. Wivel, A. Bagg, G.P. Gao, J.M. Wilson, M.L. Batshaw, Fatal systemic inflammatory response syndrome in a ornithine transcarbamylase deficient patient following adenoviral gene transfer, Mol. Genet. Metab., 80 (2003) 148-158.

[162] S. Hacein-Bey-Abina, C. von Kalle, M. Schmidt, F. Le Deist, N. Wulffraat, E. McIntyre, I. Radford, J.L. Villeval, C.C. Fraser, M. Cavazzana-Calvo, A. Fischer, A serious adverse event after successful gene therapy for X-linked severe combined immunodeficiency, N. Engl. J. Med., 348 (2003) 255-256.

[163] S. Hacein-Bey-Abina, C. Von Kalle, M. Schmidt, M.P. McCormack, N. Wulffraat, P. Leboulch, A. Lim, C.S. Osborne, R. Pawliuk, E. Morillon, R. Sorensen, A. Forster, P. Fraser, J.I. Cohen, G. de Saint Basile, I. Alexander, U. Wintergerst, T. Frebourg, A. Aurias, D. Stoppa-Lyonnet, S. Romana, I. Radford-Weiss, F. Gross, F. Valensi, E. Delabesse, E. Macintyre, F. Sigaux, J. Soulier, L.E. Leiva, M. Wissler, C. Prinz, T.H. Rabbitts, F. Le Deist, A. Fischer, M. Cavazzana-Calvo, LMO2-associated clonal T cell proliferation in two patients after gene therapy for SCID-X1, Science, 302 (2003) 415-419.

[164] M. Frauli, S. Ribault, P. Neuville, F. Auge, V. Calenda, Adenoviral-mediated skeletal muscle transcriptional targeting using chimeric tissue-specific promoters, Med. Sci. Monit., 9 (2003) BR78-84.

[165] N.J. Silman, A.R. Fooks, Biophysical targeting of adenovirus vectors for gene therapy, Curr. Opin. Mol. Ther., 2 (2000) 524-531.

[166] Y. Yang, F.A. Nunes, K. Berencsi, E.E. Furth, E. Gonczol, J.M. Wilson, Cellular immunity to viral antigens limits E1-deleted adenoviruses for gene therapy, Proc. Natl. Acad. Sci. U. S. A., 91 (1994) 4407-4411.

[167] Q. Liu, D.A. Muruve, Molecular basis of the inflammatory response to adenovirus vectors, Gene Ther., 10 (2003) 935-940.

[168] Y. Yang, Q. Su, J.M. Wilson, Role of viral antigens in destructive cellular immune responses to adenovirus vector-transduced cells in mouse lungs, J. Virol., 70 (1996) 7209-7212.

[169] Y. Yang, J.M. Wilson, Clearance of adenovirus-infected hepatocytes by MHC class I-restricted CD4+ CTLs in vivo, J. Immunol., 155 (1995) 2564-2570.

[170] K. Boris-Lawrie, H.M. Temin, The retroviral vector. Replication cycle and safety considerations for retrovirus-mediated gene therapy, Ann. N. Y. Acad. Sci., 716 (1994) 59-70; discussion 71.

[171] in: J.M. Coffin, S.H. Hughes, H.E. Varmus (Eds.) Retroviruses, Cold Spring Harbor (NY), 1997.

[172] H. Fan, C. Johnson, Insertional oncogenesis by non-acute retroviruses: implications for gene therapy, Viruses, 3 (2011) 398-422.

[173] N. Muzyczka, K. Berns, Parvoviridae: the viruses and their replication, Fields Virology, 2 (2001) 2327-2359.

[174] R.J. Samulski, Adeno-associated virus: integration at a specific chromosomal locus, Curr. Opin. Genet. Dev., 3 (1993) 74-80.

[175] B.L. Davidson, C.S. Stein, J.A. Heth, I. Martins, R.M. Kotin, T.A. Derksen, J. Zabner, A. Ghodsi, J.A. Chiorini, Recombinant adeno-associated virus type 2, 4, and 5 vectors: transduction of variant cell types and regions in the mammalian central nervous system, Proc. Natl. Acad. Sci. U. S. A., 97 (2000) 3428-3432.

[176] A.K. Malik, P.E. Monahan, D.L. Allen, B.G. Chen, R.J. Samulski, K. Kurachi, Kinetics of recombinant adeno-associated virus-mediated gene transfer, J. Virol., 74 (2000) 3555-3565.

[177] M.A. Kay, C.S. Manno, M.V. Ragni, P.J. Larson, L.B. Couto, A. McClelland, B. Glader, A.J. Chew, S.J. Tai, R.W. Herzog, V. Arruda, F. Johnson, C. Scallan, E. Skarsgard, A.W. Flake, K.A. High, Evidence for gene transfer and expression of factor IX in haemophilia B patients treated with an AAV vector, Nat. Genet., 24 (2000) 257-261.

[178] J.Y. Dong, P.D. Fan, R.A. Frizzell, Quantitative analysis of the packaging capacity of recombinant adeno-associated virus, Hum. Gene Ther., 7 (1996) 2101-2112.

[179] D. Grimm, A. Kern, K. Rittner, J.A. Kleinschmidt, Novel tools for production and purification of recombinant adenoassociated virus vectors, Hum. Gene Ther., 9 (1998) 2745-2760.

[180] L. Naldini, U. Blomer, P. Gallay, D. Ory, R. Mulligan, F.H. Gage, I.M. Verma, D. Trono, In vivo gene delivery and stable transduction of nondividing cells by a lentiviral vector, Science, 272 (1996) 263-267.

[181] J.A. Wolff, R.W. Malone, P. Williams, W. Chong, G. Acsadi, A. Jani, P.L. Felgner, Direct gene transfer into mouse muscle in vivo, Science, 247 (1990) 1465-1468.

[182] N.S. Yang, J. Burkholder, B. Roberts, B. Martinell, D. McCabe, In vivo and in vitro gene transfer to mammalian somatic cells by particle bombardment, Proc. Natl. Acad. Sci. U. S. A., 87 (1990) 9568-9572.

[183] L.C. Heller, K. Ugen, R. Heller, Electroporation for targeted gene transfer, Expert Opin. Drug Deliv., 2 (2005) 255-268.

[184] H.J. Kim, J.F. Greenleaf, R.R. Kinnick, J.T. Bronk, M.E. Bolander, Ultrasound-mediated transfection of mammalian cells, Hum. Gene Ther., 7 (1996) 1339-1346.

[185] F. Liu, Y. Song, D. Liu, Hydrodynamics-based transfection in animals by systemic administration of plasmid DNA, Gene Ther., 6 (1999) 1258-1266.

[186] G. Zhang, V. Budker, J.A. Wolff, High levels of foreign gene expression in hepatocytes after tail vein injections of naked plasmid DNA, Hum. Gene Ther., 10 (1999) 1735-1737.

[187] N.S. Dejneka, S. Wan, O.S. Bond, D.J. Kornbrust, S.J. Reich, Ocular biodistribution of bevasiranib following a single intravitreal injection to rabbit eyes, Mol. Vis., 14 (2008) 997-1005.

[188] T. Shoshani, A. Faerman, I. Mett, E. Zelin, T. Tenne, S. Gorodin, Y. Moshel, S. Elbaz, A. Budanov, A. Chajut, H. Kalinski, I. Kamer, A. Rozen, O. Mor, E. Keshet, D. Leshkowitz, P. Einat, R. Skaliter, E. Feinstein, Identification of a novel hypoxia-inducible factor 1-responsive gene, RTP801, involved in apoptosis, Mol. Cell. Biol., 22 (2002) 2283-2293.

[189] E. Neumann, M. Schaefer-Ridder, Y. Wang, P.H. Hofschneider, Gene transfer into mouse lyoma cells by electroporation in high electric fields, EMBO J., 1 (1982) 841-845.

[190] A.V. Titomirov, S. Sukharev, E. Kistanova, In vivo electroporation and stable transformation of skin cells of newborn mice by plasmid DNA, Biochim. Biophys. Acta, 1088 (1991) 131-134.

[191] F. Andre, L.M. Mir, DNA electrotransfer: its principles and an updated review of its therapeutic applications, Gene Ther., 11 Suppl 1 (2004) S33-42.

[192] M. Fechheimer, J.F. Boylan, S. Parker, J.E. Sisken, G.L. Patel, S.G. Zimmer, Transfection of mammalian cells with plasmid DNA by scrape loading and sonication loading, Proc. Natl. Acad. Sci. U. S. A., 84 (1987) 8463-8467.

[193] M. Endoh, N. Koibuchi, M. Sato, R. Morishita, T. Kanzaki, Y. Murata, Y. Kaneda, Fetal gene transfer by intrauterine injection with microbubble-enhanced ultrasound, Mol. Ther., 5 (2002) 501-508.

[194] N.A. Geis, H.A. Katus, R. Bekeredjian, Microbubbles as a vehicle for gene and drug delivery: current clinical implications and future perspectives, Curr. Pharm. Des., 18 (2012) 2166-2183.

[195] G. Zhang, X. Gao, Y.K. Song, R. Vollmer, D.B. Stolz, J.Z. Gasiorowski, D.A. Dean, D. Liu, Hydroporation as the mechanism of hydrodynamic delivery, Gene Ther., 11 (2004) 675-682.

[196] J.W. Fabre, A. Grehan, M. Whitehorne, G.J. Sawyer, X. Dong, S. Salehi, L. Eckley, X. Zhang, M. Seddon, A.M. Shah, M. Davenport, M. Rela, Hydrodynamic gene

delivery to the pig liver via an isolated segment of the inferior vena cava, Gene Ther., 15 (2008) 452-462.

[197] T.M. Klein, E. Wolf, R. Wu, J. Sanford, High-velocity microprojectiles for delivering nucleic acids into living cells, Nature, 327 (1987) 70-73.

[198] P.L. Felgner, T.R. Gadek, M. Holm, R. Roman, H.W. Chan, M. Wenz, J.P. Northrop, G.M. Ringold, M. Danielsen, Lipofection: a highly efficient, lipid-mediated DNA-transfection procedure, Proc. Natl. Acad. Sci. U. S. A., 84 (1987) 7413-7417.

[199] A. Hirko, F. Tang, J.A. Hughes, Cationic lipid vectors for plasmid DNA delivery, Curr. Med. Chem., 10 (2003) 1185-1193.

[200] O. Zelphati, F.C. Szoka, Jr., Mechanism of oligonucleotide release from cationic liposomes, Proc. Natl. Acad. Sci. U. S. A., 93 (1996) 11493-11498.

[201] E. Lai, J.H. van Zanten, Evidence of lipoplex dissociation in liquid formulations, J. Pharm. Sci., 91 (2002) 1225-1232.

[202] F. Boffi, A. Bonincontro, F. Bordi, E. Bultrini, C. Cametti, A. Congiu-Castellano, F. De Luca, G. Risuleo, Two-step mechanism in cationic lipoplex formation as observed by dynamic light scattering, dielectric relaxation and circular dichroism methods, Phys. Chem. Chem. Phys., 4 (2002) 2708-2713.

[203] H. Zhao, H. Hemmi, S. Akira, S.H. Cheng, R.K. Scheule, N.S. Yew, Contribution of Toll-like receptor 9 signaling to the acute inflammatory response to nonviral vectors, Mol. Ther., 9 (2004) 241-248.

[204] P. Harvie, F.M. Wong, M.B. Bally, Use of poly(ethylene glycol)-lipid conjugates to regulate the surface attributes and transfection activity of lipid-DNA particles, J. Pharm. Sci., 89 (2000) 652-663.

[205] O. Boussif, F. Lezoualc'h, M.A. Zanta, M.D. Mergny, D. Scherman, B. Demeneix, J.P. Behr, A versatile vector for gene and oligonucleotide transfer into cells in culture and in vivo: polyethylenimine, Proc. Natl. Acad. Sci. U. S. A., 92 (1995) 7297-7301.

[206] J.P. Behr, The proton sponge: a trick to enter cells the viruses did not exploit, CHIMIA, 51 (1997) 1-2.

[207] A. Akinc, M. Thomas, A.M. Klibanov, R. Langer, Exploring polyethylenimine-mediated DNA transfection and the proton sponge hypothesis, J. Gene Med., 7 (2005) 657-663.

[208] N.D. Sonawane, F.C. Szoka, Jr., A.S. Verkman, Chloride accumulation and swelling in endosomes enhances DNA transfer by polyamine-DNA polyplexes, J. Biol. Chem., 278 (2003) 44826-44831.

[209] M. Bertschinger, G. Backliwal, A. Schertenleib, M. Jordan, D.L. Hacker, F.M. Wurm, Disassembly of polyethylenimine-DNA particles in vitro: implications for polyethylenimine-mediated DNA delivery, J. Control. Release, 116 (2006) 96-104.

[210] D. Fischer, T. Bieber, Y. Li, H.P. Elsasser, T. Kissel, A novel non-viral vector for DNA delivery based on low molecular weight, branched polyethylenimine: effect of molecular weight on transfection efficiency and cytotoxicity, Pharm. Res., 16 (1999) 1273-1279.

[211] W.T. Godbey, K.K. Wu, A.G. Mikos, Poly(ethylenimine)-mediated gene delivery affects endothelial cell function and viability, Biomaterials, 22 (2001) 471-480.

[212] Y.H. Kim, J.H. Park, M. Lee, T.G. Park, S.W. Kim, Polyethylenimine with acid-labile linkages as a biodegradable gene carrier, J. Control. Release, 103 (2005) 209-219.

[213] H. Petersen, P.M. Fechner, A.L. Martin, K. Kunath, S. Stolnik, C.J. Roberts, D. Fischer, M.C. Davies, T. Kissel, Polyethylenimine-graft-poly(ethylene glycol) copolymers: influence of copolymer block structure on DNA complexation and biological activities as gene delivery system, Bioconjug. Chem., 13 (2002) 845-854.

[214] M.L. Forrest, J.T. Koerber, D.W. Pack, A degradable polyethylenimine derivative with low toxicity for highly efficient gene delivery, Bioconjug. Chem., 14 (2003) 934-940.

[215] Q. Peng, Z. Zhong, R. Zhuo, Disulfide cross-linked polyethylenimines (PEI) prepared via thiolation of low molecular weight PEI as highly efficient gene vectors, Bioconjug. Chem., 19 (2008) 499-506.

[216] S.-o. Han, R.I. Mahato, S.W. Kim, Water-Soluble Lipopolymer for Gene Delivery, Bioconjug. Chem., 12 (2001) 337-345.

[217] G.Y. Wu, C.H. Wu, Receptor-mediated in vitro gene transformation by a soluble DNA carrier system, J. Biol. Chem., 262 (1987) 4429-4432.

[218] D.W. Pack, D. Putnam, R. Langer, Design of imidazole-containing endosomolytic biopolymers for gene delivery, Biotechnol. Bioeng., 67 (2000) 217-223.

[219] A.M. Funhoff, C.F. van Nostrum, M.C. Lok, J.A. Kruijtzer, D.J. Crommelin, W.E. Hennink, Cationic polymethacrylates with covalently linked membrane destabilizing peptides as gene delivery vectors, J. Control. Release, 101 (2005) 233-246.

[220] P. Chollet, M.C. Favrot, A. Hurbin, J.L. Coll, Side-effects of a systemic injection of linear polyethylenimine-DNA complexes, J. Gene Med., 4 (2002) 84-91.

[221] D. Putnam, R. Langer, Poly (4-hydroxy-L-proline ester): Low-temperature polycondensation and plasmid DNA complexation, Macromolecules, 32 (1999) 3658-3662.

[222] Y.B. Lim, C.H. Kim, K. Kim, S.W. Kim, J.S. Park, Development of a safe gene delivery system using biodegradable polymer, poly[α-(4-aminobutyl)-L-glycolic acid] [19], J. Am. Chem. Soc., 122 (2000) 6524-6525.

[223] H.F. Gilbert, Thiol/disulfide exchange equilibria and disulfide bond stability, Methods Enzymol., 251 (1995) 8-28.

[224] S. Raina, D. Missiakas, Making and breaking disulfide bonds, Annu. Rev. Microbiol., 51 (1997) 179-202.

[225] G. Wu, Y.Z. Fang, S. Yang, J.R. Lupton, N.D. Turner, Glutathione metabolism and its implications for health, J. Nutr., 134 (2004) 489-492.

[226] A. Andersson, A. Lindgren, B. Hultberg, Effect of thiol oxidation and thiol export from erythrocytes on determination of redox status of homocysteine and other thiols in plasma from healthy subjects and patients with cerebral infarction, Clin. Chem., 41 (1995) 361-366.

[227] S.M. Deneke, Thiol-based antioxidants, Curr. Top. Cell. Regul., 36 (2000) 151-180.

[228] F.Q. Schafer, G.R. Buettner, Redox environment of the cell as viewed through the redox state of the glutathione disulfide/glutathione couple, Free Radic. Biol. Med., 30 (2001) 1191-1212.

[229] M.A. Gosselin, W. Guo, R.J. Lee, Efficient gene transfer using reversibly cross-linked low molecular weight polyethylenimine, Bioconjug. Chem., 12 (2001) 989-994.

[230] Y. Wang, P. Chen, J. Shen, The development and characterization of a glutathione-sensitive cross-linked polyethylenimine gene vector, Biomaterials, 27 (2006) 5292-5298.

[231] C. Lin, Z. Zhong, M.C. Lok, X. Jiang, W.E. Hennink, J. Feijen, J.F. Engbersen, Linear poly(amido amine)s with secondary and tertiary amino groups and variable amounts of disulfide linkages: synthesis and in vitro gene transfer properties, J. Control. Release, 116 (2006) 130-137.

[232] C. Lin, Z. Zhong, M.C. Lok, X. Jiang, W.E. Hennink, J. Feijen, J.F. Engbersen, Novel bioreducible poly(amido amine)s for highly efficient gene delivery, Bioconjug. Chem., 18 (2007) 138-145.

[233] K.A. Mislick, J.D. Baldeschwieler, Evidence for the role of proteoglycans in cation-mediated gene transfer, Proc. Natl. Acad. Sci. U. S. A., 93 (1996) 12349-12354.

[234] G.T. Hess, W.H.t. Humphries, N.C. Fay, C.K. Payne, Cellular binding, motion, and internalization of synthetic gene delivery polymers, Biochim. Biophys. Acta, 1773 (2007) 1583-1588.

[235] M. Ogris, S. Brunner, S. Schuller, R. Kircheis, E. Wagner, PEGylated DNA/transferrin-PEI complexes: reduced interaction with blood components, extended circulation in blood and potential for systemic gene delivery, Gene Ther., 6 (1999) 595-605.

[236] M. Lee, S.W. Kim, Polyethylene glycol-conjugated copolymers for plasmid DNA delivery, Pharm. Res., 22 (2005) 1-10.

[237] S.J. Sung, S.H. Min, K.Y. Cho, S. Lee, Y.J. Min, Y.I. Yeom, J.K. Park, Effect of polyethylene glycol on gene delivery of polyethylenimine, Biol. Pharm. Bull., 26 (2003) 492-500.

[238] J.A. Hughes, G.A. Rao, Targeted polymers for gene delivery, Expert Opin. Drug Deliv., 2 (2005) 145-157.

[239] A. Elouahabi, J.M. Ruysschaert, Formation and intracellular trafficking of lipoplexes and polyplexes, Mol. Ther., 11 (2005) 336-347.

[240] B.E. Strauer, M. Brehm, T. Zeus, M. Kostering, A. Hernandez, R.V. Sorg, G. Kogler, P. Wernet, Repair of infarcted myocardium by autologous intracoronary mononuclear bone marrow cell transplantation in humans, Circulation, 106 (2002) 1913-1918.

[241] B. Assmus, V. Schachinger, C. Teupe, M. Britten, R. Lehmann, N. Dobert, F. Grunwald, A. Aicher, C. Urbich, H. Martin, D. Hoelzer, S. Dimmeler, A.M. Zeiher, Transplantation of Progenitor Cells and Regeneration Enhancement in Acute Myocardial Infarction (TOPCARE-AMI), Circulation, 106 (2002) 3009-3017.

[242] A.M. Mozid, S. Arnous, E.C. Sammut, A. Mathur, Stem cell therapy for heart diseases, Br. Med. Bull., 98 (2011) 143-159.

[243] A.I. Caplan, J.E. Dennis, Mesenchymal stem cells as trophic mediators, J. Cell. Biochem., 98 (2006) 1076-1084.

[244] K.C. Wollert, H. Drexler, Clinical applications of stem cells for the heart, Circ. Res., 96 (2005) 151-163.

[245] L.C. Amado, A.P. Saliaris, K.H. Schuleri, M. St John, J.S. Xie, S. Cattaneo, D.J. Durand, T. Fitton, J.Q. Kuang, G. Stewart, S. Lehrke, W.W. Baumgartner, B.J. Martin, A.W. Heldman, J.M. Hare, Cardiac repair with intramyocardial injection of allogeneic mesenchymal stem cells after myocardial infarction, Proc. Natl. Acad. Sci. U. S. A., 102 (2005) 11474-11479.

[246] Y. Miyahara, N. Nagaya, M. Kataoka, B. Yanagawa, K. Tanaka, H. Hao, K. Ishino, H. Ishida, T. Shimizu, K. Kangawa, S. Sano, T. Okano, S. Kitamura, H. Mori, Monolayered mesenchymal stem cells repair scarred myocardium after myocardial infarction, Nat. Med., 12 (2006) 459-465.

[247] M. Gnecchi, H. He, N. Noiseux, O.D. Liang, L. Zhang, F. Morello, H. Mu, L.G. Melo, R.E. Pratt, J.S. Ingwall, V.J. Dzau, Evidence supporting paracrine hypothesis for Akt-modified mesenchymal stem cell-mediated cardiac protection and functional improvement, FASEB J., 20 (2006) 661-669.

[248] A.P. Beltrami, L. Barlucchi, D. Torella, M. Baker, F. Limana, S. Chimenti, H. Kasahara, M. Rota, E. Musso, K. Urbanek, A. Leri, J. Kajstura, B. Nadal-Ginard, P. Anversa, Adult cardiac stem cells are multipotent and support myocardial regeneration, Cell, 114 (2003) 763-776.

[249] A. Linke, P. Muller, D. Nurzynska, C. Casarsa, D. Torella, A. Nascimbene, C. Castaldo, S. Cascapera, M. Bohm, F. Quaini, K. Urbanek, A. Leri, T.H. Hintze, J. Kajstura, P. Anversa, Stem cells in the dog heart are self-renewing, clonogenic, and multipotent and regenerate infarcted myocardium, improving cardiac function, Proc. Natl. Acad. Sci. U. S. A., 102 (2005) 8966-8971.

[250] H. Oh, S.B. Bradfute, T.D. Gallardo, T. Nakamura, V. Gaussin, Y. Mishina, J. Pocius, L.H. Michael, R.R. Behringer, D.J. Garry, M.L. Entman, M.D. Schneider, Cardiac progenitor cells from adult myocardium: homing, differentiation, and fusion after infarction, Proc. Natl. Acad. Sci. U. S. A., 100 (2003) 12313-12318.

[251] A. Leri, J. Kajstura, P. Anversa, Cardiac stem cells and mechanisms of myocardial regeneration, Physiol. Rev., 85 (2005) 1373-1416.

[252] L. Barile, I. Chimenti, R. Gaetani, E. Forte, F. Miraldi, G. Frati, E. Messina, A. Giacomello, Cardiac stem cells: isolation, expansion and experimental use for myocardial regeneration, Nat. Clin. Pract. Cardiovasc. Med., 4 Suppl 1 (2007) S9-S14.

[253] R. Bolli, A.R. Chugh, D. D'Amario, J.H. Loughran, M.F. Stoddard, S. Ikram, G.M. Beache, S.G. Wagner, A. Leri, T. Hosoda, F. Sanada, J.B. Elmore, P. Goichberg, D. Cappetta, N.K. Solankhi, I. Fahsah, D.G. Rokosh, M.S. Slaughter, J. Kajstura, P. Anversa, Cardiac stem cells in patients with ischaemic cardiomyopathy (SCIPIO): initial results of a randomised phase 1 trial, Lancet, 378 (2011) 1847-1857.

[254] R.R. Makkar, R.R. Smith, K. Cheng, K. Malliaras, L.E. Thomson, D. Berman, L.S. Czer, L. Marban, A. Mendizabal, P.V. Johnston, S.D. Russell, K.H. Schuleri, A.C. Lardo, G. Gerstenblith, E. Marban, Intracoronary cardiosphere-derived cells for heart regeneration after myocardial infarction (CADUCEUS): a prospective, randomised phase 1 trial, Lancet, 379 (2012) 895-904.

[255] J.A. Thomson, J. Itskovitz-Eldor, S.S. Shapiro, M.A. Waknitz, J.J. Swiergiel, V.S. Marshall, J.M. Jones, Embryonic stem cell lines derived from human blastocysts, Science, 282 (1998) 1145-1147.

[256] I. Kehat, D. Kenyagin-Karsenti, M. Snir, H. Segev, M. Amit, A. Gepstein, E. Livne, O. Binah, J. Itskovitz-Eldor, L. Gepstein, Human embryonic stem cells can differentiate into myocytes with structural and functional properties of cardiomyocytes, J. Clin. Invest., 108 (2001) 407-414.

[257] K.R. Boheler, J. Czyz, D. Tweedie, H.T. Yang, S.V. Anisimov, A.M. Wobus, Differentiation of pluripotent embryonic stem cells into cardiomyocytes, Circ. Res., 91 (2002) 189-201.

[258] M.A. Laflamme, C.E. Murry, Regenerating the heart, Nat. Biotechnol., 23 (2005) 845-856.

[259] J. Nussbaum, E. Minami, M.A. Laflamme, J.A. Virag, C.B. Ware, A. Masino, V. Muskheli, L. Pabon, H. Reinecke, C.E. Murry, Transplantation of undifferentiated murine embryonic stem cells in the heart: teratoma formation and immune response, FASEB J., 21 (2007) 1345-1357.

[260] E. Poon, C.W. Kong, R.A. Li, Human pluripotent stem cell-based approaches for myocardial repair: from the electrophysiological perspective, Mol. Pharm., 8 (2011) 1495-1504.

[261] P.S. Zammit, T.A. Partridge, Z. Yablonka-Reuveni, The skeletal muscle satellite cell: the stem cell that came in from the cold, J. Histochem. Cytochem., 54 (2006) 1177-1191.

[262] P. Menasche, Skeletal myoblasts and cardiac repair, J. Mol. Cell. Cardiol., 45 (2008) 545-553.

[263] M. Khan, V.K. Kutala, D.S. Vikram, S. Wisel, S.M. Chacko, M.L. Kuppusamy, I.K. Mohan, J.L. Zweier, P. Kwiatkowski, P. Kuppusamy, Skeletal myoblasts transplanted in the ischemic myocardium enhance in situ oxygenation and recovery of contractile function, Am. J. Physiol. Heart Circ. Physiol., 293 (2007) H2129-2139.

[264] M. Kino-Oka, S.R. Chowdhury, Y. Muneyuki, M. Manabe, A. Saito, Y. Sawa, M. Taya, Automating the expansion process of human skeletal muscle myoblasts with suppression of myotube formation, Tissue Eng. Part C Methods, 15 (2009) 717-728.

[265] P. Menasche, Skeletal myoblasts as a therapeutic agent, Prog. Cardiovasc. Dis., 50 (2007) 7-17.

[266] H. Reinecke, V. Poppa, C.E. Murry, Skeletal muscle stem cells do not transdifferentiate into cardiomyocytes after cardiac grafting, J. Mol. Cell. Cardiol., 34 (2002) 241-249.

[267] M. Jain, H. DerSimonian, D.A. Brenner, S. Ngoy, P. Teller, A.S. Edge, A. Zawadzka, K. Wetzel, D.B. Sawyer, W.S. Colucci, C.S. Apstein, R. Liao, Cell therapy attenuates deleterious ventricular remodeling and improves cardiac performance after myocardial infarction, Circulation, 103 (2001) 1920-1927.

[268] M. Scorsin, A. Hagege, J.T. Vilquin, M. Fiszman, F. Marotte, J.L. Samuel, L. Rappaport, K. Schwartz, P. Menasche, Comparison of the effects of fetal cardiomyocyte and skeletal myoblast transplantation on postinfarction left ventricular function, J. Thorac. Cardiovasc. Surg., 119 (2000) 1169-1175.

[269] N. Dib, E.B. Diethrich, A. Campbell, N. Goodwin, B. Robinson, J. Gilbert, D.W. Hobohm, D.A. Taylor, Endoventricular transplantation of allogenic skeletal myoblasts in a porcine model of myocardial infarction, J. Endovasc. Ther., 9 (2002) 313-319.

[270] J.J. Gavira, M. Perez-Ilzarbe, G. Abizanda, A. García-Rodríguez, J. Orbe, J.A. Páramo, M. Belzunce, G. Rábago, J. Barba, J. Herreros, A comparison between percutaneous and surgical transplantation of autologous skeletal myoblasts in a swine model of chronic myocardial infarction, Cardiovasc. Res., 71 (2006) 744-753.

[271] S. Ghostine, C. Carrion, L.C. Souza, P. Richard, P. Bruneval, J.T. Vilquin, B. Pouzet, K. Schwartz, P. Menasche, A.A. Hagege, Long-term efficacy of myoblast transplantation on regional structure and function after myocardial infarction, Circulation, 106 (2002) I131-136.

[272] K.L. He, G.H. Yi, W. Sherman, H. Zhou, G.P. Zhang, A. Gu, R. Kao, H.B. Haimes, J. Harvey, E. Roos, D. White, D.A. Taylor, J. Wang, D. Burkhoff, Autologous skeletal myoblast transplantation improved hemodynamics and left ventricular function in chronic heart failure dogs, J. Heart Lung Transplant., 24 (2005) 1940-1949.

[273] P. Menasche, A.A. Hagège, J.-T. Vilquin, M. Desnos, E. Abergel, B. Pouzet, A. Bel, S. Sarateanu, M. Scorsin, K. Schwartz, P. Bruneval, M. Benbunan, J.-P. Marolleau, D. Duboc, Autologous skeletal myoblast transplantation for severe postinfarction left ventricular dysfunction, J. Am. Coll. Cardiol., 41 (2003) 1078-1083.

[274] J. Herreros, F. Prosper, A. Perez, J.J. Gavira, M.J. Garcia-Velloso, J. Barba, P.L. Sanchez, C. Canizo, G. Rabago, J.M. Marti-Climent, M. Hernandez, N. Lopez-Holgado, J.M. Gonzalez-Santos, C. Martin-Luengo, E. Alegria, Autologous intramyocardial injection of cultured skeletal muscle-derived stem cells in patients with non-acute myocardial infarction, Eur. Heart J., 24 (2003) 2012-2020.

[275] T. Siminiak, R. Kalawski, D. Fiszer, O. Jerzykowska, J. Rzezniczak, N. Rozwadowska, M. Kurpisz, Autologous skeletal myoblast transplantation for the treatment of postinfarction myocardial injury: phase I clinical study with 12 months of follow-up, Am. Heart J., 148 (2004) 531-537.

[276] P.C. Smits, R.J. van Geuns, D. Poldermans, M. Bountioukos, E.E. Onderwater, C.H. Lee, A.P. Maat, P.W. Serruys, Catheter-based intramyocardial injection of autologous skeletal myoblasts as a primary treatment of ischemic heart failure: clinical experience with six-month follow-up, J. Am. Coll. Cardiol., 42 (2003) 2063-2069.

[277] P. Menasche, O. Alfieri, S. Janssens, W. McKenna, H. Reichenspurner, L. Trinquart, J.T. Vilquin, J.P. Marolleau, B. Seymour, J. Larghero, S. Lake, G. Chatellier, S. Solomon, M. Desnos, A.A. Hagege, The Myoblast Autologous Grafting in Ischemic Cardiomyopathy (MAGIC) trial: first randomized placebo-controlled study of myoblast transplantation, Circulation, 117 (2008) 1189-1200.

[278] N. Dib, R.E. Michler, F.D. Pagani, S. Wright, D.J. Kereiakes, R. Lengerich, P. Binkley, D. Buchele, I. Anand, C. Swingen, M.F. Di Carli, J.D. Thomas, W.A. Jaber,

S.R. Opie, A. Campbell, P. McCarthy, M. Yeager, V. Dilsizian, B.P. Griffith, R. Korn, S.K. Kreuger, M. Ghazoul, W.R. MacLellan, G. Fonarow, H.J. Eisen, J. Dinsmore, E. Diethrich, Safety and feasibility of autologous myoblast transplantation in patients with ischemic cardiomyopathy: four-year follow-up, Circulation, 112 (2005) 1748-1755.

[279] N. Dib, P. McCarthy, A. Campbell, M. Yeager, F.D. Pagani, S. Wright, W.R. MacLellan, G. Fonarow, H.J. Eisen, R.E. Michler, P. Binkley, D. Buchele, R. Korn, M. Ghazoul, J. Dinsmore, S.R. Opie, E. Diethrich, Feasibility and safety of autologous myoblast transplantation in patients with ischemic cardiomyopathy, Cell Transplant., 14 (2005) 11-19.

[280] F.D. Pagani, H. DerSimonian, A. Zawadzka, K. Wetzel, A.S. Edge, D.B. Jacoby, J.H. Dinsmore, S. Wright, T.H. Aretz, H.J. Eisen, K.D. Aaronson, Autologous skeletal myoblasts transplanted to ischemia-damaged myocardium in humans. Histological analysis of cell survival and differentiation, J. Am. Coll. Cardiol., 41 (2003) 879-888.

[281] J.C. Chachques, J. Herreros, J. Trainini, A. Juffe, E. Rendal, F. Prosper, J. Genovese, Autologous human serum for cell culture avoids the implantation of cardioverter-defibrillators in cellular cardiomyoplasty, Int. J. Cardiol., 95 Suppl 1 (2004) S29-33.

[282] M. Ou, T.I. Kim, J.W. Yockman, B.A. Borden, D.A. Bull, S.W. Kim, Polymer transfected primary myoblasts mediated efficient gene expression and angiogenic proliferation, J. Control. Release, 142 (2010) 61-69.

[283] A.N. McGinn, H.Y. Nam, M. Ou, N. Hu, C.M. Straub, J.W. Yockman, D.A. Bull, S.W. Kim, Bioreducible polymer-transfected skeletal myoblasts for VEGF delivery to acutely ischemic myocardium, Biomaterials, 32 (2011) 942-949.

[284] J.B. Gurdon, The developmental capacity of nuclei taken from intestinal epithelium cells of feeding tadpoles, J. Embryol. Exp. Morphol., 10 (1962) 622-640.

[285] K. Takahashi, S. Yamanaka, Induction of pluripotent stem cells from mouse embryonic and adult fibroblast cultures by defined factors, Cell, 126 (2006) 663-676.

[286] Z. Pasha, Y. Wang, R. Sheikh, D. Zhang, T. Zhao, M. Ashraf, Preconditioning enhances cell survival and differentiation of stem cells during transplantation in infarcted myocardium, Cardiovasc. Res., 77 (2008) 134-142.

[287] L. Qian, Y. Huang, C.I. Spencer, A. Foley, V. Vedantham, L. Liu, S.J. Conway, J.D. Fu, D. Srivastava, In vivo reprogramming of murine cardiac fibroblasts into induced cardiomyocytes, Nature, 485 (2012) 593-598.

[288] M. Kawamura, S. Miyagawa, K. Miki, A. Saito, S. Fukushima, T. Higuchi, T. Kawamura, T. Kuratani, T. Daimon, T. Shimizu, T. Okano, Y. Sawa, Feasibility, safety, and therapeutic efficacy of human induced pluripotent stem cell-derived cardiomyocyte sheets in a porcine ischemic cardiomyopathy model, Circulation, 126 (2012) S29-37.

[289] C. Mauritz, A. Martens, S.V. Rojas, T. Schnick, C. Rathert, N. Schecker, S. Menke, S. Glage, R. Zweigerdt, A. Haverich, U. Martin, I. Kutschka, Induced pluripotent stem cell (iPSC)-derived Flk-1 progenitor cells engraft, differentiate, and improve heart function in a mouse model of acute myocardial infarction, Eur. Heart J., 32 (2011) 2634-2641.

[290] M. Hockel, K. Schlenger, S. Doctrow, T. Kissel, P. Vaupel, Therapeutic angiogenesis, Arch. Surg., 128 (1993) 423-429.

[291] N. Ferrara, VEGF-A: a critical regulator of blood vessel growth, Eur. Cytokine Netw., 20 (2009) 158-163.

[292] N. Ferrara, K. Carver-Moore, H. Chen, M. Dowd, L. Lu, K.S. O'Shea, L. Powell-Braxton, K.J. Hillan, M.W. Moore, Heterozygous embryonic lethality induced by targeted inactivation of the VEGF gene, Nature, 380 (1996) 439-442.

[293] S. Yla-Herttuala, T.T. Rissanen, I. Vajanto, J. Hartikainen, Vascular endothelial growth factors: biology and current status of clinical applications in cardiovascular medicine, J. Am. Coll. Cardiol., 49 (2007) 1015-1026.

[294] H. Gerhardt, M. Golding, M. Fruttiger, C. Ruhrberg, A. Lundkvist, A. Abramsson, M. Jeltsch, C. Mitchell, K. Alitalo, D. Shima, C. Betsholtz, VEGF guides angiogenic sprouting utilizing endothelial tip cell filopodia, J. Cell Biol., 161 (2003) 1163-1177.

[295] R.K. Jain, Molecular regulation of vessel maturation, Nat. Med., 9 (2003) 685-693.

[296] C. Hellberg, A. Ostman, C.H. Heldin, PDGF and vessel maturation, Recent Results Cancer Res., 180 (2010) 103-114.

[297] K. Gaengel, G. Genove, A. Armulik, C. Betsholtz, Endothelial-mural cell signaling in vascular development and angiogenesis, Arterioscler. Thromb. Vasc. Biol., 29 (2009) 630-638.

[298] P. Carmeliet, D. Collen, Role of vascular endothelial growth factor and vascular endothelial growth factor receptors in vascular development, Curr. Top. Microbiol. Immunol., 237 (1999) 133-158.

[299] Y. Dor, V. Djonov, R. Abramovitch, A. Itin, G.I. Fishman, P. Carmeliet, G. Goelman, E. Keshet, Conditional switching of VEGF provides new insights into adult neovascularization and pro-angiogenic therapy, EMBO J., 21 (2002) 1939-1947.

[300] C. Kupatt, R. Hinkel, A. Pfosser, C. El-Aouni, A. Wuchrer, A. Fritz, F. Globisch, M. Thormann, J. Horstkotte, C. Lebherz, E. Thein, A. Banfi, P. Boekstegers, Cotransfection of vascular endothelial growth factor-A and platelet-derived growth factor-B via recombinant adeno-associated virus resolves chronic ischemic malperfusion role of vessel maturation, J. Am. Coll. Cardiol., 56 (2010) 414-422.

[301] T.P. Richardson, M.C. Peters, A.B. Ennett, D.J. Mooney, Polymeric system for dual growth factor delivery, Nat. Biotechnol., 19 (2001) 1029-1034.

[302] D.E. Johnson, L.T. Williams, Structural and functional diversity in the FGF receptor multigene family, Adv. Cancer Res., 60 (1993) 1-41.

[303] A. Beenken, M. Mohammadi, The FGF family: biology, pathophysiology and therapy, Nat. Rev. Drug Discov., 8 (2009) 235-253.

[304] M. Murakami, L.T. Nguyen, Z.W. Zhuang, K.L. Moodie, P. Carmeliet, R.V. Stan, M. Simons, The FGF system has a key role in regulating vascular integrity, J. Clin. Invest., 118 (2008) 3355-3366.

[305] C.L. Grines, M.W. Watkins, G. Helmer, W. Penny, J. Brinker, J.D. Marmur, A. West, J.J. Rade, P. Marrott, H.K. Hammond, R.L. Engler, Angiogenic Gene Therapy (AGENT) trial in patients with stable angina pectoris, Circulation, 105 (2002) 1291-1297.

[306] T.D. Henry, C.L. Grines, M.W. Watkins, N. Dib, G. Barbeau, R. Moreadith, T. Andrasfay, R.L. Engler, Effects of Ad5FGF-4 in patients with angina: an analysis of pooled data from the AGENT-3 and AGENT-4 trials, J. Am. Coll. Cardiol., 50 (2007) 1038-1046.

CHAPTER 3

BIOREDUCIBLE POLYMER-TRANSFECTED SKELETAL MYOBLASTS FOR VEGF DELIVERY TO ACUTELY ISCHEMIC MYOCARDIUM[1]

3.1 Abstract

Implantation of skeletal myoblasts to the heart has been investigated as a means to regenerate and protect the myocardium from damage after myocardial infarction. While several animal studies utilizing skeletal myoblasts have reported positive findings, results from clinical studies have been mixed. In this study we utilize a newly developed bioreducible polymer system to transfect skeletal myoblasts with a plasmid encoding vascular endothelial growth factor (VEGF) prior to implantation into acutely ischemic myocardium. VEGF has been demonstrated to promote revascularization of the myocardium following myocardial infarction. We report that implanting VEGF expressing skeletal myoblasts into acutely ischemic myocardium produces superior results compared to implantation of untransfected skeletal myoblasts. Skeletal myoblasts expressing secreted VEGF were able to restore cardiac function to nondiseased levels as measured by ejection fraction, to limit remodeling of the heart chamber as measured by

[1] Reprinted from *Biomaterials*, 32/3, A.N. McGinn, H.Y. Nam, M. Ou, N. Hu, C.M. Straub, J.W. Yockman, D.A. Bull, S.W. Kim, Bioreducible polymer-transfected skeletal myoblasts for VEGF delivery to acutely ischemic myocardium, 942-949, (2011), with permission from Elsevier.

end systolic and diastolic volumes, and to prevent myocardial wall thinning. Additionally, arteriole and capillary formation, retention of viable cardiomyocytes, and prevention of apoptosis was significantly improved by VEGF expressing skeletal myoblasts compared to untransfected myoblasts. This work demonstrates the feasibility of using bioreducible cationic polymers to create engineered skeletal myoblasts to treat acutely ischemic myocardium.

3.2 Introduction

Myocardial infarction (MI) is the leading cause of death in developed nations and one of the most common causes of death in the world. Unfortunately, current pharmacological treatment regimens for myocardial infarction do not reliably limit remodeling of the left ventricle (LV) postinfarction and prevent progression to heart failure. Novel potential treatments, including gene and cell therapies, offer a means to directly treat the pathophysiology underlying the long-term complications of myocardial infarction—loss of cardiomyocytes due to necrosis and apoptosis.

Implantation of cells to the myocardium has long been investigated as a means to recover myocardial tissue and improve outcomes post-MI. Skeletal myoblasts are a class of progenitor muscle cells that may recover infarcted myocardium and limit remodeling of the left [1-3] and the right ventricle [4]. Several studies have demonstrated the ability of skeletal myoblasts to regenerate myocardium through mechanisms including *in situ* proliferation and fusion with resident myotubes and myofibers [5, 6]. While initial results using skeletal myoblasts for implantation to the myocardium have been positive, the long-term benefits remain uncertain. Implantation of cells is limited by the rapid loss of cells from the injection site. With the majority of cells being lost by mechanical means

soon after injection, the primary benefit of skeletal myoblast implantation is thought to derive from the paracrine effects of the growth factors and cytokines secreted by the injected cells [7, 8].

In addition to cell-based approaches, other investigators have focused on angiogenic therapies to treat myocardial infarction. Therapies using angiogenic factors, such as vascular endothelial growth factor (VEGF) and basic fibroblast growth factor (bFGF), have demonstrated the beneficial effects of angiogenesis on protection of endogenous cardiomyocytes and on the retention of functionally contractile myocardium [9-11]. The most common technique for expressing angiogenic factors has been the utilization of viral vectors to deliver VEGF into endogenous cardiomyocytes [12]. In addition to direct transduction of myocardial tissue, examples of viral transduction of skeletal myoblasts have been published [13-15]. While viral gene therapy offers high transfection efficiencies, its clinical utility is limited by host immune responses, oncogenic potential, limitations in viral loading, and difficulty in large-scale manufacturing. For these reasons, the development of safer, nonviral methods for gene delivery is increasingly important.

Nonviral polymer gene therapy is a technique that has been rapidly advancing over the past 10 years. Polymer gene carriers are nonimmunogenic, stable, have a large DNA loading capacity and are also easily manufactured. They are, however, when compared to viral vectors, less efficient at transfecting cells and producing prolonged gene expression. Among cationic polymers for gene therapy, polyethyleneimine (PEI) has recently been used to transfect human skeletal myoblasts with VEGF for implantation into the myocardium for cardiac repair following myocardial infarction [16]. While PEI

has long been considered the gold standard for polymer transfection, it is known to be highly toxic to most cell types and it lacks the ability to rapidly release its DNA cargo upon internalization to the cell. We have recently reported the synthesis and validation of disulfide-containing bioreducible polymers which improve upon PEI by allowing for the rapid release of DNA cargo upon internalization to the cell. These newly described polymers, poly(cystaminebisacrylamide-diaminohexane) [poly(CBA-DAH)] and poly(cystaminebisacrylamide-diaminohexane-arginine) [poly(CBA-DAH-R)], showed 11- and 16-fold higher expression of luciferase, respectively, with significantly less toxicity than branched PEI. We have also demonstrated that these polymers can efficiently transfect the functional gene $VEGF_{165}$, the predominant isoform of VEGF which possesses high angiogenic potency, into primary myoblasts [17]. The production of therapeutic levels of secreted VEGF by these transfected skeletal myoblasts suggests that transfected primary skeletal myoblasts can be used as bioreactors for angiogenic VEGF expression *in vivo* [17].

In this study, we utilized an *in vivo* animal model to evaluate the therapeutic efficacy of polymer-transfected primary skeletal myoblasts in limiting the size of myocardial infarction. Rats were treated with skeletal myoblasts that had been transfected with poly(CBA-DAH) containing a plasmid encoding human $VEGF_{165}$. These $VEGF_{165}$-expressing skeletal myoblast-treated animals were compared to: 1) treatment with untransfected myoblasts; 2) no treatment (ligation only); and 3) thoracotomy only. Magnetic resonance imaging (MRI), histology and immuno-histochemistry were used to determine differences in cardiac function, infarct size, arteriole and/or capillary density, and apoptosis between the study groups.

3.3 Materials and Methods

All experiments were approved by the University of Utah's Institutional Animal Care and Use Committee and followed the guidelines provided by the National Institutes of Health in *Guide for the Care and Use of Laboratory Animals*.

3.3.1 Isolation, Culture and Characterization of Rat Primary Skeletal Myoblasts

The process of isolating, culturing and characterizing rat skeletal primary myoblasts was reported in our previous work [17] with slight modifications from published protocols [18, 19].

Briefly, rat skeletal primary myoblasts were obtained from young rat hindlimbs. Isolated rat skeletal primary myoblasts were maintained in growth medium consisting of Ham's F-10 supplemented with 20% FBS, 2.5 ng/ml human bFGF, penicillin (200 μg/ml), and streptomycin (200 μg/ml) and incubated at 37 °C in 5% CO_2. Primary cultures derived from skeletal muscle consisting of myoblasts and fibroblasts were incubated in Ham's F-10 medium, giving a growth advantage to myoblasts over fibroblasts. Primary myoblasts were separated from contaminating cells, such as fibroblasts, by taking advantage of their differential adherence to the flask over several passages. After two weeks of selective growth, cells were trypsinized, suspended in 90% serum and 10% dimethyl sulfoxide (DMSO) and frozen in liquid nitrogen.

To select the primary myoblasts, cells were immunostained using the primary antibody (mouse-anti-human desmin IgG_1/κ) and the secondary antibody (Streptavidin-horseradish peroxidase, SAv-HRP conjugated biotinylated anti-mouse IgG), fixed by 2% paraformaldehyde in PBS for 30 minutes, washed with PBS and then with blocking buffer (3% BSA with 0.5% Triton X-100 in PBS) for 1 hour at room temperature. The

samples were incubated with 1:100 primary anti-desmin IgG at 4 °C overnight. The next day, cells were washed with PBS, diluted in secondary antibody (1:100 biotinylated anti-mouse IgG) for 1 hour at room temperature, and washed three times in PBS. SAv-HRP was applied and the samples were incubated for 30 minutes at room temperature. DAB substrate solution was applied to the slides and incubated until the desired color intensity was reached (around 5 minutes). The cells were dehydrated using 95% alcohol and xylene and covered with Fluoromount ^{TM} Mount Gel (Sigma-Aldrich, St. Louis, MO). After several weeks in culture, the vast majority of the cells stained positive for the myoblast specific protein desmin.

3.3.2 Preparation of Polymer, Poly(CBA-DAH), and Plasmid, pCMV-VEGF$_{165}$

The poly(disulfide amine) polymer, poly(CBA-DAH), was synthesized as detailed previously [20]. Briefly, poly(CBA-DAH) was synthesized by Michael reaction of *N*-Boc-DAH and CBA in MeOH/H_2O solution (9:1, v/v) and the reaction was protected from light under nitrogen at 60 °C for 3 days with stirring. After the third day, 10% molar ratio of *N*-Boc-DAH was added to the reaction mixture to consume any unreacted acrylamide functional groups and the reaction was allowed to proceed for an additional 2 hours. The reaction products were precipitated with anhydrous diethyl ether followed by deprotection of the *N*-Boc groups with the reagent solution (TFA:triisobutylsilane:H_2O , 95:2.5:2.5, v/v) in an ice bath for 30 minutes. The crude product was again precipitated with anhydrous diethyl ether and dried under vacuum. The final product was dialyzed against deionized water overnight (MWCO=1000 Da, Spectrum Laboratories, Inc., Rancho Dominguez, CA), and lyophilized to obtain

poly(CBA-DAH). The poly(CBA-DAH) was analyzed by ^{1}H NMR (400 MHz, D_2O) to confirm successful synthesis of the desired product.

The plasmid, pCMV-$VEGF_{165,}$ containing the vascular endothelial growth factor gene 165 was amplified in *E. coli* DH5α cells and purified by standard Maxiprep kit (Invitrogen, Carlsbad, CA).

3.3.3 Rat Myocardial Infarction Model

Male Sprague-Dawley rats were anesthetized under 4% isoflurane for induction, intubated and kept under 2% isoflurane for maintenance of anesthesia. The left chest was shaved and a thoracotomy was performed in the 4^{th} or 5^{th} intercostal space, exposing the heart. The left anterior descending coronary artery (LAD) was permanently ligated using a single stitch of 6-0 prolene suture (Ethicon). After confirming successful ligation of the LAD by observation of visible blanching of the left ventricle, the animals were assigned to one of three treatment groups: 1) Ligation only (n = 7), 2) injection of untreated skeletal myoblasts (n = 7), and 3) injection of $VEGF_{165}$-transfected skeletal myoblasts (n = 7). Animals assigned to cell injection groups received 2×10^6 cells in 200 µl PBS in three separate injections to the border zone of the infarct. After the injection of cells, the chest was closed in layers and the animal was allowed to recover under a warming lamp. Additionally, some animals received a full thoracotomy with exposure of the heart, but no ligation of the LAD to act as sham operation controls (n = 5).

Primary myoblasts were transfected with poly(CBA-DAH)/pCMV-$VEGF_{165}$ at the ratio of 20:1 (w/w) 24 hours prior to the surgery. Cells were injected at the border zone of the infarct with three injections for a total number of cells ~2×10^6/200 µl in PBS.

3.3.4 VEGF Expression Study

To verify expression of VEGF in the heart following injection of VEGF-transfected myoblasts into the myocardium, VEGF levels were measured three days after surgery using a commercially available human $VEGF_{165}$ ELISA kit (R&D Systems, Minneapolis, MN). A total of eight animals were treated with myoblasts transfected with VEGF, eight animals were treated with untransfected myoblasts, while eight control animals received no myoblasts and underwent ligation only. Hearts were weighed, and homogenized in 1× TE buffer containing protease inhibitors. 100 µl of the supernatant was used for determination of VEGF levels by ELISA assay.

The quantification of VEGF protein was determined using a UV absorbance plate reader (Model 680, Bio-Rad Lab, Hercules, CA). All experiments were performed in triplicate and quantitated using the supplied VEGF standard.

3.3.5 Magnetic Resonance Imaging (MRI)

Magnetic resonance imaging (MRI) was performed to determine changes in indices of heart function in all animals. Four weeks following surgery, the animals were analyzed by cardiac MRI to measure parameters of heart function. Anesthesia induction was achieved in each animal by exposure to 4% isoflurane and maintained with 2% isoflurane. The rats were placed prone on a pressure sensor to measure respiration, and a pulse oximeter was attached to the rat's foot. The heart was imaged using a Bruker Biospec 7T/30 cm system operated with Bruker AVANCE II electronics (Bruker BioSpin MRI GmbH, Ettlingen, Germany). A Bruker birdcage quadrature resonator (72 mm inner diameter) was used for signal transmission and reception (Bruker BioSpin MRI GmbH, Ettlingen, Germany). The images were acquired using black blood FLASH CINE

parameters with double-gating off respiration and ECG. The instrument settings were as follows: repetition time (TR) = 31 ms, echo time (TE) = 2.8 ms, number of averages (NEX) = 4, field of view (FOV) = 8 cm × 8 cm, in-plane resolution = 408 × 312 µm, slice thickness = 2 mm, number of movie frames = 5. Prospective gating was achieved using SAII monitoring and gating systems (SA Instruments, Stony Brook, NY, USA).

Resultant CINE MRI sequences were analyzed for left ventricular ejection fraction, wall thickness, and volume using the freely available software Segment v1.8 (Segment; http://segment.heiberg.se) [21]. The left ventricle was analyzed in a semi-automated manner by an investigator blinded to the treatment groups. Wall thickness was measured at the mid-ventricular level in a short-axis view at end diastole and end systole. Measurements of left ventricle end diastolic and end systolic volume were calculated from one 2 mm slice at the height of the base of the papillary muscles in order to normalize across groups.

3.3.6 Histology and Immunohistochemistry

The day after MRI, rats were sacrificed by overdose of isoflurane gas inhalation. The hearts were excised, perfused with 20 ml of Heparin-PBS, 20 ml of 2.56 M KCl, 20 ml of 10% formalin, and fixed in 10% formalin at 4 °C till sectioning. Hearts were sectioned sagittally via the LV into 4 µm sections. Immunohistochemical staining was performed on the sections of formalin-fixed, paraffin-embedded tissue. Sections were air-dried at room temperature and then placed in a 60 °C oven for 30 minutes to melt the paraffin. All of the staining steps were performed at 37 °C using an automated immunostainer (BenchMark® XT, Ventana Medical Systems, Tucson, AZ).

Collagen in the heart sections was stained using Masson's trichrome. The infarct size of myocardium was calculated by the total infarction area divided by the total LV area using a Zeiss Stemi 2000-C Stereo Microscope (Edmund Optics Inc. Barrington, NJ, USA). To evaluate the arteriolar and capillary density and the loss of cardiomyocytes with the myocardial infarction, heart sections were immunohistochemically stained using α-smooth muscle actin, endocardial cell specific CD31 (Purified Mouse Anti-Rat CD31, Abcam), and cardiomyocyte specific cTnT (Monoclonal Anti-Troponin T antibody, Sigma). The sections were detected using the IView DAB detection kit-research (Ventana Medical Systems), which is an open secondary, Streptavidin-HRP system, utilizing DAB (3-3' diaminobenzidine) as the chromogen. The sections were counterstained with hematoxylin (Ventana Medical Systems) for 4 minutes.

Capillaries positive for CD31 and α-smooth muscle actin-positive arterioles over the infarcted region were counted in five random high power fields (hpf) per specimen as the average number of capillaries per field (Nikon Eclipse TE300 Microscope). Arterioles were defined as vessels with an internal diameter of <50 μm; vessels with a diameter of <10 μm were considered capillaries. The loss or recovery of cardiomyocytes by cTnT staining was determined throughout the border zone of five hpf per specimen. The determination of apoptosis was performed using a commercially available kit (ApopTag Apoptosis Detection Kit, Intergen). Apoptosis in the infarcted regions was examined in five random hpf per section. For all the histology, every hpf was randomly chosen within the infarct border zone by an investigator blinded to the treatment groups. Analysis of all images was carried out with NIH ImageJ software (NIH, Bethesda, MD).

3.3.7 Statistical Analysis

Results are expressed as the mean value ± standard error of the mean (SEM). Differences between groups were identified by one-way analysis of variance (ANOVA) followed by Tukey *post hoc* analysis to identify significance between groups using GraphPad Prizm 4.03 software (GraphPad Software, La Jolla, CA). Statistical shorthand of $P < 0.05$, $P < 0.01$, and $P < 0.001$ are indicated as *, **, and ***, respectively, throughout the manuscript figures.

3.4 Results

An acute myocardial infarction (MI) model was used to evaluate the therapeutic efficacy of VEGF-transfected skeletal primary myoblasts. Myocardial infarction in Sprague-Dawley rats was induced by ligation of the left anterior descending coronary (LAD) artery as previously described [22]. Animals were randomly placed into one of four groups: thoracotomy only (n = 5 short-term study, n = 5 long-term study), thoracotomy followed by ligation only (n = 5 short-term study, n = 7 long-term study), thoracotomy with ligation followed by injection of primary untransfected myoblasts (n = 5 short-term study, n = 7 long-term study), and thoracotomy with ligation followed by injection with primary myoblasts transfected with poly(CBA-DAH)/pCMV-$VEGF_{165}$ (n = 5 short-term study, n = 7 long-term study). The primary myoblasts were transfected with poly(CBA-DAH)/pCMV-$VEGF_{165}$ at a 20:1 w/w ratio 24 hours before surgery and the transfected cells were injected at the border zone of the infarction. Our previously published results have demonstrated the efficacy of this approach in successfully transfecting primary myoblasts and achieving sustained VEGF expression and secretion [17].

3.4.1 Short-Term VEGF Expression Study

To determine whether transfected primary myoblast transplantation affected VEGF expression, the levels of VEGF in hearts with acute myocardial infarction were measured using an ELISA assay three days following surgery.

VEGF levels in the ligation only group averaged 15.6 ± 6.3 pg/g heart tissue, while levels in the untransfected myoblast group averaged 33.7 ± 8.5 pg/g heart tissue. The VEGF-transfected myoblast transplantation group showed a much higher level of VEGF expression than both the ligation only and untransfected myoblast groups (66.3 ± 8.1 pg/g, $P < 0.001$ *vs.* ligation only, $P < 0.05$ *vs.* myoblast only) (Figure 3.1). Detection of human $VEGF_{165}$ in the ligation only and untransfected myoblast groups was most likely due to cross-reactivity between human VEGF and endogenous rat VEGF.

3.4.2 Cardiac MRI Analysis

Four weeks following treatment, cardiac MRI was performed on all animals. The thoracotomy only group had an LV ejection fraction of $67.56 \pm 2.86\%$, which falls within the range of expected ejection fractions for normal rat hearts [23]. The hearts that underwent ligation of the LAD to induce a myocardial infarction followed by injection of VEGF-transfected myoblasts showed no significant decrease in LV ejection fraction ($61.68 \pm 2.83\%$) compared to the control, i.e., thoracotomy only, animals. Compared to both the thoracotomy only and $VEGF_{165}$-transfected myoblast injection groups, the LV ejection fraction was significantly decreased in both the ligation only ($48.18 \pm 2.53\%$, $P < 0.01$) and untransfected myoblast injection ($48.02 \pm 1.68\%$, $P < 0.01$) groups (Figure 3.2a).

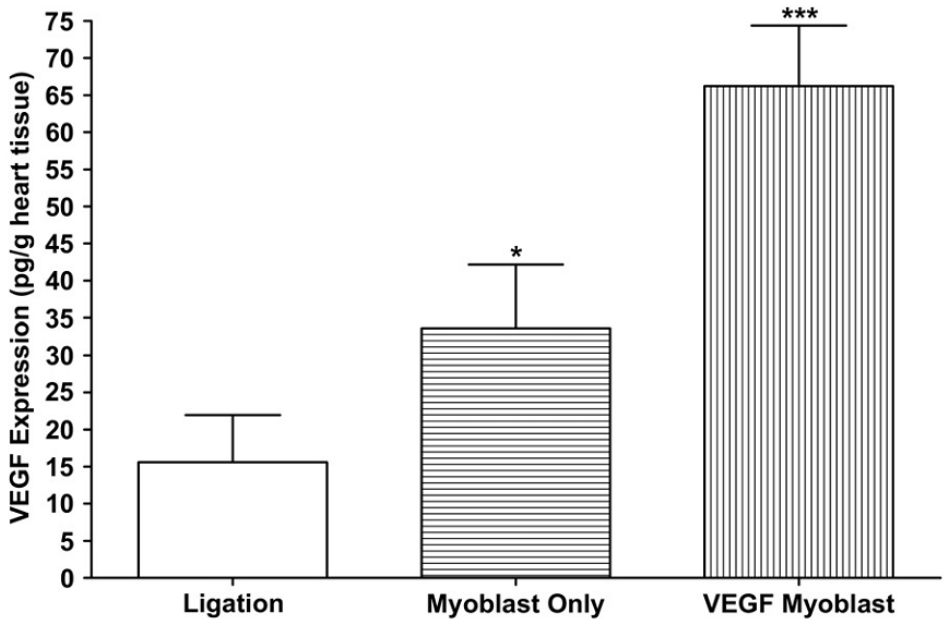

Figure 3.1. Human VEGF expression in rat hearts three days after surgery as measured by ELISA. VEGF levels were significantly higher in the $VEGF_{165}$-transfected myoblast group than the ligation and myoblast only groups ($P<0.001$ *vs* ligation; $P<0.05$ *vs* myoblast only). All data are presented as mean values ± SEM (n=8 ligation, n=8 myoblast only, n=8 VEGF myoblast group).

Measurement of end diastolic volume (EDV) and end systolic volume (ESV) revealed a similar trend, with the VEGF-transfected myoblast treatment group showing no significant increase in EDV or ESV compared to the thoracotomy only control group (EDV, 81.2 ± 3.9 µl *vs*. 75.55 ± 10.3 µl, respectively and ESV 24.9 ± 3.8 µl *vs*. 24.2 ± 0.7 µl, respectively). The ligation only control group (EDV, 113.0 ± 4.0 µl; ESV 42.3 ± 3.7 µl) and untransfected myoblast treatment group (EDV, 110.7 ± 6.2 µl; ESV 42.4 ± 3.7 µl) displayed significant increases in EDV and ESV over the 4-week time period compared to both the thoracotomy only and VEGF-transfected myoblast treatment groups ($P < 0.01$, both groups) (Figures 3.2b, c).

The final cardiac parameters measured from MRI were end diastolic wall thickness (EDWT) and end systolic wall thickness (ESWT). The thoracotomy only control group and VEGF-transfected myoblast treatment group showed no difference in wall thickness in either diastole or systole (EDWT, 2.91 ± 0.18 mm *vs*. 2.73 ± 0.09 mm, respectively; ESWT, 3.94 ± 0.13 mm *vs*. 3.98 ± 0.19 mm, respectively). The ligation only and the untransfected myoblast treatment groups displayed significant thinning of the left ventricular wall at both end diastole (EDWT, 2.09 ± 0.09 mm and 2.14 ± 0.10 mm, respectively) and end systole (ESWT, 2.91 ± 0.14 mm and 2.73 ± 0.12 mm, respectively) compared to the thoracotomy only ($P < 0.001$) and VEGF-transfected myoblast treatment groups ($P < 0.001$), (Figure 3.2d).

3.4.3 Effect of Transfected Myoblast Transplantation on Infarct Size

Four weeks following surgery, hearts were cut sagittally and stained with Masson's trichrome. Figures 3.3b–e show representative Masson's trichrome staining in rat hearts from the following groups: thoracotomy only (Figure 3.3b); ligation only (no

Figure 3.2. Cardiac parameters measured by MRI four weeks after treatment. (a) Cardiac ejection fraction. Both the VEGF myoblast and thoracotomy control groups displayed significantly higher ejection fractions than the ligation and myoblast only groups ($P < 0.01$). There was no significant difference in ejection fraction between the thoracotomy control group and the $VEGF_{165}$-transfected myoblast group. (b) End diastolic volume (EDV). EDV significantly increased in the ligation and myoblast only groups compared to both thoracotomy controls and $VEGF_{165}$-transfected myoblasts ($P < 0.01$). There was no significant increase in EDV between thoracotomy controls and the VEGF myoblast group. (c) End systolic volume (ESV). ESV significantly increased in the ligation and myoblast only groups compared to both thoracotomy controls and $VEGF_{165}$-transfected myoblasts ($P < 0.05$). There was no significant increase in ESV between thoracotomy controls and the VEGF myoblast group. (d) End diastolic wall thickness (EDWT) four weeks post treatment. The EDWT significantly decreased in the ligation and myoblast only groups compared to both thoracotomy controls and $VEGF_{165}$-transfected myoblasts ($P < 0.001$). There was no significant decrease in EDWT between thoracotomy controls and the VEGF myoblast group. (e) End systolic wall thickness (ESWT). ESWT significantly decreased in the ligation and myoblast only groups compared to both thoracotomy controls and $VEGF_{165}$-transfected myoblasts ($P<0.001$). There was no significant decrease in ESWT between thoracotomy controls and the VEGF myoblast group. All data are presented as mean ± SEM (n = 5 thoracotomy, n = 7 ligation, n = 7 myoblast only, and n = 7 VEGF myoblast group).

a

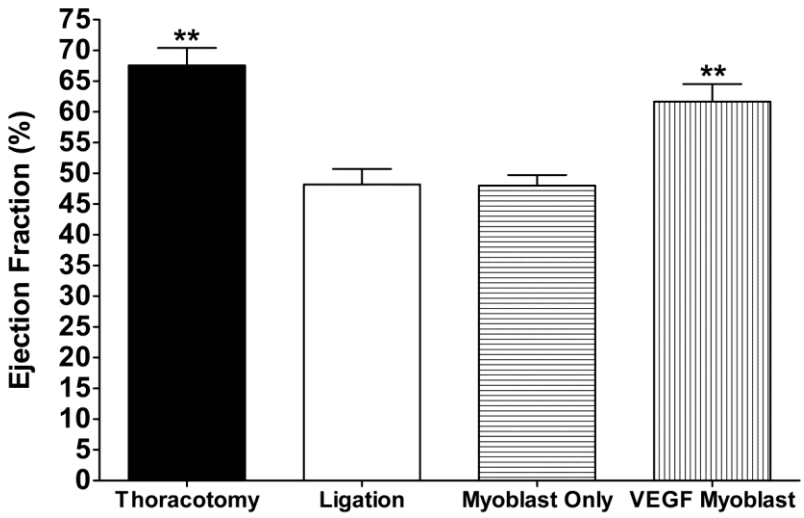
Ejection Fraction (%)
75
70
65
60
55
50
45
40
35
30
25
20
15
10
5
0
**
**
Thoracotomy
Ligation
Myoblast Only
VEGF Myoblast

b

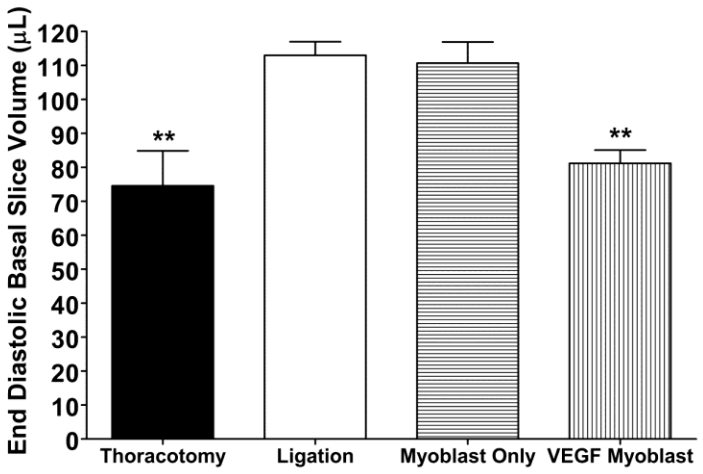

c

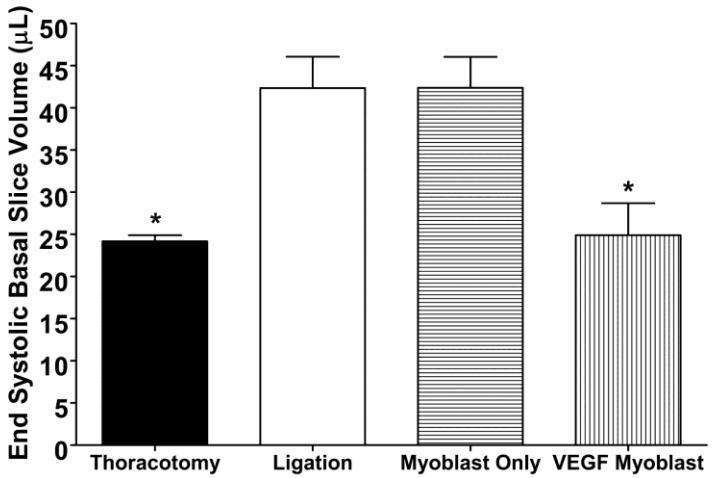

Figure 3.2. Continued.

d

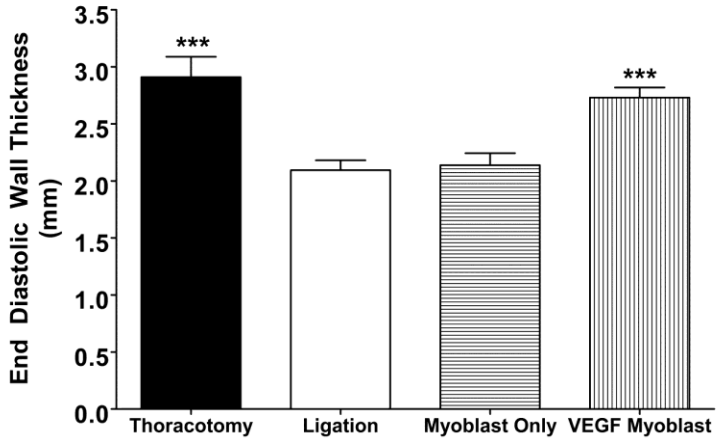

e

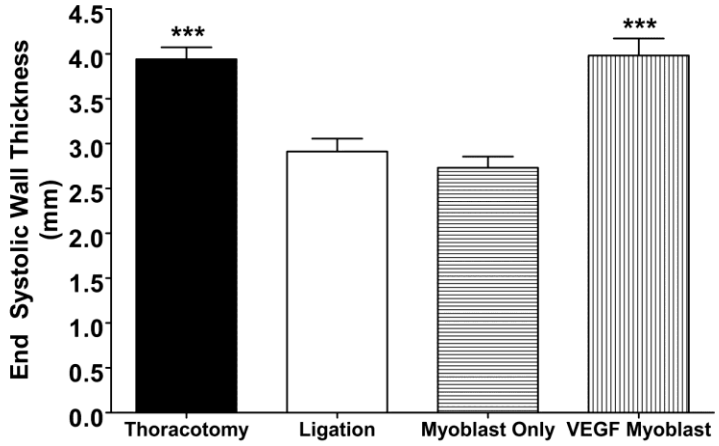

Figure 3.2. Continued.

injection, Figure 3.3c); injection of untransfected primary myoblasts only (Figure 3.3d); and injection of primary myoblasts transfected with poly(CBA-DAH)/pCMV-$VEGF_{165}$ (Figure 3.3e). On Masson's trichrome staining, the infarct scar, characterized by high collagen content, is indicated by bluish staining. Ligation only, without treatment, resulted in infarction of 32.8 ± 7.4% of the left ventricle (Figure 3.3a). With injection of untransfected primary myoblasts, the infarct size decreased to 14.9 ± 1.2% of the left ventricle ($P < 0.05$ versus ligation only group). With injection of VEGF transfected myoblasts, the infarct size was further reduced to only 5.4 ± 3.3% of the left ventricle, ($P < 0.001$ versus the ligation only group).

3.4.4 Enhancement of Vascular Density in Ischemic Myocardium

Capillary endothelial cells were detected by immunostaining of the infarcted myocardium with antibodies to CD31. Capillaries positive for CD31 were counted in 5 random microscope high power fields (hpf) in the ischemic border zone of each section, and capillary density was expressed as the average number of capillaries per field. As shown in representative micrographs of sections from each treatment group (Figures 3.4 c–j), an increased number of capillaries and arterioles were present in the $VEGF_{165}$-transfected myoblast injection group than in the thoracotomy only, ligation only or untransfected myoblast injection groups. As shown in Figure 3.4a, immunohistochemical staining for smooth muscle α-actin (SMA) revealed more arterioles present in the VEGF transfected myoblast treatment group than any of the other groups. Mean arterioles positive for SMA per hpf increased from 9.2 ± 1.0 in the ligation only group to 20.4 ± 1.9 in the VEGF transfected myoblast group ($P < 0.05$). Mean capillaries positive for CD31 per hpf in the VEGF transfected myoblast group (13.6 ± 1.2) were significantly higher

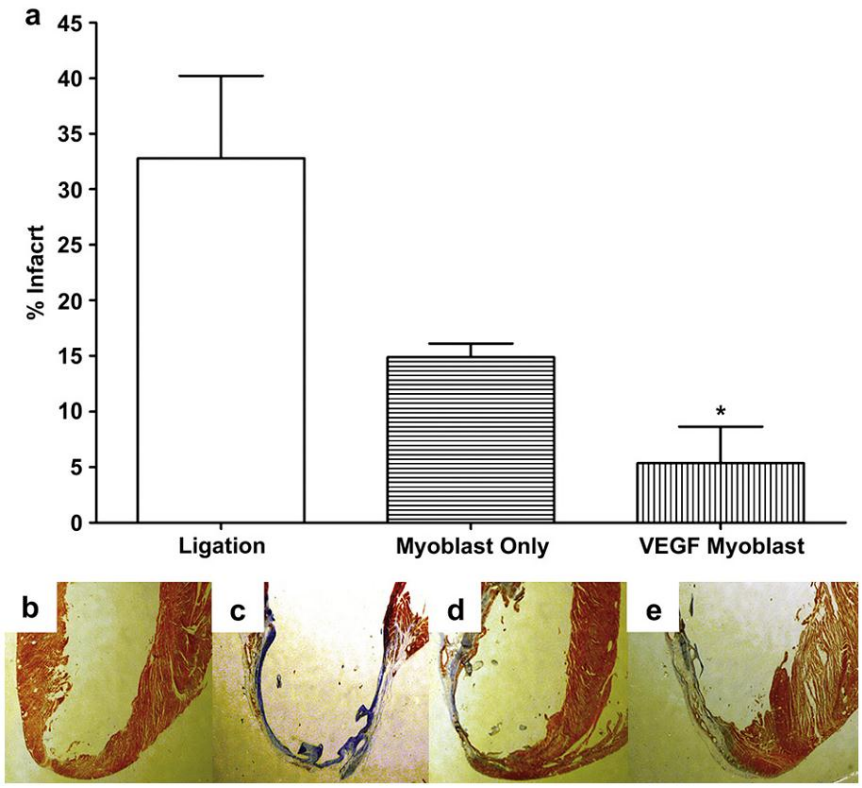

Figure 3.3. Masson's trichrome staining for infarct size, four weeks after surgery. (a) Infarcted area as a percentage of the left ventricle. $P < 0.05$ for ligation only versus VEGF myoblast group (b–e) Representative myocardial tissue sections stained with Masson's trichrome. Bluish staining indicates high collagen content, indicating infarction; (b) Thoracotomy only, control group, (c) ligation only, (d) untransfected myoblast injection group, (e) $VEGF_{165}$-transfected myoblast injection group. All data are presented as mean ± SEM (n = 5 thoracotomy, n = 7 ligation, n = 7 myoblast only, and n = 7 VEGF myoblast group).

($P < 0.05$) than in the thoracotomy only (4.1 ± 0.3), ligation only (5.2 ± 0.4) and untransfected myoblast (8.5 ± 0.8) groups (Figure 3.4b).

3.4.5 Cardiomyocyte Loss in Myocardial Infarction

Immunohistochemical staining 4 weeks after surgery was used to identify troponin T (cTnT) in rat heart myocardium. With troponin-T (cTnT) immunostaining, necrotic cardiomyocytes lose their normal brownish staining. As shown in Figure 3.5, cTnT in the left ventricular infarct zone was barely visible in the primary $VEGF_{165}$-transfected myoblast group ($6.9 \pm 0.9\%$), and not significantly different than the thoracotomy only control group ($9.0 \pm 1.7\%$). There was a significant increase in the number of cardiomyocytes lost in the ligation only ($65.9 \pm 4.8\%$) and untransfected myoblast ($34.2 \pm 5.1\%$) groups.

3.4.6 Reduction of Apoptotic Activity in Ischemic Myocardium

Apoptotic activity in the infarcted myocardium after treatment was measured by TUNEL staining. Figure 3.6 compares representative images of the TUNEL staining from the ischemic region in the left ventricle following thoracotomy only, ligation only, untransfected myoblast injection and $VEGF_{165}$-transfected myoblast injection. Five random hpf in the ischemic border zone were selected and TUNEL-positive cells were counted. TUNEL-positive cells per hpf were 27.5 ± 2.3 in the ligation only group and 21.6 ± 2.0 in the untransfected myoblast group. The number of TUNEL-positive cells in the infarcted zone was significantly reduced in the VEGF-transfected myoblast group (11.9 ± 1.4, $P < 0.001$ *vs.* ligation only).

Figure 3.4. Representative immunohistochemistry stains for SM α-actin and CD31 in the infarct border zone, 4-weeks after myocardial infarction. (c, g) Thoracotomy only, (d, h) ligation only, (e, i) untransfected myoblast injection and (f, j) $VEGF_{165}$-transfected myoblast injection group. (a) Average number of smooth muscle actin (SMA)-positive arterioles from five random high-power fields (hpf) per animal from the ischemic border zone of the infarct. The number of arterioles in the $VEGF_{165}$-transfected myoblast group was significantly greater than all other groups $P < 0.001$. (b) Average number of CD31-positive capillaries from five random hpf per animal from the ischemic border zone of the infarct. The number of capillaries in the $VEGF_{165}$-transfected myoblast group was significantly greater than all other groups $P < 0.001$. The average number of capillaries in the myoblast only group was significantly higher than both thoracotomy and ligation groups; $P < 0.01$ and $P < 0.05$, respectively. All data are presented as mean ± SEM (n = 5 thoracotomy, n = 7 ligation, n = 7 myoblast only, and n = 7 VEGF myoblast group).

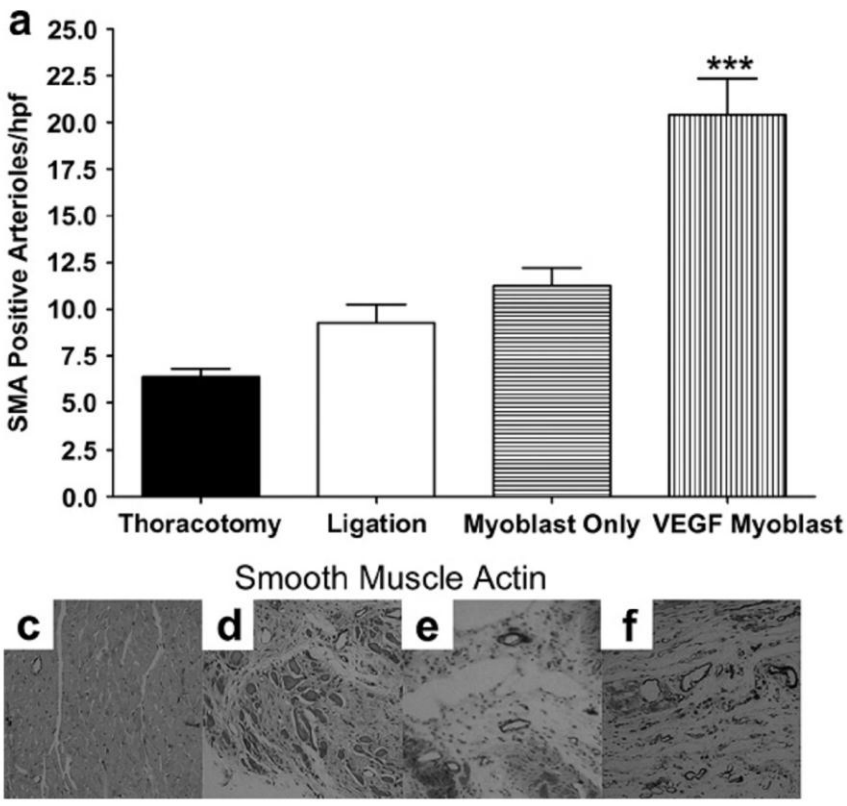
a
25.0
22.5
20.0
17.5
15.0
12.5
10.0
7.5
5.0
2.5
0.0
SMA Positive Arterioles/hpf
***
Thoracotomy
Ligation
Myoblast Only
VEGF Myoblast
Smooth Muscle Actin
c
d
e
f

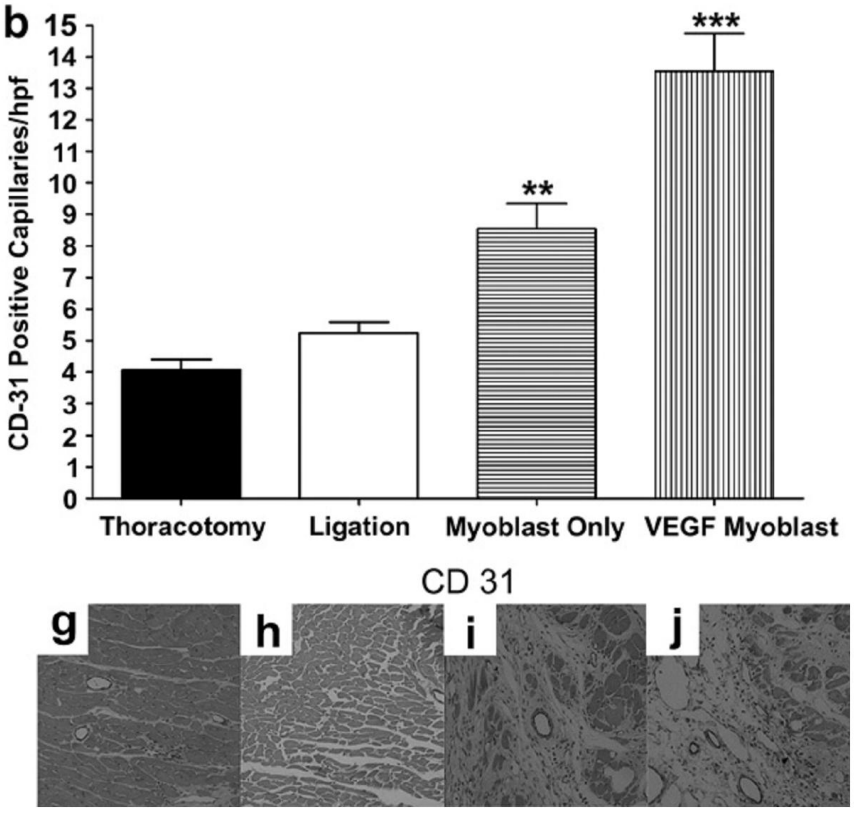

Figure 3.4. Continued.

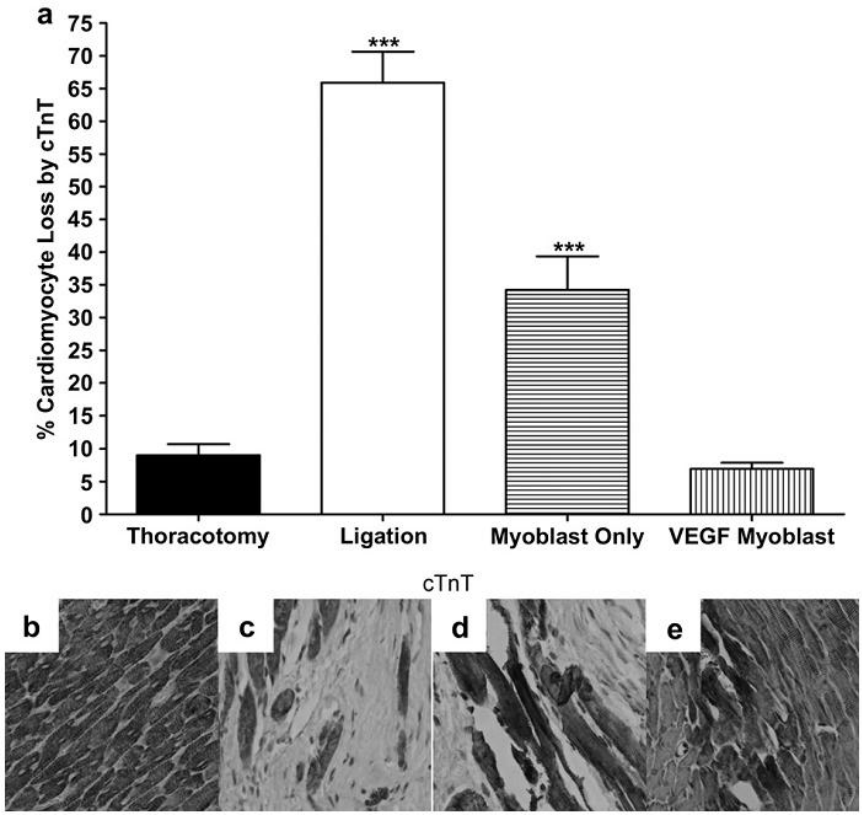

Figure 3.5. The loss of cardiomyocytes, 4-weeks after surgery as indicated by loss of immunohistochemical staining for cTnT; (a) Loss of cardiomyocytes from the infarct border zone 4-weeks after surgery identified from cTnT staining and represented as percent cardiomyocytes lost per hpf. Five random hpf were counted per animal. The loss of cardiomyocytes was significantly prevented in both the myoblast only group ($P < 0.001$ *vs.* ligation) and the VEGF myoblast group ($P < 0.001$ *vs.* ligation and myoblast only). Additionally, the ligation and myoblast only groups were statistically greater than the thoracotomy control ($P < 0.001$), whereas the VEGF myoblast treatment group was not statistically different from thoracotomy control. Representative micrographs of cTnT staining for (b) thoracotomy control group, (c) ligation, (d) myoblast only injection group and (e) $VEGF_{165}$-transfected myoblast injection group. With cell death, myofibers lose their usual normal brownish staining. All data are presented as mean ± SEM (n = 5 thoracotomy, n = 7 ligation, n = 7 myoblast only, and n = 7 VEGF myoblast group).

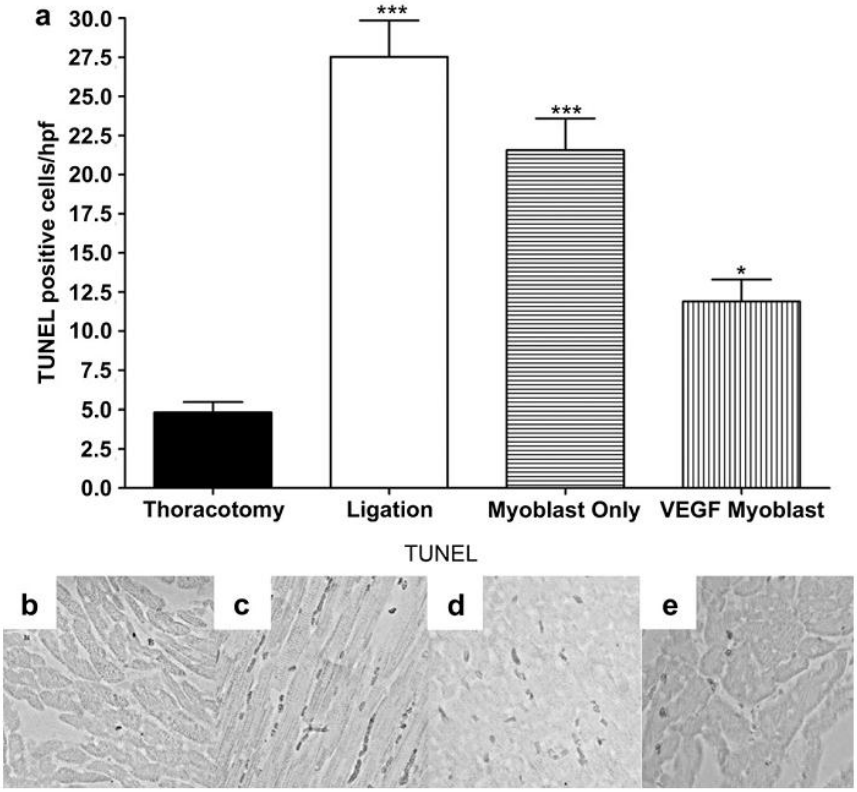

Figure 3.6. TUNEL staining for apoptotic activity, 4-weeks after surgery. (a) TUNEL staining for apoptotic cells 4-weeks after surgery. TUNEL-positive apoptotic cells were counted in the five random hpf per animal in the ischemic border zone. The average number of apoptotic cells was statistically greater between thoracotomy control and all groups with less significance between thoracotomy and the VEGF myoblast group. ($P < 0.001$ thoracotomy *vs.* ligation and myoblast only; $P < 0.05$ between thoracotomy and VEGF myoblast group). The VEGF myoblast group had significantly fewer apoptotic cells than the ligation group ($P < 0.001$) and the myoblast only group ($P < 0.01$). There was no significant difference between the myoblast only treatment group and ligation controls. Representative micrographs of apoptotic nuclei by TUNEL staining in (b) thoracotomy control group, (c) ligation, (d) myoblast only injection group and (e) $VEGF_{165}$-transfected myoblast injection group. All data are presented as mean ± SEM (n = 5 thoracotomy, n = 7 ligation, n = 7 myoblast only, and n = 7 VEGF myoblast group).

3.5 Discussion

Exogenous primary myoblast transplantation into ischemic myocardium offers many potential benefits for the treatment of myocardial infarction, including improvement and restoration of cardiac function. The improvement in cardiac function is thought to be due to the enhancement of the contractile properties of endogenous cardiomyocytes and the differentiation and proliferation of implanted myoblasts into functional myocardium within ischemic hearts. Recent studies have demonstrated the feasibility of primary myoblast transplantation for the treatment of ischemic heart disease [18, 24]. In addition, we have previously reported that VEGF gene therapy, particularly ischemia-inducible VEGF gene therapy, significantly improves myocardial function and reduces left ventricular infarct size following acute myocardial infarction [25, 26]. Because ischemic heart disease is characterized by reduced blood supply to the myocardium, therapeutic angiogenesis using angiogenic growth factors like VEGF may restore blood supply by stimulating neovascularization. Excessive VEGF expression, however, has been associated with heart failure and death, due to vascular tumor formation instead of the formation of functioning vessels [27]. We have reported that the new poly(disulfide amine)s, poly(CBA-DAH) and poly(CBA-DAH-R), are efficient and nontoxic polymeric gene carriers for the transfection of primary myoblasts and that they mediate controlled and optimal VEGF expression. Our previous studies laid the foundation for this current study by demonstrating the functional benefit of this approach for treating acute myocardial infarction in an *in vivo* rat model [17].

In the present study, VEGF-transfected myoblasts induced angiogenesis in a paracrine fashion. Immunostaining for capillaries in the ischemic zone revealed that

neovascularization was more pronounced around the injection sites in the infarct border zone. This enhancement of capillary and arteriolar density in the left ventricle by VEGF-transfected myoblasts correlated with VEGF expression levels (Figure 3.1), and resulted in a decrease in infarct size and preservation of ventricular function.

Mechanisms by which implanted myoblasts may improve ischemic heart function include: 1) reinforcement of the ventricular wall and 2) limitation of postinfarct scar expansion through strengthening and enhancement of the extracellular matrix.[1, 24] In addition, one of the major routes of cardiomyocyte loss in myocardial infarction is via apoptosis and necrosis, resulting in heart failure. There are several reports which show that cTnT staining levels in the infarcted myocardium are highly correlated with infarct size and can be used as a useful biomarker to detect myocardial injury [28, 29]. As a result of its high cardiac specificity, cTnT immuno-staining can identify myocardial damage, especially necrosis [30]. As shown by our cTnT immunostaining results, the transplantation of skeletal primary myoblasts transfected with VEGF more efficiently protects against the loss of cardiomyocytes than does injection with untransfected myoblasts. VEGF-transfected myoblast transplantation into ischemic myocardium increases VEGF expression, increases the vascular density of arterioles and capillaries, protects endogenous cardiomyocytes from death by apoptosis and necrosis, and ultimately preserves cardiac function to a significantly greater degree than untransfected myoblast transplantation.

Consistent with our previous *in vitro* study using poly-disulfide polymers and bPEI for the transfection of primary myoblasts, transplantation of poly(CBA-DAH)-VEGF myoblasts demonstrated the utility of a dual therapeutic approach to maintain

cardiac function and inhibit left ventricular remodeling after myocardial infarction. The sustained VEGF release from skeletal myoblasts resulted in: 1) increased vessel density and 2) decreased apoptosis and cardiomyocyte loss.

3.6 Conclusions

In conclusion, our study demonstrates the enhanced angiogenic efficacy of VEGF-transfected myoblasts using the bioreducible cationic polymer poly(CBA-DAH) as a transfection agent. Treatment with poly(CBA-DAH)/VEGF-transfected myoblasts preserved cardiac wall thickness, restored left ventricular function, induced neovascularization and reduced cardiac apoptosis more effectively than untransfected myoblasts. This work demonstrates that combining cellular implantation therapies with gene therapy can potentially increase the efficacy of surgical implantation of cells and produce better patient outcomes. Additionally, this work illustrates the *in vivo* safety and efficacy of poly(CBA-DAH) when used in combination with implanted cells.

3.7 Acknowledgements

This work was supported by NIH grants HL071541 (D.A.B.) and HL065477 (S.W.K.). The authors would also like to thank Sheryl Tripp of ARUP laboratories and Aida Garzarelli for their assistance in the preparation of the hearts for immunohistochemistry and histological analysis. All authors have no financial conflicts of interest influencing the work performed in this manuscript.

3.8 References

[1] P. Menasche, Skeletal myoblasts and cardiac repair, J. Mol. Cell. Cardiol., 45 (2008) 545-553.

[2] P. Menasche, A.A. Hagège, J.-T. Vilquin, M. Desnos, E. Abergel, B. Pouzet, A. Bel, S. Sarateanu, M. Scorsin, K. Schwartz, P. Bruneval, M. Benbunan, J.-P. Marolleau, D. Duboc, Autologous skeletal myoblast transplantation for severe postinfarction left ventricular dysfunction, J. Am. Coll. Cardiol., 41 (2003) 1078-1083.

[3] D.A. Taylor, Cellular cardiomyoplasty with autologous skeletal myoblasts for ischemic heart disease and heart failure, Curr. Control. Trials Cardiovasc. Med., 2 (2001) 208-210.

[4] T. Hoashi, G. Matsumiya, S. Miyagawa, H. Ichikawa, T. Ueno, M. Ono, A. Saito, T. Shimizu, T. Okano, N. Kawaguchi, N. Matsuura, Y. Sawa, Skeletal myoblast sheet transplantation improves the diastolic function of a pressure-overloaded right heart, J. Thorac. Cardiovasc. Surg., 138 (2009) 460-467.

[5] F.D. Pagani, H. DerSimonian, A. Zawadzka, K. Wetzel, A.S. Edge, D.B. Jacoby, J.H. Dinsmore, S. Wright, T.H. Aretz, H.J. Eisen, K.D. Aaronson, Autologous skeletal myoblasts transplanted to ischemia-damaged myocardium in humans. Histological analysis of cell survival and differentiation, J. Am. Coll. Cardiol., 41 (2003) 879-888.

[6] H. Reinecke, E. Minami, V. Poppa, C.E. Murry, Evidence for fusion between cardiac and skeletal muscle cells, Circ. Res., 94 (2004) e56-60.

[7] M.G. Engelmann, W.M. Franz, Stem cell therapy after myocardial infarction: ready for clinical application?, Curr. Opin. Mol. Ther., 8 (2006) 396-414.

[8] P. Menasche, Skeletal myoblasts as a therapeutic agent, Prog. Cardiovasc. Dis., 50 (2007) 7-17.

[9] Y. Lei, H. Haider, J. Shujia, E.S. Sim, Therapeutic angiogenesis. Devising new strategies based on past experiences, Basic Res. Cardiol., 99 (2004) 121-132.

[10] T.D. Henry, B.H. Annex, G.R. McKendall, M.A. Azrin, J.J. Lopez, F.J. Giordano, P.K. Shah, J.T. Willerson, R.L. Benza, D.S. Berman, C.M. Gibson, A. Bajamonde, A.C. Rundle, J. Fine, E.R. McCluskey, The VIVA trial: vascular endothelial growth factor in ischemia for vascular angiogenesis, Circulation, 107 (2003) 1359-1365.

[11] H. Haider, L. Ye, S. Jiang, R. Ge, P.K. Law, T. Chua, P. Wong, E.K. Sim, Angiomyogenesis for cardiac repair using human myoblasts as carriers of human vascular endothelial growth factor, J. Mol. Med., 82 (2004) 539-549.

[12] T.K. Rosengart, L.Y. Lee, S.R. Patel, T.A. Sanborn, M. Parikh, G.W. Bergman, R. Hachamovitch, M. Szulc, P.D. Kligfield, P.M. Okin, R.T. Hahn, R.B. Devereux, M.R. Post, N.R. Hackett, T. Foster, T.M. Grasso, M.L. Lesser, O.W. Isom, R.G. Crystal,

Angiogenesis gene therapy: phase I assessment of direct intramyocardial administration of an adenovirus vector expressing VEGF121 cDNA to individuals with clinically significant severe coronary artery disease, Circulation, 100 (1999) 468-474.

[13] M.I. Niagara, H. Haider, L. Ye, V.S. Koh, Y.T. Lim, K.K. Poh, R. Ge, E.K. Sim, Autologous skeletal myoblasts transduced with a new adenoviral bicistronic vector for treatment of hind limb ischemia, J. Vasc. Surg., 40 (2004) 774-785.

[14] K. Suzuki, B. Murtuza, R.T. Smolenski, I.A. Sammut, N. Suzuki, Y. Kaneda, M.H. Yacoub, Cell transplantation for the treatment of acute myocardial infarction using vascular endothelial growth factor-expressing skeletal myoblasts, Circulation, 104 (2001) I207-212.

[15] A. Germani, A. Di Carlo, A. Mangoni, S. Straino, C. Giacinti, P. Turrini, P. Biglioli, M.C. Capogrossi, Vascular endothelial growth factor modulates skeletal myoblast function, Am. J. Pathol., 163 (2003) 1417-1428.

[16] L. Ye, H. Kh Haider, R. Tan, W. Toh, P.K. Law, W. Tan, L. Su, W. Zhang, R. Ge, Y. Zhang, Y. Lim, E.K.W. Sim, Transplantation of nanoparticle transfected skeletal myoblasts overexpressing vascular endothelial growth factor-165 for cardiac repair, Circulation, 116 (2007) I-113-120.

[17] M. Ou, T.I. Kim, J.W. Yockman, B.A. Borden, D.A. Bull, S.W. Kim, Polymer transfected primary myoblasts mediated efficient gene expression and angiogenic proliferation, J. Control. Release, 142 (2010) 61-69.

[18] G. von Degenfeld, A. Banfi, M.L. Springer, H.M. Blau, Myoblast-mediated gene transfer for therapeutic angiogenesis and arteriogenesis, Br. J. Pharmacol., 140 (2003) 620-626.

[19] A. Banfi, M.L. Springer, H.M. Blau, Myoblast-mediated gene transfer for therapeutic angiogenesis, Methods Enzymol., 346 (2002) 145-157.

[20] M. Ou, X.L. Wang, R. Xu, C.W. Chang, D.A. Bull, S.W. Kim, Novel biodegradable poly(disulfide amine)s for gene delivery with high efficiency and low cytotoxicity, Bioconjug. Chem., 19 (2008) 626-633.

[21] E. Heiberg, L. Wigstrom, M. Carlsson, A. Bolger, M. Karlsson, Time resolved three-dimensional automated segmentation of the left ventricle, Comput. Cardiol., (2005) 599-602.

[22] N.F. Huang, R.E. Sievers, J.S. Park, Q. Fang, S. Li, R.J. Lee, A rodent model of myocardial infarction for testing the efficacy of cells and polymers for myocardial reconstruction, Nat. Protocols, 1 (2006) 1596-1609.

[23] K. Montet-Abou, J.L. Daire, M.K. Ivancevic, J.N. Hyacinthe, D. Nguyen, M. Jorge-Costa, D.R. Morel, J.P. Vallee, Optimization of cardiac cine in the rat on a clinical 1.5-T MR system, MAGMA, 19 (2006) 144-151.

[24] P. Menasche, Skeletal muscle satellite cell transplantation, Cardiovasc. Res., 58 (2003) 351-357.

[25] D.A. Bull, S.H. Bailey, J.J. Rentz, J.S. Zebrack, M. Lee, S.E. Litwin, S.W. Kim, Effect of Terplex/VEGF-165 gene therapy on left ventricular function and structure following myocardial infarction: VEGF gene therapy for myocardial infarction, J. Control. Release, 93 (2003) 175-181.

[26] J.W. Yockman, D. Choi, M.G. Whitten, C.W. Chang, A. Kastenmeier, H. Erickson, A. Albanil, M. Lee, S.W. Kim, D.A. Bull, Polymeric gene delivery of ischemia-inducible VEGF significantly attenuates infarct size and apoptosis following myocardial infarct, Gene Ther., 16 (2009) 127-135.

[27] R.S. Ernst, T.S. Mark, P. Mike, S.H. Sharon, M.I. Jeffrey, H.K. Laurence, A.K. Robert, Evaluation of the effects of intramyocardial injection of DNA expressing vascular endothelial growth factor (VEGF) in a myocardial infarction model in the rat? Angiogenesis and angioma formation, J. Am. Coll. Cardiol., 35 (2000) 1323-1330.

[28] P.J. O'Brien, D.E.C. Smith, T.J. Knechtel, M.A. Marchak, I. Pruimboom-Brees, D.J. Brees, D.P. Spratt, F.J. Archer, P. Butler, A.N. Potter, J.P. Provost, J. Richard, P.A. Snyder, W.J. Reagan, Cardiac troponin I is a sensitive, specific biomarker of cardiac injury in laboratory animals, Lab Anim., 40 (2006) 153-171.

[29] V. Ricchiuti, J. Zhang, F.S. Apple, Cardiac troponin I and T alterations in hearts with severe left ventricular remodeling, Clin. Chem., 43 (1997) 990-995.

[30] S.H. Hansen, K. Rossen, Evaluation of cardiac troponin I immunoreaction in autopsy hearts: a possible marker of early myocardial infarction, Forensic Sci. Int., 99 (1999) 189-196.

CHAPTER 4

SIRNA-MEDIATED KNOCKDOWN OF BNIP3 IN RAT CARDIOMYOCYTES USING AN EFFICIENT AND NONTOXIC POLYMER GENE CARRIER

4.1 Abstract

Nonviral polymer gene carriers are a valuable tool for achieving nucleic acid delivery to a variety of cell types with high efficiency and low cytotoxicity. Specifically, bioreducible, disulfide-containing cationic polymers have been demonstrated to mediate transfection in difficult-to-transfect cell types such as primary cardiomyocytes. We tested a variety of novel bioreducible gene carriers for their ability to deliver DNA to rat cardiomyocytes efficiently while displaying low cytotoxicity. We also evaluated the ability of these polymers to condense nucleic acids into compact nanoparticles to protect from degradation. A variety of siRNA sequences towards BNIP3, a novel apoptotic target, were screened to identify the sequence with the greatest potency in knocking down BNIP3 mRNA levels. Upregulation of BNIP3 has been shown to play an important role in predisposing cardiomyocytes to premature cell death following myocardial infarction, and is known to be a potent mediator of apoptosis, autophagy, and necrosis in cardiomyocytes. We demonstrated that *in vitro* knockdown of BNIP3 siRNA in rat primary cardiomyocytes protected the cells from hypoxic cell death, increasing cellular viability and function while decreasing apoptotic/necrotic cell death. This work

highlights both the utility of bioreducible polymers to transfect primary cardiomyocytes and the potential for BNIP3 inhibition to become a therapeutic strategy to limit hypoxic-cell death in the myocardium.

4.2 Introduction

The potential of genetic manipulation in treating human disease has been hypothesized almost since the discovery of DNA as the carrier of genetic information. Actual attempts at gene therapy in humans have been investigated for over 40 years now for its potential to treat a variety of human diseases [1, 2]. Classically, gene delivery has been accomplished using either physical methods such as electroporation or direct naked polynucleotide injection, or using attenuated viruses to deliver the genetic payload. The physical methods, however, are limited due to their impracticality and low efficiencies [3, 4]. The viral methods have received a great deal more attention, but problems still arise due to the immunogenic nature of viruses, difficulty in manufacture and quality control, and in the potential for insertional mutagenesis with some vectors [5].

Nonviral chemical methods were developed in response to these concerns and limitations and seek to utilize chemicals in the forms of cationic lipids and polymers to act as viral mimetics—protecting nucleic acids while mediating their delivery to target tissues [6]. Of these two methods, cationic polymer gene therapy has emerged as a promising candidate for clinical gene delivery.

Cationic polymers typically contain a high degree of primary, secondary, and tertiary amines, which give the polymer its cationic character and allow it to form nano-sized complexes with nucleic acids via electrostatic interaction between the positively charged amines and the negatively charged nucleotide phosphate backbone. Polymer

characteristic such as molecular weight, degree of branching, amine content, amine pKa, and polydispersity affect the attributes of the condensed polymer/nucleic acid nanoparticle (polyplex). Polyplexes are most efficient when they are approximately 200 nm in diameter with a slight excess positive charge on the particle surface. This size allows for high loading capacity, while allowing for cell entry via endocytosis, while the positive charge encourages interaction with the predominantly negatively charged cell membrane.

The incorporation of bioreducible disulfide bonds into polymer gene carriers was a major innovation in increasing polymer-mediated gene transfer efficiency while decreasing toxicity. The first cationic polymers (such as polyethyleneimine [7] and poly-L-lysine [8]) demonstrated highly efficient gene transfer abilities, but were limited by their high toxicity. A major reason for the high toxicity seen with these carriers is the nondegradable nature of the polymers, which causes cellular accumulation and delayed toxicity [9, 10]. Cationic polymers with hydrolyzable linking units were some of the next major innovations to decrease accumulation-mediated toxicity, but the effectiveness of these polymers is limited by the nonspecific hydrolysis of their bonds and the resultant rapid polymer degradation [11]. Building polymers using disulfide-linked monomers introduces several improvements over other degradable bonds: disulfide bonds are very stable and resistant to degradation in blood and other extracellular sites; however, despite, their strength, they are rapidly reduced via reaction with glutathione in the reductive intracellular cytoplasmic environment.

One of the most common areas for applying gene therapy is cardiovascular disease. Despite significant advances in preventive, pharmacological, and interventional

care, cardiovascular disease remains the most common cause of death in the United States and developed nations [12]. Within the spectrum of cardiovascular diseases, myocardial infarction (MI) is one of the most common and devastating forms of heart disease. The deadliness of the disease is highlighted by the fact that once a patient experiences an MI event, their chance of dying within the next 5 years is 36% if the patient is a man or 47% if the patient is a woman [12]. A large portion of these deaths are due to heart failure caused by left ventricular remodeling, set in motion by the initial MI, where the infarct zone continues to expand long after blood supply has been reestablished [13, 14]. Multiple gene therapy strategies have been attempted to limit adverse left ventricular remodeling, with angiogenic, procontractile, and antiapoptotic therapies being some of the more common approaches [15-18].

In this work, we first set out to identify the polymer transfection agent that displays the highest transfection efficiency of cardiomyocytes while also minimizing cellular toxicity. This polymer was then used in further study to evaluate the effect of siRNA-mediated knockdown of Bcl-2/adenovirus E1B nineteen-kilodalton interacting protein 3 (BNIP3), a proapoptotic protein upregulated specifically under hypoxia [19-21].

4.3 Materials and Methods

4.3.1 Materials

21-mer siRNA sequences were obtained from Thermo Scientific (Waltham, MA, USA). Target sequences were as follows: siRNA 1 [22], 5`-UGAGAGGUAGCAGGGCAGCdTdT-3`; siRNA 2, 5`-UACCAACAGA-GCUGAAAUAdTdT-3`; siRNA 3, 5`-AAACUCAGAUUGGAUAUGGdTdT-3`; siRNA 4, 5`-CAGCUUCCGUCUCUAUUUAdTdT-3`.

4.3.2 Primary Rat Ventricular Cardiomyocyte Isolation

Rat primary cardiomyocytes were isolated from 2-day-old neonatal rats using a commercially available neonatal cardiomyocyte isolation system (Worthington Biochemical, Lakewood, NJ) [23]. Briefly, hearts were quickly excised from rat pups under isoflurane anesthesia, rinsed twice in ice-cold HBSS, and the atria removed, leaving only ventricular myocytes. The ventricles were minced with dissecting scissors and the tissue was digested overnight at 4 °C in 50 µg/ml trypsin. The following day, 2000 µg trypsin inhibitor were added and the myocytes were warmed and digested further with 1,500 Units collagenase at 37 °C for 45 minutes. The tissue was then dissociated gently by pipetting up and down with a 5 ml pipette and strained through a 70 µm cell strainer (BD Falcon, Franklin Lakes, NJ). The cell solution was then centrifuged for 5 minutes at 100× g and the cell pellet resuspended in DMEM media supplemented with 10% horse serum and then plated on rat tail collagen-coated cell culture plates at least 24 hours before use.

4.3.3 Synthesis of ABP and Other Polymers

The arginine-grafted bioreducible polymer (ABP) used in this study was synthesized as previously detailed [24], using the backbone polymer poly(CBA-DAH) synthesized previously in our lab [25]. Briefly, poly(CBA-DAH) was synthesized via Michael reaction of equimolar amounts of *N*-Boc-DAH and CBA in a 9:1 v/v solution of MeOH/H_2O. The reaction was run under nitrogen at 60 °C for 5 days and protected from light. The polymerization was terminated by addition of 10% *N*-Boc-DAH and the reaction was maintained for an additional 2 days. The product was precipitated with diethyl ether and the Boc groups were removed by addition of TFA:triisobutylsilane:H_2O

95:2.5:2.5, v/v in an ice bath for 30 minutes. The deprotected product was precipitated 2 additional times with diethyl ether and dialyzed against ultrapure water using a dialysis membrane (MWCO= 1000 Da, Spectrum Laboratories, Inc., Rancho Dominguez, CA, USA). The solution was then lyophilized to yield pure poly(CBA-DAH).

Arginine was grafted onto poly(CBA-DAH) by addition of 4 equivalents of Fmoc-Arg(pbf)-OH and HBTU, and 8 equivalents of DIPEA in DMF for 2 days at room temperature. The product was precipitated with diethyl ether 2 times in order to remove unreacted starting materials then mixed with an equal volume of piperidine (30% solution in DMF) for 30 minutes at room temperature to remove Fmoc groups. The product was again precipitated 2 times with diethyl ether and a solution of TFA:triisopropylsilane:H_2O 95:2.5:2.5, v/v was added to the precipitate at room temperature for 30 minutes to deprotect the pbf groups on the arginine. After one final diethyl ether precipitation, the final arginine-grafted bioreducible poly(disulfide amine) was dialyzed against ultrapure water and lyophilized to yield a sticky solid.

The polymer poly(cystaminebisacrylamide triethylenetetramine) (CBA-TETA) was synthesized by following a previously published protocol developed by our lab [26]. The polymer polyethylenimine-grafted-polyethyleneglycol (PEI-g-PEG) was also synthesized as previously detailed in the literature [27].

4.3.4 Luciferase Transfection Efficiency Assay

Transfection efficiency of the various polymers was evaluated using a single luciferase flash reporter assay. Isolated primary rat cardiomyocytes were plated into 24-well plates at 125,000 cells/mm^2 and incubated until they had reached approximately 60% confluence. On the day of transfection, 0.5 μg DNA was complexed with the

cationic polymers in a 5% glucose, 20 mM HEPES buffer solution at a variety of weight ratios to identify the most efficient formulation. The polyplexes were allowed to form spontaneously at room temperature for 30 minutes prior to transfection. The serum-supplemented media was removed from all wells and replaced with serum-free media. The polyplexes were then added directly to the wells and the plate was incubated at 37 °C for 4 hours. After polyplex incubation, the serum-free media was replaced again with supplemented media and the cells incubated at 37 °C for 48 hours. The cells were washed with room temperature PBS, treated with 200 µl lysis buffer, and exposed to 2 freeze/thaw cycles to complete the lysis. The well contents were transferred to microcentrifuge tubes and the cellular debris was cleared by centrifugation at 14,000× g for 5 minutes. To measure total protein concentration, 10 µl of the supernatant was transferred to a clear 96-well plate and quantified using a BCA protein assay kit (Pierce, Rockford, IL) with bovine serum albumin as a standard. An additional 25 µl aliquot was transferred to a white 96-well plate to measure luminescence. A Perkin Elmer Victor plate reader (Perkin Elmer, Waltham, MA) was used to automatically dispense 100 µl of luciferase assay buffer containing luciferin (Pierce, Rockford, IL) to the wells and measure the relative luminescence units (RLUs) for each well. The RLU data were then normalized as RLU/mg total protein. All transfection assays were performed with triplicate replicates and repeated three times.

4.3.5 MTT Viability Assay

Cellular viability was analyzed using a 3-(4,5-dimethylthiazol-2-yl)-2,5-diphenyltetrazolium bromide (MTT) assay. MTT is reduced in living cells to form an insoluble purple formazan crystal and is an indicator of cellular viability. Primary rat

cardiomyocytes were plated into 24-well plates at 125,000 cells/mm^2 and incubated at 37 °C until they had reached 80% confluence. DNA was complexed with the cationic polymers at predetermined w/w ratios in a 5% glucose, 20 mM HEPES buffer solution and allowed to form nanoparticles at room temperature for 30 minutes. The supplemented media was removed and replaced with serum free media and the polyplexes were added to each well. The polyplexes were incubated with the cells for 4 hours at 37 °C, after which the media was removed and replaced with serum supplemented media. The cells were returned to the incubator for approximately 16 hours. An MTT solution (50 µl of 2 mg/ml MTT) was added to each well and the cells were returned for a further 4 hours of incubation. After formation of purple crystals at the bottom of the well was evident, the media was carefully aspirated and 300 µl of DMSO was added to each well to solubilize the formazan crystals. Absorbance was read at 570 nm on a microplate reader (Bio-Rad, Hercules, CA). Percent relative viability was determined using untreated cells as a 100% control level. All samples were performed in triplicate and each experiment was repeated a minimum of three times.

4.3.6 Gel Retardation

A 0.8% agarose gel containing SYBR green was prepared using tris-acetate-EDTA (TAE) buffer. ABP:siRNA complexes were prepared with 500 ng of siRNA at various w/w ratios in a 5% glucose, 20 mM HEPES buffer solution and allowed to form polyplexes for 30 minutes at room temperature. A loading dye was added to each sample and the polyplexes were loaded into the wells of the prepared gel. The gel was electrophoresed at 110 V for 15 minutes and the RNA bands were then visualized with UV light on a Bio-Rad Gel Doc system (Bio-Rad, Hercules, CA). Polyplex reduction was

achieved by incubating siRNA polyplexes with 5 mM dithiothreitol (DTT) at 37 °C for 30 minutes. The reduced samples were then run as described above.

4.3.7 *In Vitro* Knockdown

To perform the siRNA knockdown studies, rat primary caridomyocytes were seeded onto 6-well plates at 125,000 cells/cm^2 and allowed to grow to 75% confluence. The cells were then treated with 50 nM siRNA complexed with ABP at a 1:20 w/w ratio in serum free media for 4 hours. The media was then replaced with supplemented media and the cells were incubated a further 48 hours. The cells were then lysed and the mRNA isolated using a PureLink total RNA extraction kit (Life Technologies, Carlsbad, CA).

qRT-PCR was performed using the TaqMan One-Step RT-PCR kit (Life Technologies, Carlsbad, CA). Primers were acquired for rat BNIP3 (part number Rn00821447), and compared against the housekeeping gene L32 (part number Rn00820748). All probe/primer combinations were designed, validated, and purchased from Applied Biosciences/Life Technologies (Life Technologies, Carlsbad, CA).

4.3.8 BNIP3 Protein ELISA

Rat primary cardiomyocytes were seeded onto 35 mm plates at 125,000 cells/cm^2 and allowed to grow to 75% confluence. As above, the cells were then treated with 50 nM siRNA complexed with ABP at a 1:20 w/w ratio in serum free media for 4 hours. The media was then replaced with supplemented media and the cells were incubated for an additional 2, 3, 5, and 7 days. The cells were then lysed and the protein isolated using standard microbiology techniques described briefly below.

Whole cell lysates were prepared by aspirating the cell media, and adding complete RIPA lysis buffer (20 mM Tris-HCl (pH 7.5), 150 mM NaCl, 1 mM Na_2EDTA,

1 mM EGTA, 1% NP-40, 1% sodium deoxycholate, 2.5 mM sodium pyrophosphate, 1 mM ß-glycerophosphate, 1 mM Na_3VO_4, 1 µg/ml leupeptin). After a single freeze-thaw cycle, the cells were scraped and pipetted to ensure complete lysis. The lysates were transferred to a microcentrifuge tube and centrifuged for 5 minutes at 14,000× g to separate the debris. The supernatant was then analyzed using a 96-well plate ELISA specific for rat BNIP3 (Kamiya Biomedical, Seattle, WA).

4.3.9 Contracting Cardiomyocytes

To analyze cardiomyocyte contractile function after hypoxia exposure, rat primary cardiomyocytes were seeded into 35 mm plates at 125,000 cells/cm^2 and allowed to grow until intercellular junctions could form and the plate of cells were beating synchronously (approximately 80% confluence). The cells were then treated with 50 nM luciferase or BNIP3 siRNA complexed with ABP at a 1:20 w/w ratio in serum free media for 4 hours. The media was then replaced with reduced serum media and the cells were incubated under hypoxic conditions (1% O_2, 5% CO_2, 94% N_2) for 24 hours. Immediately after 24 hours exposure to hypoxia, the cells were removed from the incubator and imaged on an EVOS fluorescent microscope (AMG, Bothell, WA) using the transmitted light setting at 20× magnification. The total number of cardiomyocytes in each high power field still showing contractile activity was then counted. All results were normalized against the number of cells beating in the untreated hypoxic control group.

4.3.10 *In Vitro* Live/Dead Assay

Primary rat cardiomyocytes isolated as above were seeded onto 35 mm plates at a density of 125,000 cells/cm^2 and allowed to grow to 75% confluence. Cells were then treated with 50 nM siRNA with ABP (1:20 w/w) in serum free media for 4 hours. The

media was then replaced with reduced serum media and the cells were incubated under hypoxic conditions (1% O_2, 5% CO_2, 94% N_2) for 48 hours. The cells were then treated with ethidium homodimer-1 and calcein AM dyes from Invitrogen's mammalian LIVE/DEAD Viability/Cytotoxicity Kit (Life Technologies, Carlsbad, CA, USA) and analyzed on an EVOS fl fluorescent microscope (AMG, Bothell, WA, USA). The number of positive cells in both the live and dead channels was counted from a total of 3 random fields from each sample. Data were reported as fold normoxia control levels.

To perform the *in vitro* live/dead assay, primary rat neonatal cardiomyocytes were seeded onto 35 mm cell culture plates coated with a collagen-based attachment factor at approximately 150,000 cells/cm^2. Once the cells had reached 60–75% confluence, the FBS-supplemented media was replaced with serum free medium and the cells were treated with 50 nM of BNIP3 siRNA complexed at 1:20 w/w with ABP, 50 nM luciferase siRNA complexed at 1:20 w/w with ABP, or no siRNA at all. The serum free media was replaced with FBS-supplemented media after 4 hours and the cells were incubated for 24 hours under normal cell culture conditions. After 24 hours, the cells were transferred to a hypoxia chamber containing 1% O_2, 5% CO_2, 94% N_2 and incubated in reduced serum (1% FBS) for an additional 24 hours.

After incubation under hypoxia, the plates were removed from the incubator and rinsed three times with Dubelcco's phosphate-buffered saline to reduce extracellular esterase activity. They were then immediately treated with 2 µM calcein AM and 4 µM ethidium homodimer-1. The cells were then incubated in the dark for 45 minutes at room temperature. After incubation, the cells were viewed on an EVOS fluorescent microscope (AMG, Bothell, WA) using a 470/22 nm excitation with 525/50 nm emission window for

calcein AM, and a 531/40 nm excitation with 593/40 nm emission window for ethidium homodimer-1.

4.3.11 Statistical Analysis

All results are reported as the mean value ± standard error of the mean (SEM). Statistical analysis was performed in GraphPad Prism 4.03 (GraphPad Software, La Jolla, CA, USA) using one-way analysis of variance (ANOVA) followed by Tukey's *post hoc* test to identify significance between groups. $P < 0.05$ was considered statistically significant throughout.

4.4 Results

The polymer ABP was synthesized according to the reaction scheme in Figure 4.1. The structure was confirmed by NMR, mass-spectrometry, and FTIR (data not shown). The structures of the other polymers evaluated for transfection efficiency and cytotoxicity are included in Figure 4.2. The structure of CBA-TETA was unique from the other bioreducible compounds evaluated as it forms a branched cationic polymer as opposed to a linear polymer, as shown in Figure 4.1.

4.4.1 Transfection Efficiency

Luciferase expression is commonly used to evaluate transfection efficiency as it indicates the efficiency of cellular entry, endosomal escape, polymer dissociation from its nucleic acid cargo, nuclear penetration, and ultimately, transcription and translation of the plasmid DNA. We evaluated a large number of polymers at varying polymer:DNA weight ratios to identify not only the most efficient polymer but also to determine the most efficient weight ratio for each polymer. The bioreducible polymer ABP showed

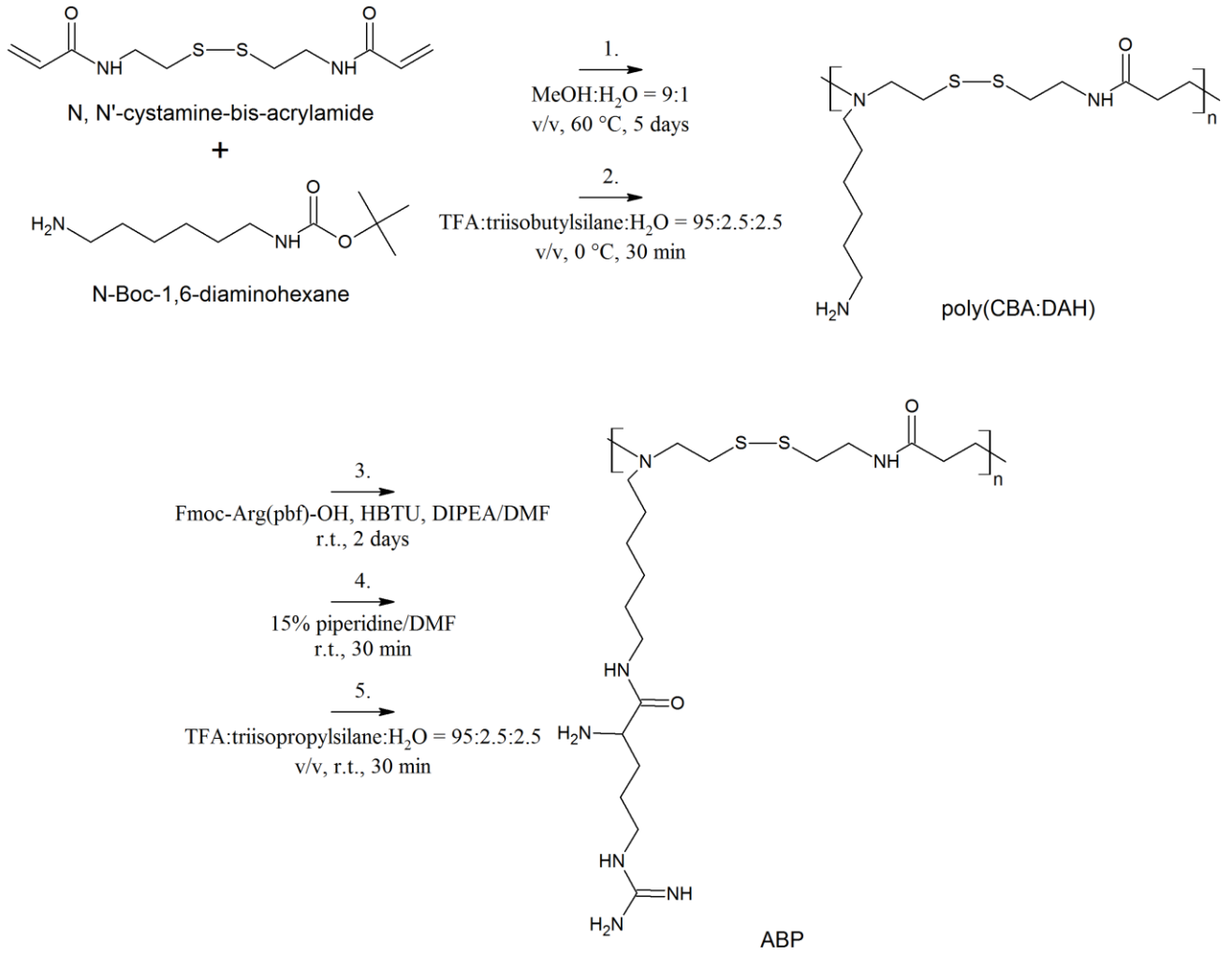

Figure 4.1. Synthesis of arginine-grafted bioreducible polymer. Adapted from [24].

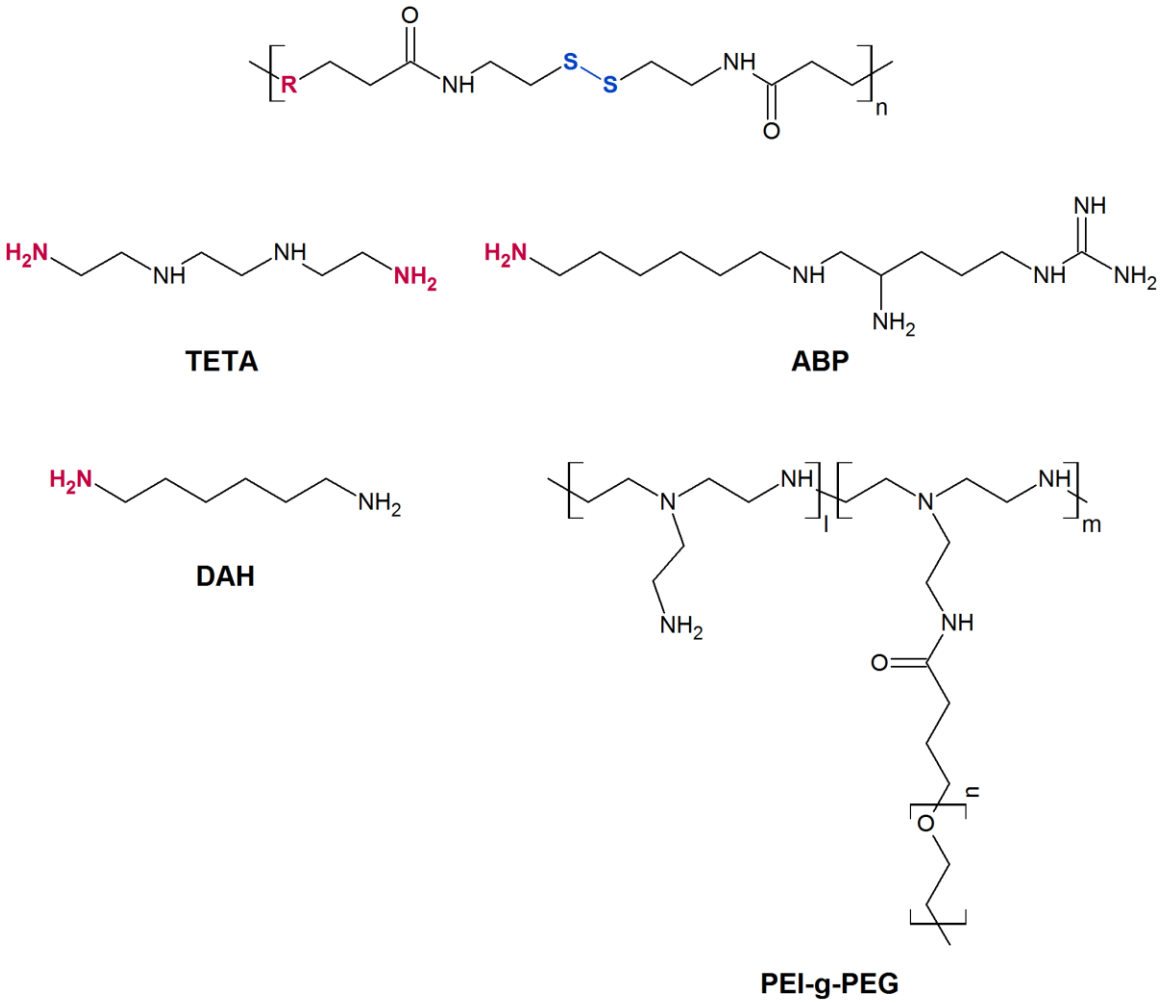

Figure 4.2. Chemical structures of cationic polymers screened to transfect rat cardiomyocytes. TETA = triethylenetetramine, ABP = arginine-grafted bioreducible polymer, DAH = diaminohexane, PEI-g-PEG = polyethyleneimine-grafted polyethyleneglycol.

higher transfection efficiency than bPEI at all weight ratios and demonstrated significantly higher transfection efficiency than all other polymer formulations, with the exception of TETA at 10:1 (Figure 4.3). Notably, most other polymers did not perform as well as the bPEI benchmark whereas ABP showed 2.9-fold higher expression at 20:1, 8.9-fold higher expression at 40:1, and 30.0-fold higher expression at 60:1. The steadily increasing transfection efficiencies as weight ratio increases is typical for polyplex delivery systems; however, as the weight ratio increases, so does toxicity.

4.4.2 MTT Viability Assay

Evaluating the cytotoxic effects of polyplex gene delivery is of obvious importance as high transgene expression is of limited value if most of the cells are killed by the treatment. Using the MTT viability assay, we evaluated the toxicity of the experimental conditions tested for luciferase expression. As expected, the toxicity of the polyplexes becomes more pronounced as the polymer:DNA weight ratio increases. Even though TETA at 10:1 showed improved transfection efficiency compared to bPEI, the treatment condition killed 10% of the cells, limiting its effectiveness (Figure 4.4). However, ABP at 20:1 showed no toxicity towards cardiomyocytes compared to untreated control cells. As the weight ratio of ABP:DNA increases, significant toxicity becomes apparent. While the 40:1 and 60:1 formulations of ABP showed progressively increasing transfection efficiencies, the accompanying increase in toxicity negated the benefit. A degree of toxicity is acceptable for *in vitro* experimentation as the transfected cells can replicate to replace the cells lost due to polyplex toxicity or a larger number of cells can be used to plan for the cells lost; however, when translating research to an *in*

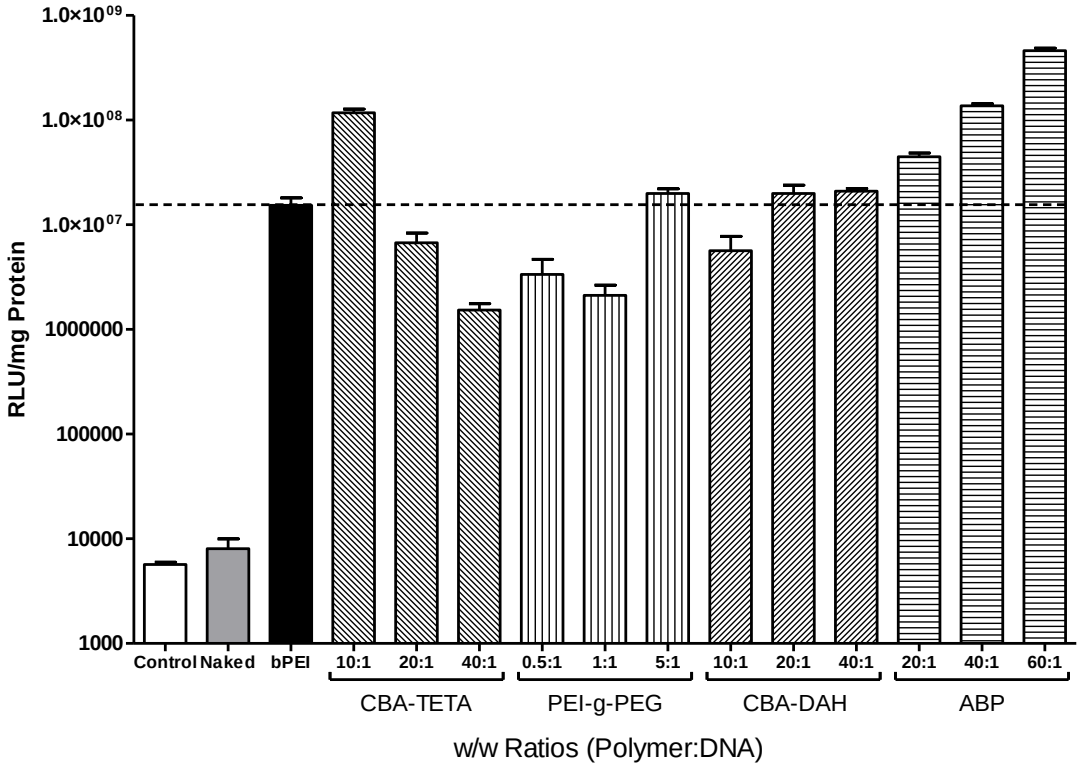

Figure 4.3. Luciferase transfection efficiency assay of various cationic polymers on rat cardiomyocytes. The dashed line indicates the expression level achieved by transfection of luciferase with 25 kDa bPEI.

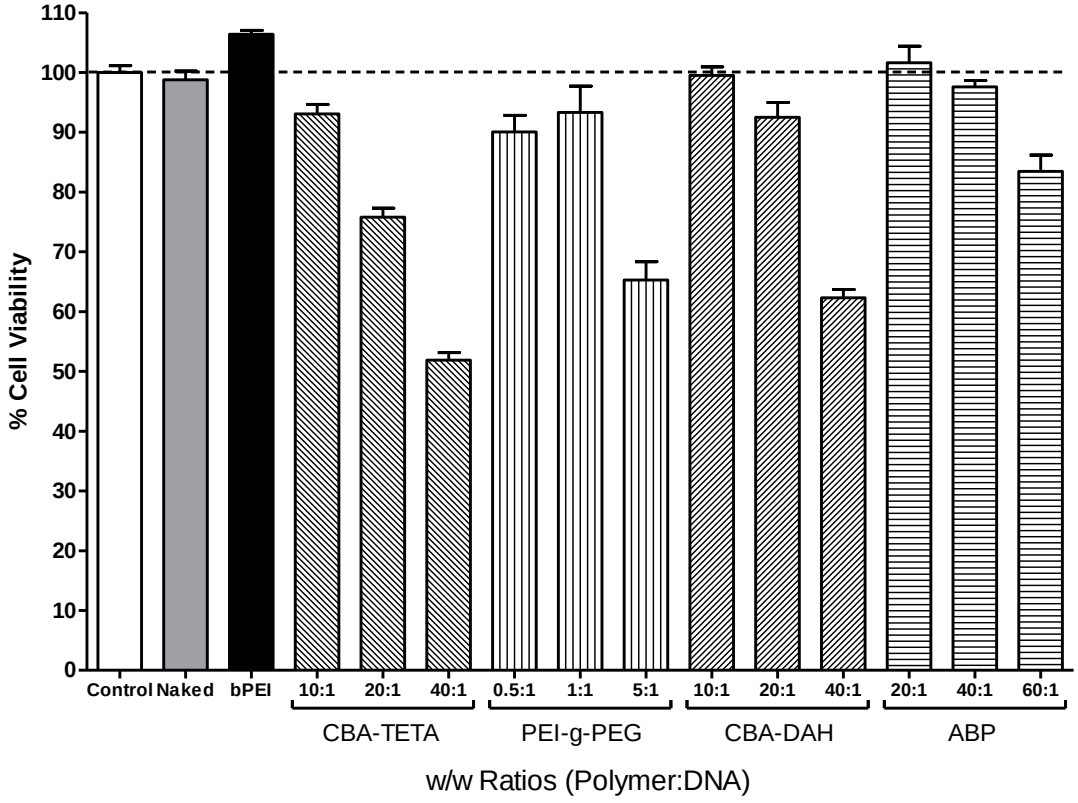

Figure 4.4. MTT viability assay of various cationic polymers on rat cardiomyocytes. All results reported as a percentage of untransfected control cells. The dashed line indicates 100% viability as determined by untransfected controls.

vivo animal model, even small levels of toxicity are unacceptable. This is especially true in the heart, which is known for very low cellular turnover and a limited capacity for self-renewal. For these reasons, all subsequent studies were performed with ABP at a weight ratio of 20:1.

4.4.3 Gel Retardation

Gel retardation assays, also known as gel electrophoresis mobility shift assays, reveal the capacity of the polyplex to bind and complex DNA tightly and efficiently. If the polyplex formulation condenses DNA or siRNA, it prevents it from migrating through the gel and no band is visible. The gel retardation study was performed on the selected ABP polymer at weight ratios of 0.5:1, 1:1, 5:1, 10:1, 20:1, and 40:1 ABP:siRNA to ensure that the polymer forms tight complexes to provide for protection from degradation by nucleases. ABP demonstrated that it can condense siRNA at weight ratios 20:1 and 40:1, as evidenced by the significantly lighter bands (Figure 4.5, top).

The addition of the chemical agent DTT reduced the disulfide bonds in the polymer, freeing the siRNA and allowing all bands to migrate (Figure 4.5, bottom). Even the higher 20:1, and 40:1 w/w ratio polyplexes were completely degraded, demonstrating the ability of the polymers to break down and dissociate from nucleic acids under reducing conditions similar to that experienced in the cytoplasm.

4.4.4 BNIP3 Sequence Selection

In order to identify the most potent siRNA for use in our future studies, we compared a previously published sequence of siRNA (siRNA 1, sense strand 5'-GCUGCCCUGCUACCUCUCAdTdT-3') [22] with three sequences designed using Thermo Scientific's proprietary algorithms and validated by the company (Table 4.1).

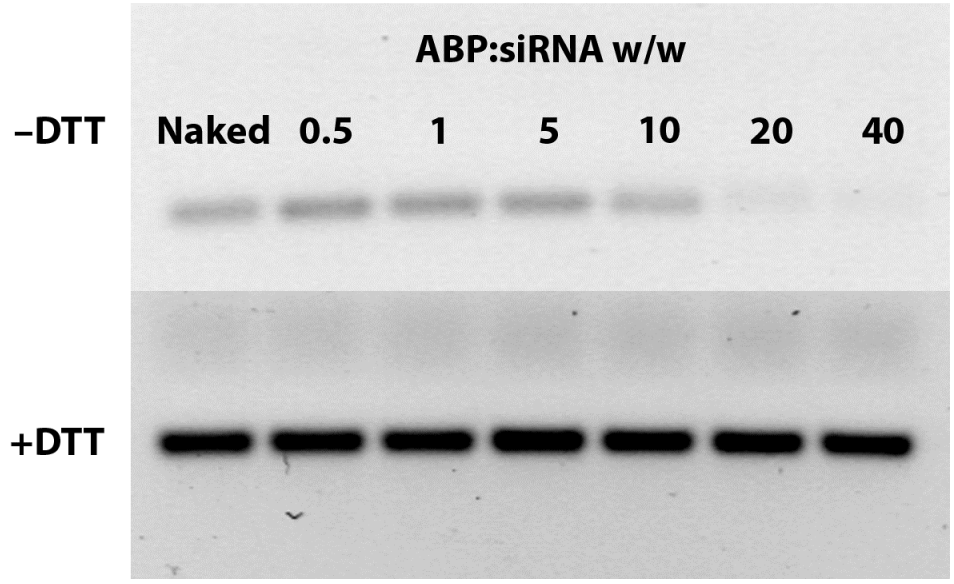

Figure 4.5. Gel retardation assay of ABP:siRNA polyplexes at 0.5:1, 1:1, 5:1, 10:1, 20:1, and 40:1 w/w ratios. The top panel is without the addition of the reducing agent DTT, while the bottom panel contains 5 mM DTT to reduce disulfide bonds.

Table 4.1. siRNA Sequences Tested for BNIP3 Knockdown Potency

Sequence Name	Target Sequence (5`-3`)
siBNIP3 1	UGAGAGGUAGCAGGGCAGCdTdT
siBNIP3 2	UACCAACAGAGCUGAAAUAdTdT
siBNIP3 3	AAACUCAGAUUGGAUAUGGdTdT
siBNIP3 4	CAGCUUCCGUCUCUAUUUAdTdT

We compared the knockdown of BNIP3 mRNA in rat primary cardiomyocytes treated with 50 nM siRNA complexed with ABP at 1:20 w/w ratio. After 48 hours, total RNA was isolated and analyzed for relative BNIP3 levels compared to untreated controls and normalized against the ribosomal protein L32 by qRT-PCR. The qRT-PCR results indicated that the previously published siRNA (siRNA 1) was the most potent, decreasing BNIP3 mRNA levels to an average of 36.8 ± 8.1% of normal versus an average of 59.0 ± 16.6%, 54.7 ± 6.3%, and 62.7 ± 3.4% for the alternative sequences (Figure 4.6).

4.4.5 BNIP3 Protein Knockdown Confirmation

In order to ensure the sequence selected above by qRT-PCR also produced knockdown of BNIP3 protein, an ELISA was used to evaluate relative protein levels. BNIP3 protein levels were immediately reduced from baseline levels as soon as 24 hours after transfection with BNIP3 siRNA (Figure 4.7). Protein levels were reduced 30% from normal and were maintained at this decreased level through day 5 ($P < 0.01$). At day 7, BNIP3 levels increased and while they remained reduced from control levels, they were no longer significantly lower.

4.4.6 Hypoxia Protection and Functional Cardiomyocytes

The fractional survival of cells exposed to hypoxia is not the only predictor of function after myocardial infarction. It is also important that cells are able to maintain function after exposure to harsh conditions that would be experienced in an infarcted region. Inhibition of BNIP3 using siRNA in rat primary cardiomyocytes significantly improved contractile function after exposure to severe hypoxic conditions for 24 hours. The siBNIP3-treated cardiomyocytes showed an almost 3-fold higher level of contractile

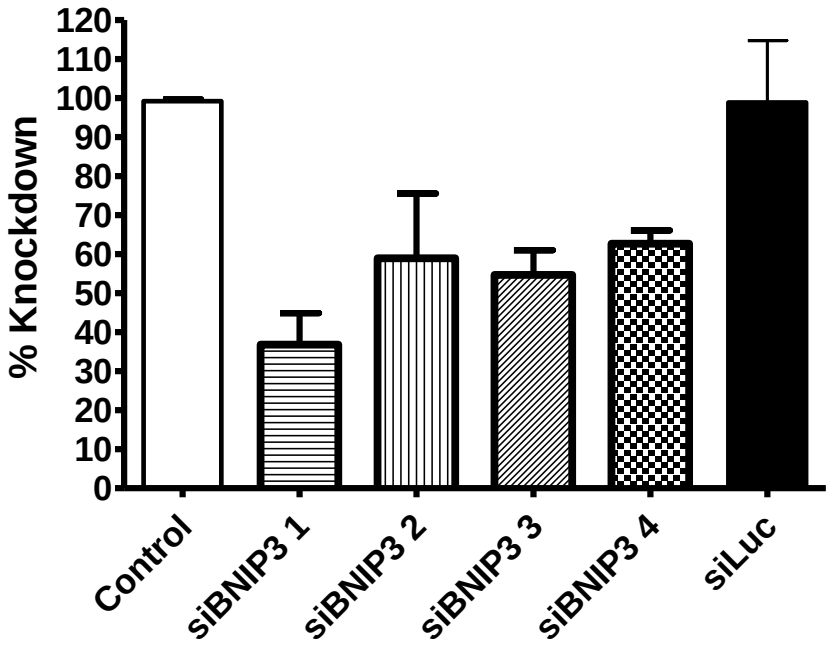

Figure 4.6. qRT-PCR knockdown of rat BNIP3 in rat primary cardiomyocytes. The graph shows that the previously published BNIP3 siRNA sequence was the most potent siRNA sequence evaluated, knocking down BNIP3 mRNA levels to $36.8 \pm 8.1\%$ of normal levels.

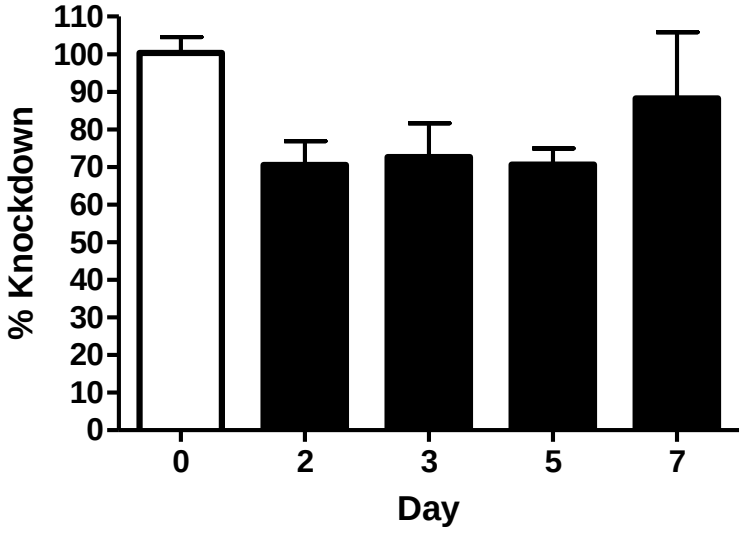

Figure 4.7. siRNA knockdown of BNIP3 protein over a 7-day period. All time points are normalized against nontransfected controls.

function compared to both untreated controls and siLuc-treated cardiomyocytes ($P < 0.001$)(Figure 4.8).

4.4.7 *In Vitro* Viability Live/Dead Assay

In order to initially validate the ability of BNIP3 inhibition to protect cardiomyocytes from apoptosis and retain cell viability, we performed a live/dead assay on primary rat ventricular cardiomyocytes under hypoxic conditions for 24 hours. Compared to normoxic controls, cells transfected with siBNIP3:ABP at a 1:20 w/w ratio remained viable (97% of normoxic, $P < 0.001$ *vs.* hypoxic controls). Significant loss of viability was observed in both untreated hypoxic cells (40% of normoxic) and in nontargeting siLuc:ABP-treated cells (50% of normoxic) (Figure 4.9a).

The same pattern of hypoxia protection was evident when evaluating dead/dying cells with condensed nuclei and disrupted cell membranes. The siBNIP3:ABP-transfected cells were not significantly increased over normoxic levels. The level of dead cells was less than 50% of that seen in untreated hypoxic controls and in nontargeted siLuc-transfected cells ($P < 0.001$)(Figure 4.9b).

4.5 Discussion

The primary barrier limiting the clinical potential of gene therapy remains the lack of nontoxic, nonimmunogenic, gene delivery agents that produce high transgene expression or mediate efficient mRNA knockdown by RNAi. Here we show that bioreducible cationic polymers can transfect rat primary cardiomyocytes, producing high expression of plasmid DNA, and efficient knockdown mediated by siRNA. We also demonstrate that we are able to attain these high gene delivery levels without causing significant cellular toxicity.

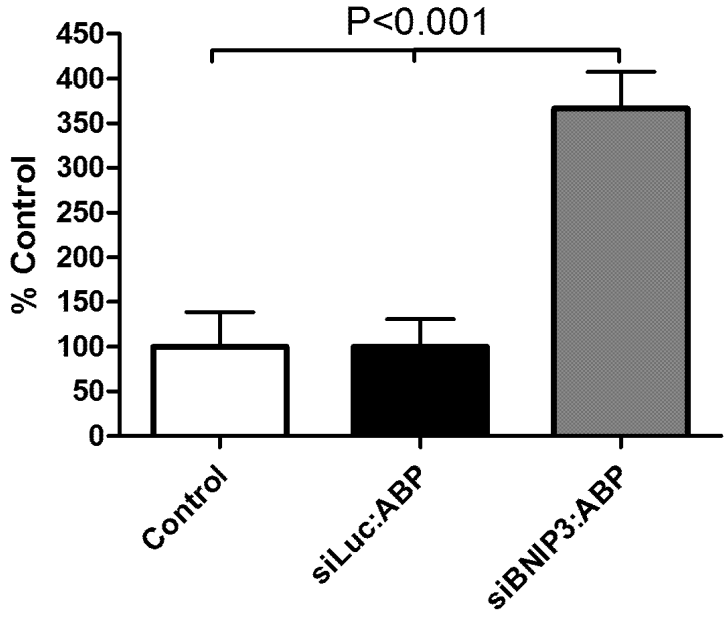

Figure 4.8. Beating cardiomyocytes after siRNA-mediated knockdown of BNIP3 and exposure to 24 hours of hypoxia.

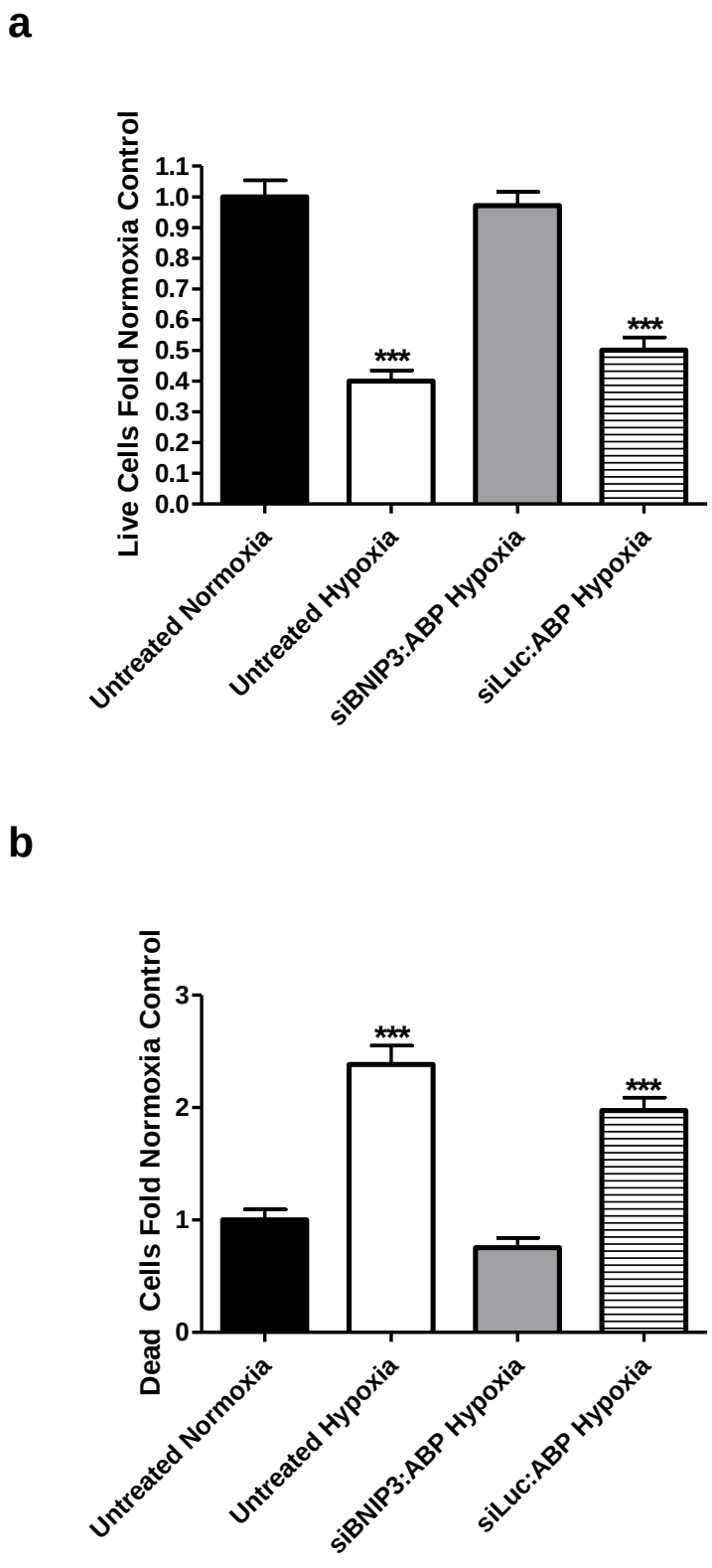

Figure 4.9. *In vitro* live/dead microscopy assay. (a) Live cells (b) Dead cells

While polymeric gene delivery had been observed before, the true potential for polymers to act as efficient gene delivery agents was not fully appreciated until Behr *et al.* reported the versatility of polyethyleneimine (PEI) for oligonucleotide transfer [7]. Since that time, PEI has become the gold standard for polymer transfection, but its usefulness is limited by its high charge density and nondegradable nature [28]. Bioreducible polymers still mediate high transfection efficiency and condense nucleic acids to nano-sized particles, but their disulfide bonds rapidly degrade upon entry to the cytosol, allowing for rapid polyplex unpackaging and clearance of the smaller molecular weight polymer fragments.

We demonstrated that of the bioreducible and nondegradable polymers investigated, ABP was both highly efficient and nontoxic to cardiomyocytes. Our lab has previously shown that ABP can transfect a wide number of cell types with low toxicity and high efficiency [24, 29]. However, the ability of ABP to transfect primary cells, especially cardiomyocytes, had not been investigated. In addition to the positive luciferase results demonstrating that ABP was the most efficient gene delivery agent for cardiomyocytes, we also determined that ABP was essentially nontoxic to cardiomyocytes at a 20:1 weight ratio. While higher transfection efficiency was observed at 40:1 and 60:1 weight ratios, the toxicity associated with those formulations precludes them from use in an *in vivo* setting, where cell loss incidental to transfection is not acceptable.

The proapoptotic protein BNIP3 has long been known to play an important role in causing cell death in a number of tissue types such as neurons [30, 31] and cardiomyocytes [21, 32-34]. Additionally, BNIP3 loss-of-function mutations and

decreased expression are common in many hypoxia-resistant, metastatic cancers [35, 36] and are indicators of poor prognosis [37]. Previous studies have demonstrated that BNIP3 deletion or interference has a protective effect on hypoxic cardiomyocytes [34, 38-42]; however, no one has demonstrated the protective effect of siRNA knockdown of BNIP3 on hypoxia survival. Here we show that BNIP3 interference via siRNA produces rapid and significant decreases in both BNIP3 mRNA and more importantly, protein levels. This rapid and significant decrease makes siRNA knockdown of BNIP3 a viable therapeutic strategy to prevent cell death due to MI possible as cell death due to ischemia is known to peak within the first few days after MI [43, 44]. While the levels of BNIP3 protein knockdown were not as significant as those observed at an mRNA level, BNIP3 is not highly expressed in normoxic cells, and in situations of elevated BNIP3 expression such as hypoxia, the knockdown of BNIP3 protein may be more significant.

Finally, we also demonstrated that the immediate decrease in BNIP3 mRNA and protein levels produced a protective response to harsh hypoxic conditions. Interference with BNIP3 transcription and translation increased the number of viable cells after hypoxia, decreased the number of necrotic/apoptotic cells, and also increased the contractile performance of cells after prolonged hypoxia exposure.

4.6 Conclusions

In conclusion, this work has established that nonviral bioreducible polymers can act as gene delivery agents to secondary and primary rat cardiomyocytes with high efficiency of gene expression/siRNA-mediated mRNA knockdown, and low toxicity. Furthermore, we demonstrated that the proapoptotic protein BNIP3 is a valid target for the prevention of cell death due to exposure to harsh hypoxia conditions, as BNIP3

mRNA inhibition resulted in increased cardiomyocyte function and viability versus untreated or nontargeting siRNA controls. Therefore, BNIP3 knockdown via RNAi is a viable option to reduce cardiomyocyte death due to hypoxic injury and should be investigated in animal models of myocardial infarction.

4.7 Acknowledgements

Thanks to Tae-Il Kim, PhD who designed and assisted in the synthesis of the polymer ABP. Additional thanks go to Mei Ou, PhD who designed and assisted in the synthesis of the backbone polymer CBA-DAH. The polymer CBA-TETA was synthesized following guidance from Jonathan Brumbach, PhD.

4.8 References

[1] S. Rogers, A. Lowenthal, H.G. Terheggen, J.P. Columbo, Induction of arginase activity with the Shope papilloma virus in tissue culture cells from an argininemic patient, J. Exp. Med., 137 (1973) 1091-1096.

[2] H.V. Aposhian, The use of DNA for gene therapy--the need, experimental approach, and implications, Perspect. Biol. Med., 14 (1970) 98.

[3] D.J. Wells, Gene therapy progress and prospects: electroporation and other physical methods, Gene Ther., 11 (2004) 1363-1369.

[4] S. Mehier-Humbert, R.H. Guy, Physical methods for gene transfer: improving the kinetics of gene delivery into cells, Adv. Drug Deliv. Rev., 57 (2005) 733-753.

[5] R. Tomanin, M. Scarpa, Why do we need new gene therapy viral vectors? Characteristics, limitations and future perspectives of viral vector transduction, Curr. Gene Ther., 4 (2004) 357-372.

[6] M.S. Al-Dosari, X. Gao, Nonviral gene delivery: principle, limitations, and recent progress, AAPS J., 11 (2009) 671-681.

[7] O. Boussif, F. Lezoualc'h, M.A. Zanta, M.D. Mergny, D. Scherman, B. Demeneix, J.P. Behr, A versatile vector for gene and oligonucleotide transfer into cells in culture and in vivo: polyethylenimine, Proc. Natl. Acad. Sci. U. S. A., 92 (1995) 7297-7301.

[8] G.Y. Wu, C.H. Wu, Receptor-mediated in vitro gene transformation by a soluble DNA carrier system, J. Biol. Chem., 262 (1987) 4429-4432.

[9] W.T. Godbey, K.K. Wu, A.G. Mikos, Poly(ethylenimine)-mediated gene delivery affects endothelial cell function and viability, Biomaterials, 22 (2001) 471-480.

[10] P. Chollet, M.C. Favrot, A. Hurbin, J.L. Coll, Side-effects of a systemic injection of linear polyethylenimine-DNA complexes, J. Gene Med., 4 (2002) 84-91.

[11] D. Putnam, R. Langer, Poly (4-hydroxy-L-proline ester): Low-temperature polycondensation and plasmid DNA complexation, Macromolecules, 32 (1999) 3658-3662.

[12] V.L. Roger, A.S. Go, D.M. Lloyd-Jones, E.J. Benjamin, J.D. Berry, W.B. Borden, D.M. Bravata, S. Dai, E.S. Ford, C.S. Fox, H.J. Fullerton, C. Gillespie, S.M. Hailpern, J.A. Heit, V.J. Howard, B.M. Kissela, S.J. Kittner, D.T. Lackland, J.H. Lichtman, L.D. Lisabeth, D.M. Makuc, G.M. Marcus, A. Marelli, D.B. Matchar, C.S. Moy, D. Mozaffarian, M.E. Mussolino, G. Nichol, N.P. Paynter, E.Z. Soliman, P.D. Sorlie, N. Sotoodehnia, T.N. Turan, S.S. Virani, N.D. Wong, D. Woo, M.B. Turner, Heart disease and stroke statistics--2012 update: a report from the American Heart Association, Circulation, 125 (2012) e2-e220.

[13] M.A. Pfeffer, Left ventricular remodeling after acute myocardial infarction, Annu. Rev. Med., 46 (1995) 455-466.

[14] B.I. Jugdutt, Ischemia/Infarction, Heart Fail. Clin., 8 (2012) 43-51.

[15] R. Hinkel, T. Trenkwalder, C. Kupatt, Gene therapy for ischemic heart disease, Expert Opin. Biol. Ther., 11 (2011) 723-737.

[16] Y. Hojo, T. Saito, H. Kondo, Role of apoptosis in left ventricular remodeling after acute myocardial infarction, J. Cardiol., (2012).

[17] A. Abbate, J. Narula, Role of apoptosis in adverse ventricular remodeling, Heart Fail. Clin., 8 (2012) 79-86.

[18] Y. Chandrashekhar, Role of apoptosis in ventricular remodeling, Curr. Heart Fail. Rep., 2 (2005) 18-22.

[19] R.K. Bruick, Expression of the gene encoding the proapoptotic Nip3 protein is induced by hypoxia, Proc. Natl. Acad. Sci. U. S. A., 97 (2000) 9082-9087.

[20] M.T. Crow, Hypoxia, BNip3 proteins, and the mitochondrial death pathway in cardiomyocytes, Circ. Res., 91 (2002) 183-185.

[21] G.W. Dorn, 2nd, L.A. Kirshenbaum, Cardiac reanimation: targeting cardiomyocyte death by BNIP3 and NIX/BNIP3L, Oncogene, 27 (2008) S158-S167.

[22] K. Prabhakaran, L. Li, L. Zhang, J.L. Borowitz, G.E. Isom, Upregulation of BNIP3 and translocation to mitochondria mediates cyanide-induced apoptosis in cortical cells, Neuroscience, 150 (2007) 159-167.

[23] M. Toraason, M.E. Luken, M. Breitenstein, J.A. Krueger, R.E. Biagini, Comparative toxicity of allylamine and acrolein in cultured myocytes and fibroblasts from neonatal rat heart, Toxicology, 56 (1989) 107-117.

[24] T.I. Kim, M. Ou, M. Lee, S.W. Kim, Arginine-grafted bioreducible poly(disulfide amine) for gene delivery systems, Biomaterials, 30 (2009) 658-664.

[25] M. Ou, X.L. Wang, R. Xu, C.W. Chang, D.A. Bull, S.W. Kim, Novel biodegradable poly(disulfide amine)s for gene delivery with high efficiency and low cytotoxicity, Bioconjug. Chem., 19 (2008) 626-633.

[26] L.V. Christensen, C.W. Chang, W.J. Kim, S.W. Kim, Z. Zhong, C. Lin, J.F. Engbersen, J. Feijen, Reducible poly(amido ethylenimine)s designed for triggered intracellular gene delivery, Bioconjug. Chem., 17 (2006) 1233-1240.

[27] H. Petersen, P.M. Fechner, A.L. Martin, K. Kunath, S. Stolnik, C.J. Roberts, D. Fischer, M.C. Davies, T. Kissel, Polyethylenimine-graft-poly(ethylene glycol)

copolymers: influence of copolymer block structure on DNA complexation and biological activities as gene delivery system, Bioconjug. Chem., 13 (2002) 845-854.

[28] H. Lv, S. Zhang, B. Wang, S. Cui, J. Yan, Toxicity of cationic lipids and cationic polymers in gene delivery, J. Control. Release, 114 (2006) 100-109.

[29] S.H. Kim, J.H. Jeong, T.I. Kim, S.W. Kim, D.A. Bull, VEGF siRNA delivery system using arginine-grafted bioreducible poly(disulfide amine), Mol. Pharm., 6 (2009) 718-726.

[30] S.T. Zhao, M. Chen, S.J. Li, M.H. Zhang, B.X. Li, M. Das, J.C. Bean, J.M. Kong, X.H. Zhu, T.M. Gao, Mitochondrial BNIP3 upregulation precedes endonuclease G translocation in hippocampal neuronal death following oxygen-glucose deprivation, BMC Neurosci., 10 (2009) 113.

[31] Z. Zhang, R. Shi, J. Weng, X. Xu, X.M. Li, T.M. Gao, J. Kong, The proapoptotic member of the Bcl-2 family Bcl-2 / E1B-19K-interacting protein 3 is a mediator of caspase-independent neuronal death in excitotoxicity, FEBS J., 278 (2011) 134-142.

[32] K.A. Webster, R.M. Graham, N.H. Bishopric, BNip3 and signal-specific programmed death in the heart, J. Mol. Cell. Cardiol., 38 (2005) 35-45.

[33] C. Vande Velde, J. Cizeau, D. Dubik, J. Alimonti, T. Brown, S. Israels, R. Hakem, A.H. Greenberg, BNIP3 and genetic control of necrosis-like cell death through the mitochondrial permeability transition pore, Mol. Cell. Biol., 20 (2000) 5454-5468.

[34] A. Hamacher-Brady, N.R. Brady, S.E. Logue, M.R. Sayen, M. Jinno, L.A. Kirshenbaum, R.A. Gottlieb, A.B. Gustafsson, Response to myocardial ischemia/reperfusion injury involves Bnip3 and autophagy, Cell Death Differ., 14 (2007) 146-157.

[35] H.R. Mellor, A.L. Harris, The role of the hypoxia-inducible BH3-only proteins BNIP3 and BNIP3L in cancer, Cancer Metastasis Rev., 26 (2007) 553-566.

[36] H. Lee, S.G. Paik, Regulation of BNIP3 in normal and cancer cells, Mol. Cells, 21 (2006) 1-6.

[37] M. Erkan, J. Kleeff, I. Esposito, T. Giese, K. Ketterer, M.W. Buchler, N.A. Giese, H. Friess, Loss of BNIP3 expression is a late event in pancreatic cancer contributing to chemoresistance and worsened prognosis, Oncogene, 24 (2005) 4421-4432.

[38] K.M. Regula, K. Ens, L.A. Kirshenbaum, Inducible expression of BNIP3 provokes mitochondrial defects and hypoxia-mediated cell death of ventricular myocytes, Circ. Res., 91 (2002) 226-231.

[39] A. Diwan, M. Krenz, F.M. Syed, J. Wansapura, X. Ren, A.G. Koesters, H. Li, L.A. Kirshenbaum, H.S. Hahn, J. Robbins, W.K. Jones, G.W. Dorn, Inhibition of ischemic

cardiomyocyte apoptosis through targeted ablation of Bnip3 restrains postinfarction remodeling in mice, J. Clin. Invest., 117 (2007) 2825-2833.

[40] D.A. Kubli, M.N. Quinsay, C. Huang, Y. Lee, A.B. Gustafsson, Bnip3 functions as a mitochondrial sensor of oxidative stress during myocardial ischemia and reperfusion, Am. J. Physiol. Heart Circ. Physiol., 295 (2008) H2025-2031.

[41] R.M. Graham, D.P. Frazier, J.W. Thompson, S. Haliko, H. Li, B.J. Wasserlauf, M.G. Spiga, N.H. Bishopric, K.A. Webster, A unique pathway of cardiac myocyte death caused by hypoxia-acidosis, J. Exp. Biol., 207 (2004) 3189-3200.

[42] L.A. Kubasiak, O.M. Hernandez, N.H. Bishopric, K.A. Webster, Hypoxia and acidosis activate cardiac myocyte death through the Bcl-2 family protein BNIP3, Proc. Natl. Acad. Sci. U. S. A., 99 (2002) 12825-12830.

[43] P.W. Thimister, L. Hofstra, I.H. Liem, H.H. Boersma, G. Kemerink, C.P. Reutelingsperger, G.A. Heidendal, In vivo detection of cell death in the area at risk in acute myocardial infarction, J. Nucl. Med., 44 (2003) 391-396.

[44] J.P. Veinot, D.A. Gattinger, H. Fliss, Early apoptosis in human myocardial infarcts, Hum. Pathol., 28 (1997) 485-492.

CHAPTER 5

BIOREDUCIBLE POLYMER-MEDIATED DELIVERY OF BNIP3 SIRNA TO RETAIN HEART FUNCTION IN A RAT MODEL OF ISCHEMIA/REPERFUSION INJURY

5.1 Abstract

Apoptosis in the myocardium following myocardial infarction is purported to be a major contributing factor to infarct expansion and negative remodeling of the left ventricle. In human patients and in animal models of myocardial ischemia/reperfusion (I/R) injury, the hypoxia-responsive, proapoptotic protein BNIP3 is consistently upregulated in the myocardial infarct zone, suggesting an important role in cardiac apoptosis. In this work, we hypothesized that polymer-mediated siRNA gene therapy to knockdown BNIP3 would reduce apoptosis in a rat model of I/R and lead to retained heart function and decreased left ventricle remodeling. After a temporary 30-minute ligation of the left anterior descending coronary artery, rats were randomly divided between five groups: 1) BNIP3 siRNA complexed with a novel cationic, disulfide-linked arginine-grafted bioreducible polymer (ABP), siBNIP3:ABP, 2) nontargeting luciferase siRNA complexed with ABP, siLuc:ABP, 3) naked siBNIP3, 4) I/R but no treatment, and 5) thoracotomy sham surgery control. After 2 weeks of treatment, siBNIP3:ABP-treated rats demonstrated elevated ejection fraction versus I/R controls ($74.4 \pm 4.4\%$ *vs.* $58.4 \pm 3.9\%$). Improvements in regional wall thickening and end systolic volume versus

untreated controls were also observed. Infarcts in siBNIP3:ABP rats were over 50% smaller than in I/R only, nontargeting siLuc:ABP, and naked BNIP3 control groups. Significant decreases in TUNEL-positive cells were also observed in the siBNIP3:ABP treatment group. Our results demonstrate the potential utility of an RNAi treatment paradigm to reduce cell death after myocardial infarction and improve heart function by targeting BNIP3.

5.2 Introduction

While rates of cardiovascular disease have been in decline over the years, it remains the top cause of death among developed countries. In the United States alone, it accounts for one out of three deaths, totaling 811,900 deaths in 2008 [1]. Myocardial infarction (MI) is a form of coronary heart disease caused by decreased blood flow and, concomitantly, oxygen supply to the myocardium, causing ischemic cell death. This reduction in blood flow is most commonly caused by a plaque or thrombotic occlusion in one of the coronary arteries. In the event of an MI, the most common medical response is to attempt to reestablish blood flow to the heart through the use of pharmacological agents which clear thrombi within the coronary arteries or via primary percutaneous coronary intervention. Research has revealed, however, that the rapid reestablishment of oxygen supply to the hypoxic myocardium results in a reperfusion injury caused by the rapid increase in reactive oxygen to tissues that have begun to compensate for the lowered oxygen state, thereby increasing their susceptibility to oxidative damage [2-5]. This complex series of events creates a multifaceted pathology that must be considered when attempting to develop new therapies to improve the treatment of MI.

Of principle importance to the treatment of infarcted myocardium is the prevention of left ventricular remodeling that occurs after MI [6]. The infarct zone is not static and even after blood flow has been restored and the vasculature has been repaired, the infarct continues to slowly expand to encompass an ever larger portion of the ventricle [7]. Infarct expansion and left ventricular remodeling occur due to complex interplay of neurohormonal, mechanical, and biochemical compensatory factors that end in maladaptive remodeling of the left ventricle, leading to heart failure [8].

Gene therapy has been investigated in both research and clinical settings as a potential treatment for myocardial infarction [9]. Most gene therapy studies, especially those with clinical data, however, have focused on proangiogenic approaches to revascularize the myocardium and promote tissue survival [10-12]. Another important therapeutic strategy for myocardial gene therapy of ischemic heart disease, however, is the prevention of cell death via apoptosis, necrosis, and autophagy to preserve endogenous cardiomyocytes [13-15]. Several research studies have evaluated viral and nonviral DNA therapy to express proteins that protect against apoptosis such as Bcl-2 [16] and TNF-α receptor 1 [17]. Other groups have evaluated siRNA treatment to lower levels of genes that directly or indirectly contribute to apoptosis such as SHP-1 [18], ALOX5 [19], PTP-1B [20], and PHD2 [21, 22].

Bcl-2/adenovirus E1B 19 kDa interacting protein 3 (BNIP3) is a proapoptotic member of the Bcl-2 apoptosis family. The BNIP3 protein is unique, however, as it is the only proapoptotic protein with a hypoxia response element (HRE) upstream [23]. This HRE is activated by the oxygen-sensitive Hif-1 transcription factor complex, upregulating expression of downstream genes during periods of hypoxic stress. Most

genes with HREs are prorecovery factors like GLUT-1 [24], VEGF [25], and erythropoietin [26], but BNIP3 appears to be the only HRE-containing gene with direct proapoptotic activity [27]. Importantly, BNIP3 has been shown to play an important role in MI [28]. In mouse models of MI, BNIP3-overexpression decreased LV function, increased apoptosis, and increased LV dilation whereas BNIP3-knockout mice showed lower levels of apoptosis, improved LV function, and lower levels of LV dilation [29].

The aim of this study was to utilize an efficient and nontoxic bioreducible polymer delivery system to locally deliver BNIP3 siRNA to the infarcted rat heart *in vivo*. We have previously established the high transfection efficiency and low toxicity of our arginine-grafted bioreducible polymer (ABP) in a variety of cell types, including myoblasts [30, 31]. We used this novel cell-penetrating polymer to deliver BNIP3 siRNA and investigate the hypothesis that transient reduction of BNIP3 levels in the infarcted heart leads to increased cardiomyocyte protection, decreased left ventricular remodeling, and retention of heart function.

5.3 Materials and Methods

All experiments were approved by the University of Utah's Institutional Animal Care and Use Committee and followed the guidelines provided by the National Institutes of Health in *Guide for the Care and Use of Laboratory Animals*.

5.3.1 Materials

BNIP3 siRNA was obtained from Thermo Scientific (Waltham, MA, USA). The target strand sequence was as follows: 5`-UGAGAGGUAGCAGGGCAGCdTdT-3`.

5.3.2 Synthesis of ABP Polymer

The arginine-grafted bioreducible polymer (ABP) used in this study was synthesized as previously detailed [30], using the backbone polymer poly(CBA-DAH) synthesized previously in our lab [32]. Briefly, poly(CBA-DAH) was synthesized via Michael reaction of equimolar amounts of *N*-Boc-DAH and CBA in a 9:1 v/v solution of MeOH/H_2O. The reaction was run under nitrogen at 60 °C for 5 days and protected from light. The polymerization was terminated by addition of 10% *N*-Boc-DAH and the reaction was maintained for an additional 2 days. The product was precipitated with diethyl ether and the Boc groups were removed by addition of TFA:triisobutylsilane:H_2O, 95:2.5:2.5 (v/v) in an ice bath for 30 minutes. The deprotected product was precipitated 2 additional times with diethyl ether and dialyzed against ultrapure water using a dialysis membrane (MWCO= 1000 Da, Spectrum Laboratories, Inc., Rancho Dominguez, CA, USA). The solution was then lyophilized to yield pure poly(CBA-DAH).

Arginine was grafted onto poly(CBA-DAH) by addition of 4 equivalents of Fmoc-Arg(pbf)-OH and HBTU, and 8 equivalents of DIPEA in DMF for 2 days at room temperature. The product was precipitated with diethyl ether 2 times in order to remove unreacted starting materials then mixed with an equal volume of piperidine (30% solution in DMF) for 30 minutes at room temperature to remove Fmoc groups. The product was again precipitated 2 times with diethyl ether and a solution of TFA:triisopropylsilane:H_2O, 95:2.5:2.5 (v/v) was added to the precipitate at room temperature for 30 minutes to deprotect the pbf groups on the arginine. After one final diethyl ether precipitation, the final arginine-grafted bioreducible poly(disulfide amine) was dialyzed against ultrapure water and lyophilized to yield a sticky solid.

5.3.3 Vertebrate Animals

All animal experiments were performed according to protocols approved by the University of Utah's Institutional Animal Care and Use Committee. Sprague Dawley rats were purchased from Charles River Laboratories International, Inc. (Wilmington, MA, USA). The rats were housed under the care of a licensed veterinarian and monitored daily for signs of sickness or pain after surgery. The animals had free access to normal rat chow and water and were kept with a 12-hour light-dark schedule.

5.3.4 Rat Ischemia/Reperfusion Model

Male Sprague Dawley rats (approximately 300 g) were anesthetized under 4% isoflurane, given an intramuscular injection of ketamine, and had their left chests shaved. After allowing 10 minutes for the ketamine to take effect, the rats were again anesthetized with 4% isoflurane and intubated by hanging the rats from their incisors and inserting a 12 G IV catheter over a 0.035" guidewire past the vocal cords into the trachea. The rat was quickly moved to a water-warmed operating table and connected to a ventilator delivering 2% isoflurane at 60 cycles/minute with a 12 ml/kg stroke volume. An incision was made between the 4^{th} and 5^{th} rib and the ribs spread using a retractor to gain access to the chest cavity. The left lung was swept dorsally to visualize the heart and held out of the way using a wet 2" × 2" gauze pad. The pericardium was carefully removed and the left anterior descending artery (LAD) identified. A 6-0 prolene suture was passed under the LAD approximately 2 mm from the edge of the left atrial appendage and the needle cut from the suture. The two ends of the suture were then threaded through a 2 cm length of PE-50 tubing (Becton Dickinson, Franklin Lakes, NJ, USA) to form a snare. The two ends of the suture were pulled tight and the tubing was

clamped with a pair of needle drivers to occlude the LAD. After confirming successful occlusion of the LAD by blanching of the myocardium and visible dyskinesia of the LV wall the animals were assigned to one of 5 groups: 1) ischemia/reperfusion (I/R) only (n = 7), 2) nontargeting siLuc:ABP (n = 5), 3) naked siBNIP3 (n = 5), 4) siBNIP3/ABP (n = 7), and 5) thoracotomy sham surgery control (n = 5). After 30 minutes, the snare was loosened, the suture removed from the myocardium, and an injection of 25 µg siRNA complexed with 500 µg ABP (1:20 w/w) for the siRNA groups or 25 µg naked siRNA in 100 µl 1X PBS were injected intramyocardially in 4 sites (3 sites around the ischemic border zone, 1 site in the central infarct zone). The chest was then closed in layers using resorbable sutures and the rats were allowed to recover under a warming lamp and given injections of pain alleviating medication (buprenorphine) and antibiotics (cefazolin). The sham surgery control animals received a thoracotomy and had a suture passed under the LAD without tightening before closing the surgical site.

5.3.5 Magnetic Resonance Imaging

Three weeks after surgery, MRI was performed to determine changes in indices of heart function in all animals. Cardiac Cine-MRI was used to measure parameters of heart function and anatomy. MRI scans were performed on isoflurane-anesthetized rats placed prone on a pressure sensor to monitor respiration and a pulse oximeter attached to the rat's foot. A Bruker Biospec 7T/30 cm MRI operated with Bruker AVANCE II electronics (Bruker BioSpin MRI GmbH, Ettlingen, Germany) with a Bruker birdcage quadrature resonator (72 mm internal diameter) was used for signal transmission and reception. The images were acquired using retrospectively gated fast-low-shot-angle (FLASH) pulse sequences in CINE mode. The instrument settings were as follows:

repetition time (TR) = 72 ms, echo time (TE) = 3 ms, flip-angle = 10°, number of repetitions = 100, field of view (FOV) = 40 mm × 55 mm, matrix size = 196 × 96 zero-padded to 392 × 192 yielding an effective in-plane resolution of 102 × 286 microns. A total of 7 short-axis scans (slice thickness = 1.5 mm, number of movie frames = 10) were acquired. Images were reconstructed using Bruker's Intragate software and exported as DICOM files for analysis. The resulting Cine-MRI images were used to analyze left ventricle ejection fraction, end-diastolic and end-systolic wall thickness, and end-diastolic and end-systolic volume using the freely available software Segment v1.8 (Segment; http://segment.heiberg.se) [33]. Papillary muscles were included for all volume and ejection fraction measurements, but were excluded to perform analysis of the ventricle wall. An investigator blinded to the treatment groups analyzed the left ventricle in a semi-automated manner and another blinded investigator reviewed the results for accuracy and quality control.

5.3.6 Histology and Immunochemistry

The day following MRI acquisition, the rats were sacrificed by overdose of isoflurane. The hearts were rapidly excised and washed/perfused 3 times each with 20 ml heparin-PBS, 20 ml 2.56 M KCl, and 10% formalin. The hearts were then fixed in 10% formalin at room temperature for 48 hours, after which they were transferred to and stored in 70% EtOH until sectioning. Hearts were sectioned along the short axis from base to apex by slicing every 2 mm using an acrylic tissue matrix and embedded in paraffin (Zivic Instruments, Pittsburg, PA, USA). The paraffin-embedded short axis slices were then air dried for at least 30 minutes at room temperature and placed in a dry 55–60 °C oven for an additional 30 minutes. The slides were then de-paraffinized in 3

changes of xylene (5 minutes each), rehydrated in ethanol (100% ×2, 95% ×2, 70% ×1, 1 minute each), and finally placed in dH_2O. All histology and immunohistochemical staining steps were performed at 37 °C with an automated immunostainer (BenchMark® XT, Ventana Medical Systems, Tucson, AZ, USA).

Heart sections were stained using Masson's trichrome to quantitatively analyze the extent of infarct formation. Trichrome-stained heart slides were scanned for analysis using a standard desktop scanner at 600 dpi (CanoScan 8800F, Canon USA, Inc., Lake Success, NY, USA). The infarct size within the left ventricle was calculated by outlining the collagen-stained area, the total left ventricle epicardial area, and the total left ventricle endocardial area in ImageJ (NIH, Bethesda, MA, USA). Percent infarct was calculated using the following equation.

$$\text{Infarct size}(\%) = \frac{\text{collagen stained area}}{(\text{epicardial area} - \text{endocardial area})} \times 100$$

Additional heart sections were stained using a rabbit anti-rat BNIP3 antibody (Abcam, Cambridge, MA, USA). Sections were incubated at room temperature with the primary BNIP3 antibody at a 1:300 dilution for 20 minutes. The secondary antibody was applied at 1:100 for 20 minutes. The sections were detected using the indirect biotin streptavidin system iVIEW DAB that uses the chromogen DAB (3-3' diaminobenzidine) (Ventana Medical Systems, Tucson, AZ, USA). Slides were counterstained with hematoxylin and dehydrated by reversing the ethanol sequence above.

Apoptotic cells were detected by staining heart sections with ApopTag® Fluorescein Apoptosis Detection Kit (Millipore, Billerica, MA, USA). Briefly, slides were air- and oven-dried as above, then de-paraffinized and rehydrated. Sections were

digested in a 1:50 dilution of proteinase K (Dako, Carpinteria, CA, USA) for 25 minutes, rinsed in TBS, and covered in equilibration buffer for 10 seconds. Tdt enzyme/buffer was added to each section and slides were incubated in a 37 °C oven for 2 hours. After stopping the reaction, slides were again rinsed in TBS and an anti-digoxigenin-fluorescein conjugate was added for 1 hour at room temperature. After a final rinse in TBS and addition of immunofluorescent mounting media (Dako, Carpinteria, CA, USA), the cover slips were added to the slides.

Immunohistochemistry and H&E stains were digitized by scanning the entire slide at 20× magnification using an Aperio CS Scanscope (Aperio Technologies, Inc., Vista, CA, USA). Immunohistochemical slides stained for BNIP3 were analyzed by manually counting BNIP3-positive nuclei from five random high power fields in each heart using Aperio ImageScope V11.2.0.780 (Aperio Technologies, Inc., Vista, CA, USA).

TUNEL immunofluorescence slides were imaged at 40× magnification using an Olympus FV1000 confocal fluorescent microscope (Olympus, Center Valley, PA, USA) and quantified by counting positively stained cells from five random high power fields for each animal.

5.3.7 Statistical Analysis

All results are reported as the mean value ± standard error of the mean (SEM). Statistical analysis was performed in GraphPad Prism 4.03 (GraphPad Software, La Jolla, CA, USA) using one-way analysis of variance (ANOVA) followed by Tukey's *post hoc* test to identify significance between groups. $P < 0.05$ was considered statistically significant throughout.

5.4 Results

5.4.1 Infarct Size and Collagen Content

The left anterior descending coronary artery supplies blood to the anterior surface of the LV and the apex of the heart. Ligation of this coronary artery produces large, fibrotic LV infarcts that are readily detectable by collagen staining (Figure 5.1). Sectioned hearts from each treatment group were stained with the collagen-specific Masson's Trichrome stain. The infarct area was measured as a percentage of the total cross-sectional area of the left ventricle at 14 days postinfarction (Figure 5.2a). As seen in Figure 5.2b–d, the siBNIP3:ABP-treated hearts showed a smaller area of infarction within the myocardial region supplied by the LAD compared to ischemia/reperfusion (I/R) control hearts. Quantitative assessment of all the hearts revealed that the siBNIP3:ABP treatment limited infarct formation to 8.29 ± 0.97% of the left ventricle. An average infarct size for the I/R controls was measured at 17.91 ± 1.80% and the infarcts for the siLuc:ABP nontargeting siRNA group and the naked siBNIP3 group measured 17.87 ± 1.83% and 16.46 ± 2.33%, respectively. The siBNIP3:ABP infarct size was statistically lower than all other groups at $P < 0.01$ versus I/R control and siLuc:ABP, and $P < 0.05$ versus naked BNIP3.

5.4.2 Functional and Anatomical MRI Analysis

To evaluate the effects of siRNA-mediated knockdown *in vivo*, we used a more physiologically relevant model of I/R in rats by ligating the LAD temporarily for 30 minutes using a suture snare and then releasing the snare to commence the indefinite reperfusion period [34]. Before treatment, the animals were randomized to one of five study arms: I/R only (n = 7), thoracotomy only (n = 4), I/R followed by injection of

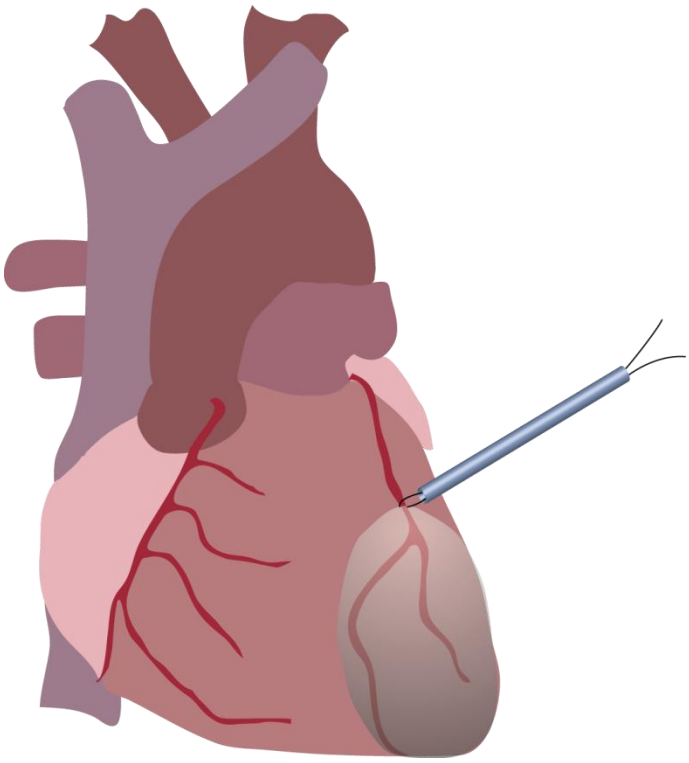

Figure 5.1. Temporary ligation of the rat heart at the left anterior descending coronary artery showing the infarct region of the left ventricle distal to the ligation site.

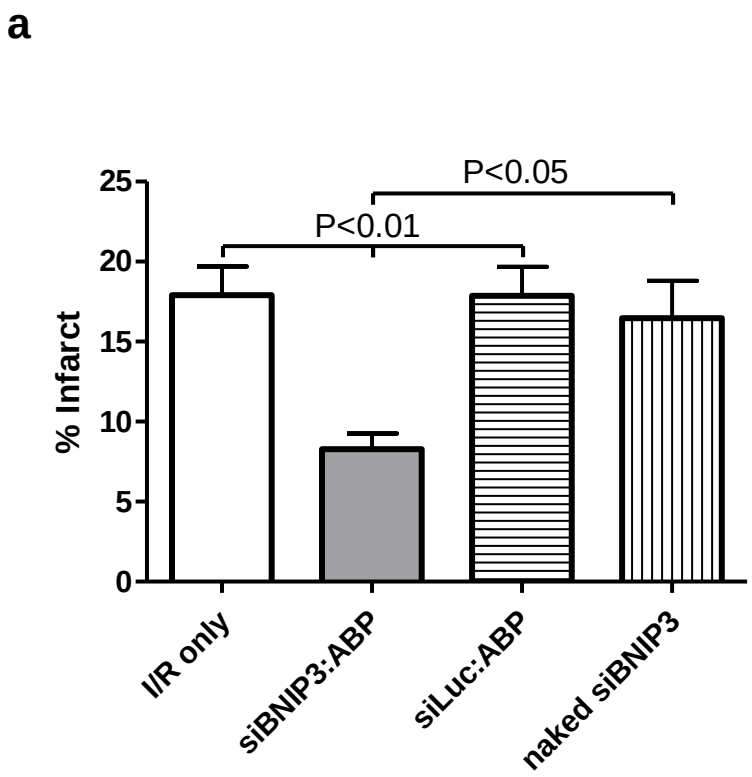

Figure 5.2. Masson's trichrome staining showing infarct formation between all treatment groups and I/R control. (a) Quantitative analysis of myocardial infarct size between all groups as a percent of the left ventricle. Representative Masson's trichrome staining showing infarct formation in (b) ischemia/reperfusion only animals, (c) thoracotomy only animals, and (d) siBNIP3:ABP-treated animals.

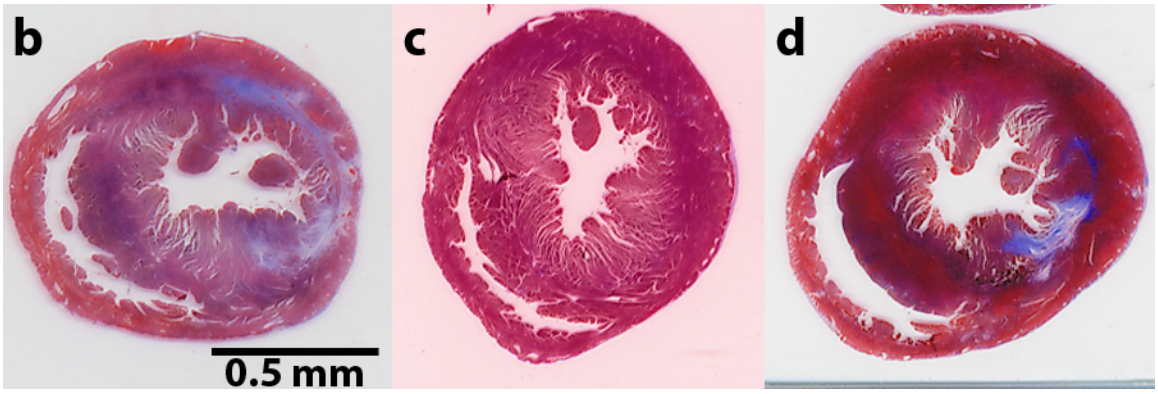

Figure 5.2 Continued.

siBNIP3 complexed with ABP (n = 7, 50 nM BNIP3 siRNA 1:20 w/w with ABP), I/R followed by injection of nontargeting siLuc complexed with ABP (n = 5, 50 nM Luc siRNA 1:20 w/w with ABP), and I/R followed by injection of 50 nM BNIP3 siRNA alone (n = 5). All treatment injections were delivered in 100 µl 1X PBS immediately after reperfusion.

To determine the treatment effects on heart function and anatomy, we used cineMRI to evaluate the *in vivo* rat hearts 14 days after surgery. The first notable result was that treatment of infarcted rat hearts with siBNIP3:ABP led to significant preservation of heart ejection fraction 14 days after surgery (74.4 ± 4.4%). This ejection fraction value was reduced but not significantly lower than thoracotomy control animals (77.4 ± 3.1%), but was significantly higher than I/R controls (58.4 ± 3.9%, $P < 0.05$). The ejection fractions of the siLuc:ABP (64.4 ± 1.4%) and naked siBNIP3 (62.3 ± 1.9%) groups were lower than both thoracotomy and siBNIP3:ABP groups, but were not significantly increased compared to the I/R control group (Figure 5.3).

In addition to the pumping efficiency indicator provided by the ejection fraction measurement, we also analyzed left ventricle volume at end diastole and end systole. The end diastolic volume (EDV) between all groups was not statistically different from either the I/R control group nor the thoracotomy control group, demonstrating that left ventricular remodeling had not yet progressed to the point where chamber dilation had occured. The mean EDV for siBNIP3:ABP-treated animals was 281 ± 15 µl while the EDV for I/R only and thoracotomy control animals was 309 ± 21 µl and 308 ± 17 µl, respectively (Figure 5.4a).

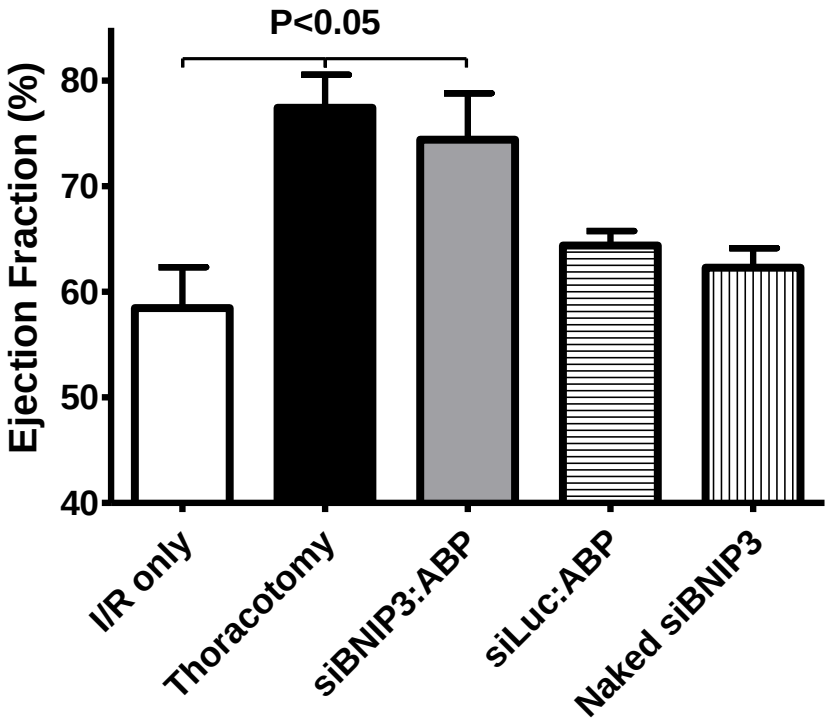

Figure 5.3. MRI analysis of rat hearts for functional analysis by ejection fraction. The ejection fraction was retained 14 days after surgery and treatment in the siBNIP:ABP group.

Evaluation of left ventricle volume at end systole revealed that the I/R only animals experienced a large and significant increase in end systolic volume (ESV) compared to both thoracotomy controls and siBNIP3:ABP-treated animals. The I/R only treatment group ESV was measured at 109 ± 9 µl while thoracotomy animals measured 71 ± 13 µl and siBNIP3:ABP animals measured 60 ± 6 µl ($P < 0.05$ I/R *vs.* thoracotomy, $P < 0.01$ *vs.* siBNIP3:ABP). The siLuc:ABP and naked siBNIP3 groups measured 94 ± 4 µl and 88 ± 7 µl, respectively, and were not statistically lower than the negative I/R only control group (Figure 5.4b).

5.4.3 Temporal Wall Thickening

Left ventricle wall thickness was evaluated throughout the entire cardiac cycle (15 individual time frames) at a midventricular level. The left ventricle was divided into 4 sectors with each sector comprising 90° of the ventricle and sector 1 beginning at a line that bisects the short-axis of the heart, equally dividing the left and right ventricles. Sector 2 comprises the anterior surface of the left ventricle, which is the portion of the left ventricle that is primarily supplied by the LAD. Notably, the I/R rats demonstrated little change between all sectors between end diastole and end systole, which is reflected in the poor ejection fraction seen in these animals. Additionally, the left ventricle wall displayed essentially no thickening throughout the cardiac cycle within sector 2. Thoracotomy controls displayed a significant difference between all sectors from end diastole to end systole with no difference between the LAD sector (sector 2) and the other sectors of the left ventricle. Finally, the siBNIP3:ABP group also showed a large change in wall thickness between all sectors from end diastole to end systole with no discernible difference between sector 2 and the other sectors of the ventricle (Figure 5.5).

a

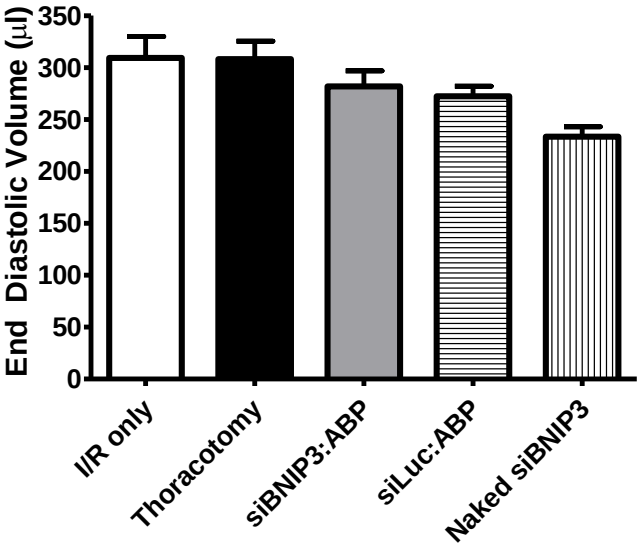

b

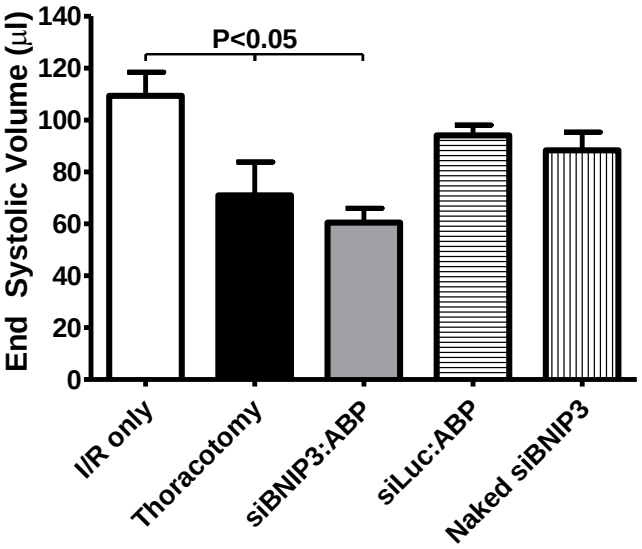

Figure 5.4. MRI analysis of rat hearts for global changes in end diastolic and end systolic left ventricle chamber volumes. (a) End diastolic volume for all treatment groups, (b) end systolic volume for each treatment group.

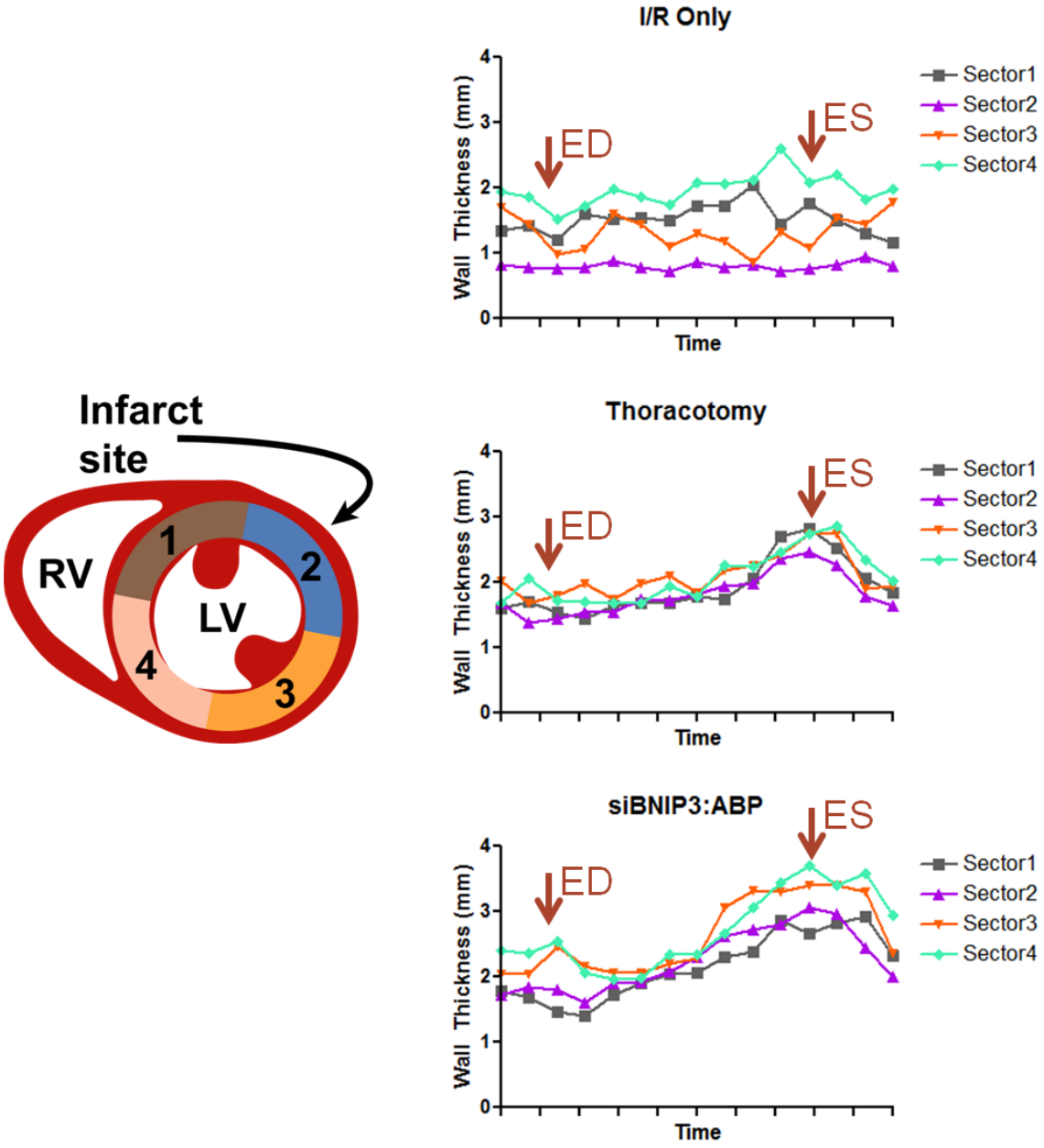

Figure 5.5. Temporal wall thickening for I/R only (top), thoracotomy (middle), and siBNIP3:ABP (bottom).

5.4.4 Cardiomyocyte Hypertrophy and Density

To evaluate the degree of remodeling, we analyzed cardiomyocyte cross-sectional surface area, and cardiomyocyte density. The cross-sectional area of cardiomyocytes in I/R only hearts was almost 3-times larger than the area of cardiomyocytes in thoracotomy control hearts ($796.7 \pm 58.3\ \mu m^2$ *vs.* $267.8 \pm 18.3\ \mu m^2$, respectively, $P < 0.001$). siBNIP3:ABP hearts showed a significantly decreased cross-sectional area at $413.3 \pm 32.6\ \mu m^2$ versus I/R hearts ($P < 0.001$). siLuc:ABP and naked siBNIP3 controls showed a similar degree of hypertrophy as I/R only controls ($691.5 \pm 60.6\ \mu m^2$ and $727.6 \pm 62.9\ \mu m^2$) (Figure 5.6a).

In agreement with the hypertrophy data, cardiomyocyte density was significantly decreased from thoracotomy controls in I/R only hearts ($1{,}100 \pm 58$ cells/mm^2 I/R *vs.* $1{,}920 \pm 103$ cells/mm^2 thoracotomy, $P < 0.001$). Density of cardiomyocytes in siBNIP3:ABP-treated hearts ($1{,}590 \pm 91.2$ cells/mm^2) was slightly decreased from thoracotomy controls ($P < 0.05$) but significantly elevated over I/R only hearts ($P < 0.001$). The density of cardiomyocytes in siLuc:ABP hearts at $1{,}210 \pm 43.3$ cells/mm^2 and in naked siBNIP3 hearts at $1{,}250 \pm 47.7$ cells/mm^2 was slightly decreased from siBNIP3:ABP hearts ($P < 0.05$) but were not significantly increased over I/R only controls (Figure 5.6b).

Figures 5.6c–d contain representative micrographs showing differences in cardiomyocyte density, and myocyte cross-section between I/R only, thoracotomy, and siBNIP3:ABP-treated rat hearts. The large increase in cardiomyocyte cross-section is readily apparent in the I/R only animals.

a

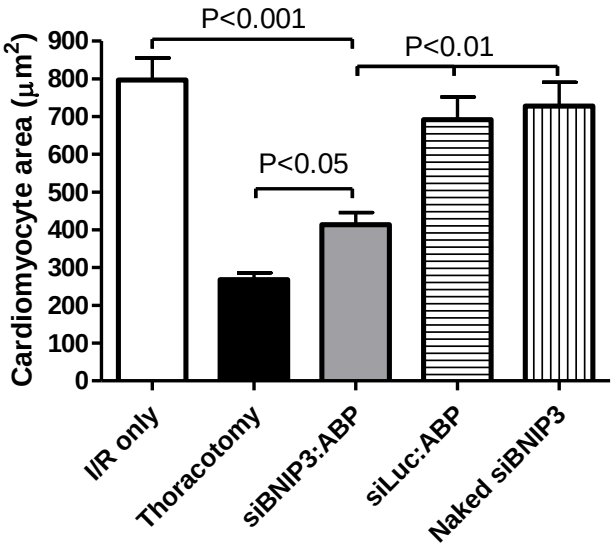

b

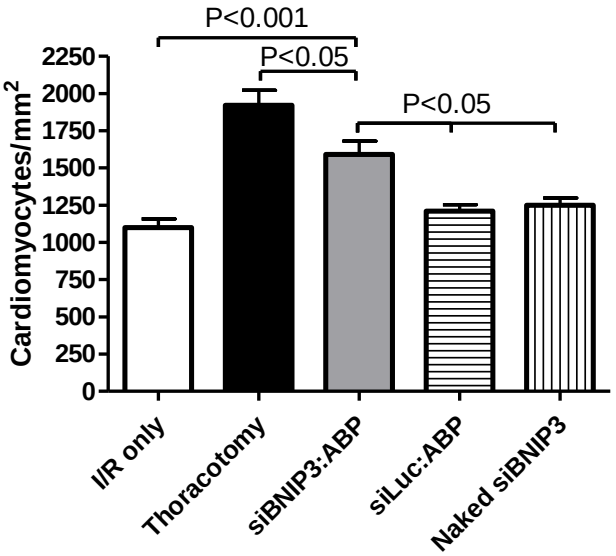

Figure 5.6. Cardiomyocyte hypertrophy and density from H&E staining. (a) Cardiomyocyte cross-sectional area in μm^2. (b) Cardiomyocyte density in cells/mm^2. Representative micrographs of (c) I/R only control animals, (d) thoracotomy controls, and (e) siBNIP3:ABP-treated rats.

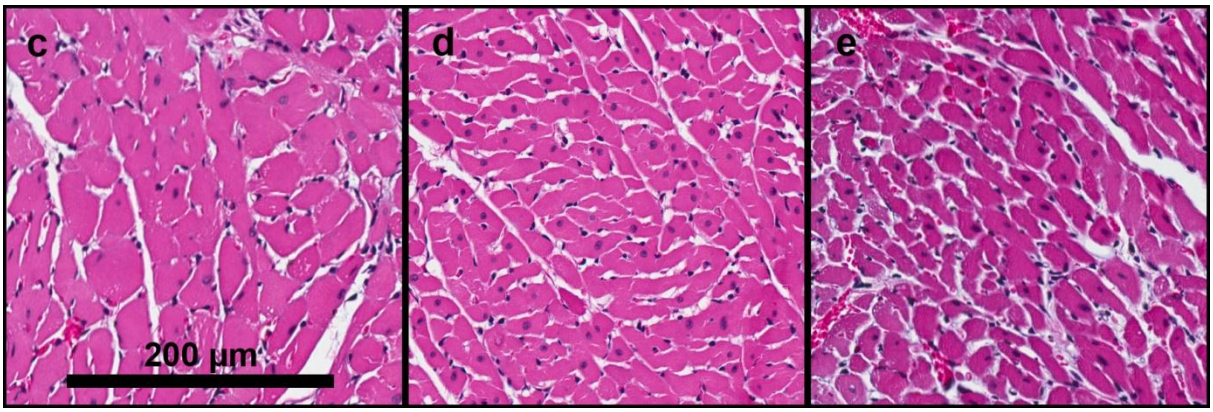

Figure 5.6 Continued.

5.4.5 BNIP3 Immunohistochemistry

Immunohistochemical analysis of the rat hearts revealed that there were a significant number of BNIP3-positive cells in the I/R only heart group, whereas there were very few positive cells in the thoracotomy control group or the siBNIP3:ABP treatment group (Figure 5.7).

5.4.6 TUNEL Immunofluorescence

Finally, to evaluate the degree of apoptosis/necrosis in the myocardium, an immunofluorescent TUNEL assay was performed on all samples. The left ventricles of all animals were analyzed for TUNEL-positive nuclei at 40× magnification in 5 random high power fields per animal. Analysis of thoracotomy surgery control animals revealed that the assay identified 69.4 ± 6.7 positive nuclei/mm^2 as a background level of apoptosis (Figure 5.8). I/R only rats had a significantly increased number of TUNEL-positive cells at 225.4 ± 14.7 cells/mm^2 ($P < 0.001$). Treatment siBNIP3:ABP hearts showed a significant decrease in apoptotic cells, but did not quite have as few positive cells as thoracotomy hearts (95.9 ± 8.1 cells/mm^2, $P < 0.001$ *vs.* I/R only, *NS vs.* thoracotomy). Naked BNIP3-treated hearts and siLuc:ABP hearts were increased to the same levels as I/R control animals and were significantly increased over both siBNIP3:ABP and thoracotomy hearts, but were not significantly different from I/R only control heart levels (264.2 ± 14.5 cells/mm^2 and 234.3 ± 22.6 cells/mm^2, respectively, $P < 0.001$ *vs.* both siBNIP3:ABP and thoracotomy, *NS vs.* I/R only).

5.5 Discussion

Considering the high incidence of acute myocardial infarction and the lack of approved therapies that effectively prevent or limit ventricular remodeling after acute MI,

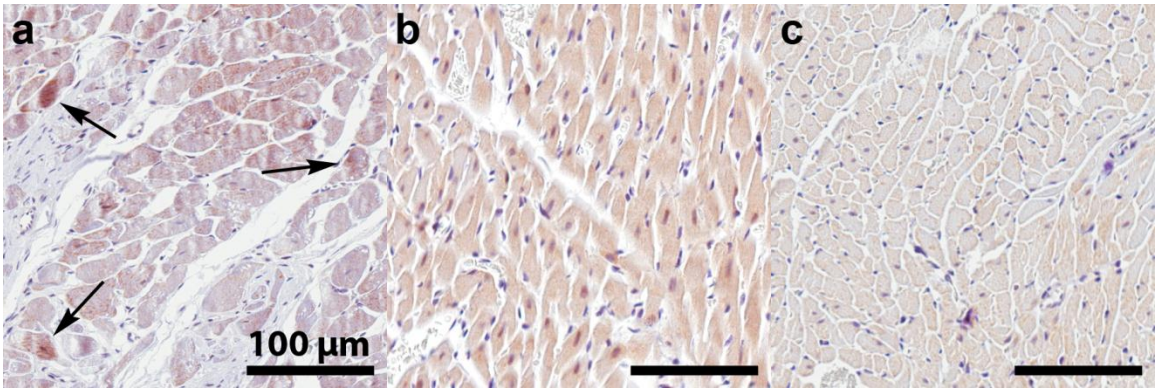

Figure 5.7. BNIP3 immunohistochemical staining showing increased BNIP3 expression in I/R only hearts (a), but with no detectable BNIP3 expression in thoracotomy (b), and siBNIP3:ABP hearts (c).

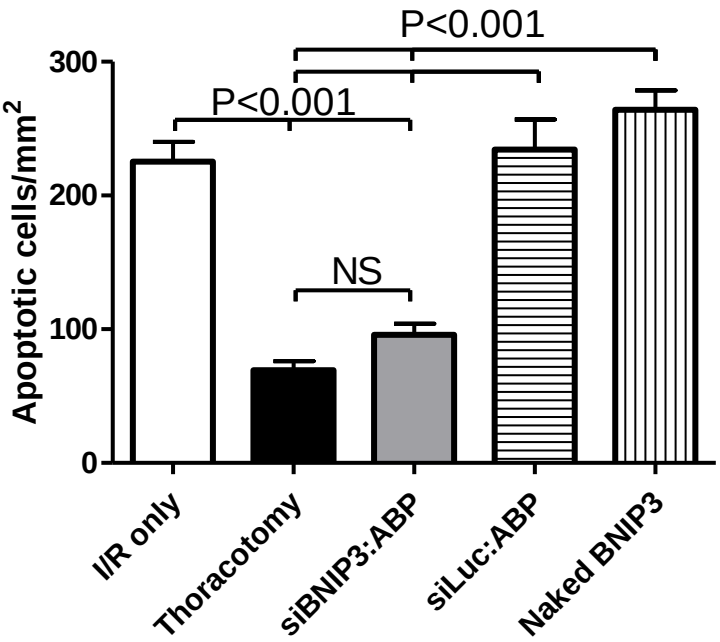

Figure 5.8. TUNEL analysis for apoptotic activity in the infarct border zone 14 days after surgery.

the exploration of new treatment strategies such as gene therapy is of extreme importance. Our work investigated the effects of bioreducible polymer-delivered BNIP3 siRNA to test the hypothesis that limiting BNIP3-mediated apoptosis in the early phase immediately after MI can result in decreased ventricular remodeling with preservation of heart function.

In previous studies performed by our group, we have shown that polymer-mediated VEGF gene therapy can be used to promote angiogenesis, reducing left ventricular remodeling and improving heart function [12, 35-37]. Angiogenic approaches, while popular, are limited in their ability to repopulate the myocardium and are better suited to retaining populations of cells that survived the initial I/R injury but are located in at-risk infarct border zones. Cell therapies have been extensively studied in both research and clinical settings and are designed to implant populations of cells that can hopefully either differentiate to cardiomyocytes or exert a positive influence on the remaining myocardial cells via paracrine effects [38-40]. This technique has seen success in some human trials, but the approach is still limited by questions as to whether the implanted cells are truly repopulating the myocardium with electromechanically competent and synchronously contracting myocytes [41-43]. An approach that focuses on retaining endogenous cardiomyocytes is attractive as it could circumvent many of the problems experienced with cell therapies by preserving the functional endogenous population of cardiomyocytes and support cells.

Our lab has investigated and demonstrated the feasibility of using polymer-mediated siRNA gene inhibition to limit apoptosis in cardiomyocytes *in vitro*; however, this work had not been expanded to *in vivo* animal models [44-46]. In this work, we

wanted to investigate not only the utility of transient siRNA-mediated inhibition of a proapoptotic gene to prevent cardiomyocyte death, but to demonstrate proof-of-principle that BNIP3 is an apropriate target for gene therapy of the myocardium post-MI.

Studies have shown that ventricular remodeling is progressive in nature with the extent of injury early after acute ischemic insult correlating to the size of the infarct and the degree of remodeling [47, 48]. The early stage is characterized by rapid metabolic changes, causing oxidative stress on cardiomyocytes and resulting in increased levels of apoptosis, necrosis, and autophagy in the myocardium [49, 50]. Annexin V staining in human patients suffering acute MI has indicated that the level of apoptosis decreases after the first week in the myocardial area-at-risk while TUNEL assays on autopsied hearts showed peak apoptosis within 3 days [50, 51]. This early loss of endogenous cells is thought to play an important role in determining the degree of LV remodeling and loss of heart function and suggests that there is a window of opportunity to gain long-term benefits by protecting cells from apoptosis in the early stage following acute MI. The short duration of siRNA therapy limits its utility for treating diseases in organs such as the heart that are difficult to access locally. However, with evidence suggesting that the myocardium is at increased risk for death over a shorter 1-week window, this creates an opportunity to see long-term benefit from siRNA therapy over a short duration.

The animal results we observed are particularly promising, showing that the knockdown of BNIP3 locally in the infarcted rat heart can produce positive global and regional functionality and demonstrate morphological improvement in LV remodeling progression. Globally, the treatment groups demonstrated preserved heart function as measured by ejection fraction. Ejection fraction is an important measure of heart function

both in animal models and in human patients, providing important prognostic information regarding the long-term expectations for the patient [47]. While we did not identify any statistical difference in end diastolic volume between any of the treatment groups, this is possibly due to the short 2-week study length, and the use of a less severe 30-minute occlusion/reperfusion protocol to induce infarction in the animals. Over this time period, remodeling in the LV may not have progressed to the point where wall thinning and cardiomyocyte slipping led to increased diastolic chamber volumes. However, we did see a significant impact on end systolic function within the hearts of I/R only control animals, siLuc:ABP nontargeting control, and naked BNIP3 delivery control animals. This is especially important since systolic function is an important determinant for long-term survival [47].

The regional results from the temporal wall-thickening measurements shed some insight into the reasons for loss of efficient systolic emptying of the LV. The I/R only animals showed significant loss of cardiomyocyte function in the LV region supplied by the experimentally ligated LAD. Over the course of a heart cycle, I/R only (and siLuc:ABP, and naked BNIP3) animals showed very little thickening of the myocardial wall in the infarct zone. This demonstrates that whether due to loss of cardiomyocytes, increased fibrosis, or cardiomyocyte dysfunction, the region of the heart where the infarct occurs was dramatically less functional than the unaffected regions. Conversely, treatment with siBNIP3:ABP demonstrated that it has a positive effect on the infarct zone with no significant difference in end diastolic to end systolic wall thickening detected.

Morphological analysis of all animal groups revealed that LV cellular remodeling in the form of increased cardiomyocyte hypertrophy was occurring in I/R only and

control groups, but was prevented in the siBNIP3:ABP group. In Figure 5.6e of the siBNIP3:ABP group, we can see that the cross-sectional area of the cardiomyocytes is significantly less than that seen in Figure 5.6c of the I/R only animals, despite the evident fibrosis in each of the panels.

Finally, our results show that as a result of our reduction in BNIP3 mRNA levels in the acute early phase of MI, we were still able to detect significantly lower levels of apoptosis after 2 weeks. This demonstrates that, as shown in long-term knockout and deletion models reported in the literature, BNIP3 removal or reduction leads to decreased levels of apoptosis/necrosis in the myocardium. Even more interestingly, this demonstrates that after MI, the myocardium does pass through a stage of increased apoptosis and that prevention of apoptosis during this short period can translate to long-term decreases in cell death. Normally, siRNA administration results in peak target knockdown between 24–48 hours with a total duration of less than 1 week. The duration of this effect can depend on factors such as target mRNA expression levels and cellular turnover.

This study and others have identified BNIP3 as a particularly attractive target for prevention of myocardial apoptosis/necrosis post-MI for myriad reasons. First, the role of BNIP3 as a hypoxia-responsive mediator of cardiomyocyte cell death has been well-established in both *in vitro* and *in vivo* models [29, 52, 53]. Also, transgenic studies show that BNIP3 deletion improves heart function and decreases LV remodeling [29], while *in vitro* studies in cardiac myocytes demonstrated that cell death is blocked by BNIP3 antisense oligonucleotides [54]. Our work shows similar protection from left ventricular remodeling, decreased infarct formation, and cell death as has been noted in permanent

BNIP3 knockout studies, but is a more practical approach that could be used as therapy post-MI.

5.6 Conclusions

In conclusion, this work demonstrated that the inhibition of BNIP3 as an antiapoptotic target serves to protect mammalian cardiomyocytes from hypoxia- and reperfusion-related injuries *in vivo*. This demonstrates BNIP3 is a novel target for the treatment of myocardial infarction and the prevention of left ventricular remodeling after heart attack. While this study examined inhibition of BNIP3 using polymer-delivered siRNA and suggest that polymer-mediated siRNA therapy could be a feasible therapeutic approach, the principles can be broadly expanded with potential applications for small molecules targeting BNIP3. Additionally, we were able to show that the novel arginine-grafted bioreducible polymer ABP can produce efficient siRNA transfection locally to hearts *in vivo* with no observed side effects or toxicity.

5.7 Acknowledgements

Special thanks are extended to Hye Yeong Nam, PhD who assisted in the synthesis of the polymer ABP used throughout this chapter.

5.8 References

[1] V.L. Roger, A.S. Go, D.M. Lloyd-Jones, E.J. Benjamin, J.D. Berry, W.B. Borden, D.M. Bravata, S. Dai, E.S. Ford, C.S. Fox, H.J. Fullerton, C. Gillespie, S.M. Hailpern, J.A. Heit, V.J. Howard, B.M. Kissela, S.J. Kittner, D.T. Lackland, J.H. Lichtman, L.D. Lisabeth, D.M. Makuc, G.M. Marcus, A. Marelli, D.B. Matchar, C.S. Moy, D. Mozaffarian, M.E. Mussolino, G. Nichol, N.P. Paynter, E.Z. Soliman, P.D. Sorlie, N. Sotoodehnia, T.N. Turan, S.S. Virani, N.D. Wong, D. Woo, M.B. Turner, Heart disease and stroke statistics--2012 update: a report from the American Heart Association, Circulation, 125 (2012) e2-e220.

[2] W. Damerau, J. Ibel, T. Thurich, H. Assadnazari, G. Zimmer, Generation of free radicals in Langendorff and working hearts during normoxia, hypoxia, and reoxygenation, Basic Res. Cardiol., 88 (1993) 141-149.

[3] K. Matsumura, R.W. Jeremy, J. Schaper, L.C. Becker, Progression of myocardial necrosis during reperfusion of ischemic myocardium, Circulation, 97 (1998) 795-804.

[4] B.J. Zimmerman, D.N. Granger, Reperfusion injury, Surg. Clin. North Am., 72 (1992) 65-83.

[5] M. Samaja, R. Motterlini, F. Santoro, G. Dell' Antonio, A. Corno, Oxidative injury in reoxygenated and reperfused hearts, Free Radic. Biol. Med., 16 (1994) 255-262.

[6] R.G. McKay, M.A. Pfeffer, R.C. Pasternak, J.E. Markis, P.C. Come, S. Nakao, J.D. Alderman, J.J. Ferguson, R.D. Safian, W. Grossman, Left ventricular remodeling after myocardial infarction: a corollary to infarct expansion, Circulation, 74 (1986) 693-702.

[7] J.A. Erlebacher, J.L. Weiss, M.L. Weisfeldt, B.H. Bulkley, Early dilation of the infarcted segment in acute transmural myocardial infarction: role of infarct expansion in acute left ventricular enlargement, J. Am. Coll. Cardiol., 4 (1984) 201-208.

[8] D.G. Kramer, T.A. Trikalinos, D.M. Kent, G.V. Antonopoulos, M.A. Konstam, J.E. Udelson, Quantitative evaluation of drug or device effects on ventricular remodeling as predictors of therapeutic effects on mortality in patients with heart failure and reduced ejection fraction: a meta-analytic approach, J. Am. Coll. Cardiol., 56 (2010) 392-406.

[9] R. Hinkel, T. Trenkwalder, C. Kupatt, Gene therapy for ischemic heart disease, Expert Opin. Biol. Ther., 11 (2011) 723-737.

[10] M. Giacca, S. Zacchigna, VEGF gene therapy: therapeutic angiogenesis in the clinic and beyond, Gene Ther., 19 (2012) 622-629.

[11] B. Eibel, C.G. Rodrigues, Giusti, II, I.A. Nesralla, P.R. Prates, R.T. Sant'Anna, N.B. Nardi, R.A. Kalil, Gene therapy for ischemic heart disease: review of clinical trials, Rev. Bras. Cir. Cardiovasc., 26 (2011) 635-646.

[12] J.W. Yockman, D. Choi, M.G. Whitten, C.W. Chang, A. Kastenmeier, H. Erickson, A. Albanil, M. Lee, S.W. Kim, D.A. Bull, Polymeric gene delivery of ischemia-inducible VEGF significantly attenuates infarct size and apoptosis following myocardial infarct, Gene Ther., 16 (2009) 127-135.

[13] A. Abbate, G.G. Biondi-Zoccai, A. Baldi, Pathophysiologic role of myocardial apoptosis in post-infarction left ventricular remodeling, J. Cell. Physiol., 193 (2002) 145-153.

[14] A. Abbate, J. Narula, Role of apoptosis in adverse ventricular remodeling, Heart Fail. Clin., 8 (2012) 79-86.

[15] G.W. Dorn, 2nd, Apoptotic and non-apoptotic programmed cardiomyocyte death in ventricular remodelling, Cardiovasc. Res., 81 (2009) 465-473.

[16] Z. Chen, C.C. Chua, Y.S. Ho, R.C. Hamdy, B.H. Chua, Overexpression of Bcl-2 attenuates apoptosis and protects against myocardial I/R injury in transgenic mice, Am. J. Physiol. Heart Circ. Physiol., 280 (2001) H2313-2320.

[17] M. Sugano, M. Koyanagi, K. Tsuchida, T. Hata, N. Makino, In vivo gene transfer of soluble TNF-alpha receptor 1 alleviates myocardial infarction, FASEB J., 16 (2002) 1421-1422.

[18] M. Sugano, K. Tsuchida, T. Hata, N. Makino, RNA interference targeting SHP-1 attenuates myocardial infarction in rats, FASEB J., 19 (2005) 2054-2056.

[19] O.O. Lisovyy, V.E. Dosenko, V.S. Nagibin, L.V. Tumanovska, M.O. Korol, O.V. Surova, O.O. Moibenko, Cardioprotective effect of 5-lipoxygenase gene (ALOX5) silencing in ischemia-reperfusion, Acta Biochim. Pol., 56 (2009) 687-694.

[20] H. Song, Z. Zhang, L. Wang, Small interference RNA against PTP-1B reduces hypoxia/reoxygenation induced apoptosis of rat cardiomyocytes, Apoptosis, 13 (2008) 383-393.

[21] R. Natarajan, F.N. Salloum, B.J. Fisher, R.C. Kukreja, A.A. Fowler, 3rd, Hypoxia inducible factor-1 activation by prolyl 4-hydroxylase-2 gene silencing attenuates myocardial ischemia reperfusion injury, Circ. Res., 98 (2006) 133-140.

[22] R. Natarajan, F.N. Salloum, B.J. Fisher, E.D. Ownby, R.C. Kukreja, A.A. Fowler, 3rd, Activation of hypoxia-inducible factor-1 via prolyl-4 hydoxylase-2 gene silencing attenuates acute inflammatory responses in postischemic myocardium, Am. J. Physiol. Heart Circ. Physiol., 293 (2007) H1571-1580.

[23] S. Kothari, J. Cizeau, E. McMillan-Ward, S.J. Israels, M. Bailes, K. Ens, L.A. Kirshenbaum, S.B. Gibson, BNIP3 plays a role in hypoxic cell death in human epithelial cells that is inhibited by growth factors EGF and IGF, Oncogene, 22 (2003) 4734-4744.

[24] B.L. Ebert, J.D. Firth, P.J. Ratcliffe, Hypoxia and mitochondrial inhibitors regulate expression of glucose transporter-1 via distinct Cis-acting sequences, J. Biol. Chem., 270 (1995) 29083-29089.

[25] J.A. Forsythe, B.H. Jiang, N.V. Iyer, F. Agani, S.W. Leung, R.D. Koos, G.L. Semenza, Activation of vascular endothelial growth factor gene transcription by hypoxia-inducible factor 1, Mol. Cell. Biol., 16 (1996) 4604-4613.

[26] B.H. Jiang, E. Rue, G.L. Wang, R. Roe, G.L. Semenza, Dimerization, DNA binding, and transactivation properties of hypoxia-inducible factor 1, J. Biol. Chem., 271 (1996) 17771-17778.

[27] A.E. Greijer, E. van der Wall, The role of hypoxia inducible factor 1 (HIF-1) in hypoxia induced apoptosis, J. Clin. Pathol., 57 (2004) 1009-1014.

[28] G.W. Dorn, 2nd, L.A. Kirshenbaum, Cardiac reanimation: targeting cardiomyocyte death by BNIP3 and NIX/BNIP3L, Oncogene, 27 (2008) S158-S167.

[29] A. Diwan, M. Krenz, F.M. Syed, J. Wansapura, X. Ren, A.G. Koesters, H. Li, L.A. Kirshenbaum, H.S. Hahn, J. Robbins, W.K. Jones, G.W. Dorn, Inhibition of ischemic cardiomyocyte apoptosis through targeted ablation of Bnip3 restrains postinfarction remodeling in mice, J. Clin. Invest., 117 (2007) 2825-2833.

[30] T.I. Kim, M. Ou, M. Lee, S.W. Kim, Arginine-grafted bioreducible poly(disulfide amine) for gene delivery systems, Biomaterials, 30 (2009) 658-664.

[31] S.H. Kim, J.H. Jeong, T.I. Kim, S.W. Kim, D.A. Bull, VEGF siRNA delivery system using arginine-grafted bioreducible poly(disulfide amine), Mol. Pharm., 6 (2009) 718-726.

[32] M. Ou, X.L. Wang, R. Xu, C.W. Chang, D.A. Bull, S.W. Kim, Novel biodegradable poly(disulfide amine)s for gene delivery with high efficiency and low cytotoxicity, Bioconjug. Chem., 19 (2008) 626-633.

[33] E. Heiberg, L. Wigstrom, M. Carlsson, A. Bolger, M. Karlsson, Time resolved three-dimensional automated segmentation of the left ventricle, Comput. Cardiol., (2005) 599-602.

[34] R.E. Sievers, U. Schmiedl, C.L. Wolfe, M.E. Moseley, W.W. Parmley, R.C. Brasch, M.J. Lipton, A model of acute regional myocardial ischemia and reperfusion in the rat, Magn. Reson. Med., 10 (1989) 172-181.

[35] D.A. Bull, S.H. Bailey, J.J. Rentz, J.S. Zebrack, M. Lee, S.E. Litwin, S.W. Kim, Effect of Terplex/VEGF-165 gene therapy on left ventricular function and structure following myocardial infarction: VEGF gene therapy for myocardial infarction, J. Control. Release, 93 (2003) 175-181.

[36] A.N. McGinn, H.Y. Nam, M. Ou, N. Hu, C.M. Straub, J.W. Yockman, D.A. Bull, S.W. Kim, Bioreducible polymer-transfected skeletal myoblasts for VEGF delivery to acutely ischemic myocardium, Biomaterials, 32 (2011) 942-949.

[37] L.V. Christensen, C.W. Chang, J.W. Yockman, R. Conners, H. Jackson, Z. Zhong, J. Feijen, D.A. Bull, S.W. Kim, Reducible poly(amido ethylenediamine) for hypoxia-inducible VEGF delivery, J. Control. Release, 118 (2007) 254-261.

[38] K.C. Wollert, H. Drexler, Clinical applications of stem cells for the heart, Circ. Res., 96 (2005) 151-163.

[39] S.D. Collins, R. Baffour, R. Waksman, Cell therapy in myocardial infarction, Cardiovasc. Revasc. Med., 8 (2007) 43-51.

[40] M. Perez-Ilzarbe, O. Agbulut, B. Pelacho, C. Ciorba, E. San Jose-Eneriz, M. Desnos, A.A. Hagege, P. Aranda, E.J. Andreu, P. Menasche, F. Prosper, Characterization of the paracrine effects of human skeletal myoblasts transplanted in infarcted myocardium, Eur. J. Heart Fail., 10 (2008) 1065-1072.

[41] N. Dib, E.B. Diethrich, A. Campbell, N. Goodwin, B. Robinson, J. Gilbert, D.W. Hobohm, D.A. Taylor, Endoventricular transplantation of allogenic skeletal myoblasts in a porcine model of myocardial infarction, J. Endovasc. Ther., 9 (2002) 313-319.

[42] H. Reinecke, V. Poppa, C.E. Murry, Skeletal muscle stem cells do not transdifferentiate into cardiomyocytes after cardiac grafting, J. Mol. Cell. Cardiol., 34 (2002) 241-249.

[43] P. Menasche, Skeletal myoblasts as a therapeutic agent, Prog. Cardiovasc. Dis., 50 (2007) 7-17.

[44] S.H. Kim, J.H. Jeong, M. Ou, J.W. Yockman, S.W. Kim, D.A. Bull, Cardiomyocyte-targeted siRNA delivery by prostaglandin E(2)-Fas siRNA polyplexes formulated with reducible poly(amido amine) for preventing cardiomyocyte apoptosis, Biomaterials, 29 (2008) 4439-4446.

[45] H.Y. Nam, A. McGinn, P.H. Kim, S.W. Kim, D.A. Bull, Primary cardiomyocyte-targeted bioreducible polymer for efficient gene delivery to the myocardium, Biomaterials, 31 (2010) 8081-8087.

[46] H.Y. Nam, J. Kim, S. Kim, J.W. Yockman, S.W. Kim, D.A. Bull, Cell penetrating peptide conjugated bioreducible polymer for siRNA delivery, Biomaterials, 32 (2011) 5213-5222.

[47] H.D. White, R.M. Norris, M.A. Brown, P.W. Brandt, R.M. Whitlock, C.J. Wild, Left ventricular end-systolic volume as the major determinant of survival after recovery from myocardial infarction, Circulation, 76 (1987) 44-51.

[48] A.D. Struthers, Pathophysiology of heart failure following myocardial infarction, Heart, 91 Suppl 2 (2005) ii14-16; discussion ii31, ii43-18.

[49] J. Kajstura, W. Cheng, K. Reiss, W.A. Clark, E.H. Sonnenblick, S. Krajewski, J.C. Reed, G. Olivetti, P. Anversa, Apoptotic and necrotic myocyte cell deaths are independent contributing variables of infarct size in rats, Lab. Invest., 74 (1996) 86-107.

[50] J.P. Veinot, D.A. Gattinger, H. Fliss, Early apoptosis in human myocardial infarcts, Hum. Pathol., 28 (1997) 485-492.

[51] P.W. Thimister, L. Hofstra, I.H. Liem, H.H. Boersma, G. Kemerink, C.P. Reutelingsperger, G.A. Heidendal, In vivo detection of cell death in the area at risk in acute myocardial infarction, J. Nucl. Med., 44 (2003) 391-396.

[52] K.M. Regula, K. Ens, L.A. Kirshenbaum, Inducible expression of BNIP3 provokes mitochondrial defects and hypoxia-mediated cell death of ventricular myocytes, Circ. Res., 91 (2002) 226-231.

[53] R.K. Bruick, Expression of the gene encoding the proapoptotic Nip3 protein is induced by hypoxia, Proc. Natl. Acad. Sci. U. S. A., 97 (2000) 9082-9087.

[54] L.A. Kubasiak, O.M. Hernandez, N.H. Bishopric, K.A. Webster, Hypoxia and acidosis activate cardiac myocyte death through the Bcl-2 family protein BNIP3, Proc. Natl. Acad. Sci. U. S. A., 99 (2002) 12825-12830.

CHAPTER 6

CONCLUSIONS, LIMITATIONS, AND FUTURE DIRECTIONS

6.1 Conclusions

Overall, the work in this dissertation demonstrates that disulfide-linked bioreducible polymers can be used to promote therapeutic gene delivery to address the deleterious effects of myocardial infarction. The therapeutic potential of gene therapy as an alternative and superior approach to treating many diseases remains to be met largely due to technical issues surrounding implementation of prolonged gene transduction in target cells. The failure of gene therapy to meet its clinical potential to date is principally due to difficulties in designing efficient gene vectors with acceptable safety profiles. We have demonstrated that polymeric systems, particularly bioreducible ones, represent a viable approach to effecting gene transfer with minimal side effects and high efficacy.

In Chapter 3, we observed that VEGF-transfected skeletal myoblasts stably express $VEGF_{165}$ and promote angiogenesis when implanted into the rat heart after permanent acute myocardial infarction. The polymer poly(CBA-DAH) was able to transfect the skeletal myoblasts and produce high transgene expression without significant toxicity. The implanted cells induced neovascularization of the myocardium as determined by CD31 and SMA immunohistochemistry, with notable increased vessel and capillary formation compared to controls. Also, ejection fraction, a clinically important measurement of heart function, was greatly increased in the VEGF-transfected

treatment group, demonstrating that the angiogenic effect of the transfected cell implantation results in retention of healthy heart function. Also, LV remodeling progressed significantly less in the rats treated with VEGF-transfected myoblasts, showing that this treatment strategy can slow the progression of global and regional remodeling of the LV wall and chamber. Finally, infarct size and apoptosis levels were dramatically decreased in the VEGF/myoblast treatment group, showing that the angiogenic therapy can promote cell survival, resulting in more viable myocardium.

Chapter 4 demonstrated that the cardiomyocyte transfection efficiency of the poly(CBA-DAH) bioreducible polymer can be improved through conjugation of nitrogen-rich arginine groups to form poly(CBA-DAH-R), an arginine-conjugated bioreducible polymer (ABP). This polymer showed minimal toxicity to primary cardiomyocytes while producing high transgene expression, suggesting its potential utility for *in vivo* use. Additionally, this chapter set the initial validation work of the hypoxia-inducible death switch BNIP3, demonstrating that siRNA towards BNIP3 can produce significant knockdown at both mRNA and protein levels. Finally, using an *in vitro* hypoxia model, we observed that BNIP3 inhibition via ABP-delivered siRNA protected cardiomyocytes from cell death and increased cell viability under harsh hypoxic conditions.

The 5th chapter expanded on the *in vitro* work performed in the previous chapter, evaluating the therapeutic benefit of polymer-delivered BNIP3 siRNA. A rat ischemia/reperfusion model of MI was used and siBNIP3 polyplexes were delivered directly to the myocardial infarct and border zone to reduce acute cell death. This approach not only produced regional improvements in the infarct region as demonstrated

by the reduced infarct sizes, but this improvement translated to improved heart function compared to control animals. Overall improvement in markers of LV remodeling such as cardiomyocyte density and hypertrophy showed that siBNIP3 therapy limits remodeling of the myocardium on a cellular level. The retention of systolic chamber volumes also demonstrated that LV remodeling is also improved on a global ventricular level also. Finally, the TUNEL analysis showed that apoptotic and necrotic cell populations 2 weeks after MI were reduced over 2-fold compared to control groups and were almost reduced to preinjury levels.

In summary, the work in this dissertation demonstrates that gene therapy approaches using nontoxic bioreducible polymers to treat MI and prevent LV remodeling are possible and of potential clinical value. This work evaluated two very different mechanisms of myocardial protection and demonstrated that while both approaches have their limitations, they can also be very effective in preventing pathological remodeling.

6.2 Limitations

Since this dissertation relies heavily on *in vivo* animal models of MI to identify novel therapeutic strategies to treat the disease, it is important to consider some of the limitations in translating positive animal results to meaningful clinical therapies. Over the past years, it has been found that many therapies that have shown excellent results in animal disease models, especially those models of cardiovascular disease, have failed to translate these research successes to the clinic [1].

These limitations are due to a variety of factors and basic limitations that come from controlling variables in lab experiments that cannot be controlled in the real world.

Some of the major differences between animal and clinical studies on MI and possible means to increase translatability are examined below.

In animal models of MI, the animals come from a homogenous group of healthy, usually young population and are also normally free of comorbidities. In human patients presenting with acute MI, the population is very heterogeneous, middle-aged or older, and often present with additional comorbidities such as hypertension, dyslipidemia, and diabetes. Many of these diseases are known to exacerbate conditions such as MI. To address these issues, researchers should look at using older populations of animals with comorbidities.

In animal models, only drugs that are involved in the therapy or that are medically necessary to perform the procedure are given. In humans, patients who present with MI are normally taking more than one medication, which can influence the impact of the therapy being studied. This is a difficult condition to control in humans, but proper recording and tracking of drugs currently being taken by patients will allow the researcher to determine potential influencing roles of classes of medication over time.

The duration of the ischemic period in animals is usually short (30–60 minutes) and all animals receive the same duration of ischemia throughout the study. In humans, the duration of ischemia is much longer with time-to-reperfusion ranging from 3 to over 12 hours in some patients due to variability in transport time, physician, and facility availability. Also, within a study, the range of ischemic durations can be highly variable, making direct comparisons difficult. This can be addressed by introducing larger variation and ischemic times in animal studies while in human studies, the subjects

should be analyzed and compared within windows of treatment such as <4 hours or between 4–8 hours.

Most animal studies produce an acute mechanical occlusion on the same healthy coronary vessel and at the same site. In humans, the location of the occlusion, the vessel patency, and the health of the coronary artery are all highly variable, making direct comparisons more challenging. Spontaneous atherosclerotic animal models exist and may make better approximations of MI in humans.

Therapeutic intervention in animal models is often timed to occur at the time of reperfusion or ischemia. This is often due to limitations of laboratory research as it is much simpler and more convenient to make interventions at the time of the surgery. This is especially a limitation in strategies that employ direct intervention with the myocardium as it is difficult and cumbersome to perform separate interventional surgeries in lab animals. In humans, as mentioned above, there is high variability in the time to intervention. Care should be taken to consider the timing of the therapy in clinical trials.

Infarcts in animal models of myocardial infarction are often much larger than those seen in human patients. Depending on the model of MI used, infarcts of between 25 to over 50% are often seen in animals. Human infarct size is typically much smaller, with infarcts from 10–20% of the LV more common. Newer animal models such as the 30-minute ischemia/reperfusion model used in Chapter 4 of this dissertation produce more modest infarcts and may be a more reliable comparator for human studies.

Finally, most animal studies are performed over a short period of time with average times ranging from 2–6 weeks for studies evaluating LV remodeling. Also, the

most common endpoints used in laboratory studies are cardiac function and geometry, and infarct size. These endpoints are not as clinically significant as evaluating the long-term effects of an intervention of health measurements such as subsequent animal illness and death. Longitudinal animal studies may be more clinically relevant and directly translatable to the impact of an intervention in human application.

Overall, the shortcomings of animal studies and their lack of translatability to human therapy are understandable when the differences between the experimental strategies are more closely examined. However, it is impractical to expect that all animal studies be performed with the degree of variability and rigor necessary to more closely model human disease. The researcher should at least have an understanding of some of these constraints so that the limitations of his or her findings can be appreciated and so that advanced studies can be planned to eliminate some of the shortcomings of realistic laboratory animal models.

6.3 Future Directions

6.3.1 Dual Plasmid for Mature Angiogenesis

As mentioned earlier, VEGF is the most common angiogenic factor used for therapeutic angiogenesis [2]. However, it has also been well established that while VEGF is the most potent factor to promote rapid neoangiogenesis, the vessels it stimulates are immature, leaky, and do not last much longer after VEGF levels return to baseline [3, 4]. To increase the functionality of the new vasculature, a dual-gene therapy approach combining the rapid VEGF factor with a vascular maturing factor such as PDGF should rapidly induce new vasculature growth while promoting vessel maturation for long-term benefit even after VEGF levels have abated [5].

6.3.2 Combined Antiapoptosis and Angiogenesis Treatment Modality

The chapters in this dissertation investigate two therapeutic modalities for the treatment of acute MI and prevention of LV remodeling: therapeutic angiogenesis and myocardial antiapoptosis. As highlighted in Figure 1.1, these two treatment strategies show maximal benefit at distinct windows after the initial ischemic insult. Therapeutic angiogenesis typically occurs outside the early phase of acute MI and serves to assist in rebuilding a functional vascular system to supply the myocardium with oxygen and nutrients. Antiapoptotic strategies have the potential to produce maximal benefit when implemented immediately after the initial ischemic phase, as this is the period of highest cardiomyocyte death [6, 7]. By devising a strategy combining fast-acting antiapoptotic siRNA and long-term pDNA-mediated angiogenesis, the benefits of both strategies could combine synergistically to produce a therapeutic effect greater than either intervention alone. Our lab is currently pursuing this strategy and has performed initial *in vitro* studies using an anti-SHP-1 (Src homology domain 2 (SH2)-containing tyrosine phosphatase-1) siRNA sequence combined with a hypoxia-inducible VEGF-expressing plasmid. Both the SHP-1 siRNA and hypoxia-inducible VEGF strategies have been evaluated *in vitro* in our lab but have not yet been combined in an *in vivo* animal model [8-12].

6.3.3 Local Heart Targeting via Systemic Delivery

The delivery approaches in this dissertation relied on local injection directly into the myocardium. Local injection at the time of insult is the most widely used technique in research due largely to its simplicity, the effectiveness of local injection, and the difficulty involved in re-accessing the site to deliver the therapy at a later time or date. However, this approach does not accurately replicate the therapeutic strategy likely to be

employed in a clinical setting. In human patients, local injection is possible but is limited to: 1) injection through the chest wall, which is difficult to perform accurately; 2) injection via catheter based systems, which again can be difficult and presents risks of complication during the procedure; and 3) injection at the time of thoracic surgery, which is the most accurate technique but only a small number of patients may actually have indications for cardiothoracic surgery. Development of systems that allow targeted delivery of genes to the ischemic myocardium are a preferable approach as these systems would allow for multiple dosing schedules through simple intravenous injection.

Our lab has been working on approaches to develop targeted bioreducible cationic polymers to target polyplexes to the ischemic myocardium. We have conjugated a short nine-residue targeting polypeptide, identified by *in vivo* phage display and capable of homing to ischemic myocardium [13], to a bioreducible polymer and demonstrated that it can selectively target the polyplex to the ischemic portion of the heart immediately after MI. Additional work with this targeted polymer gene delivery system is still needed to evaluate the ability to produce therapeutic gene expression or RNAi in animal models of MI.

6.4 References

[1] D.M. Yellon, D.J. Hausenloy, Myocardial reperfusion injury, N. Engl. J. Med., 357 (2007) 1121-1135.

[2] M. Hedman, J. Hartikainen, S. Yla-Herttuala, Progress and prospects: hurdles to cardiovascular gene therapy clinical trials, Gene Ther., 18 (2011) 743-749.

[3] P. Carmeliet, D. Collen, Role of vascular endothelial growth factor and vascular endothelial growth factor receptors in vascular development, Curr. Top. Microbiol. Immunol., 237 (1999) 133-158.

[4] Y. Dor, V. Djonov, R. Abramovitch, A. Itin, G.I. Fishman, P. Carmeliet, G. Goelman, E. Keshet, Conditional switching of VEGF provides new insights into adult neovascularization and pro-angiogenic therapy, EMBO J., 21 (2002) 1939-1947.

[5] C. Kupatt, R. Hinkel, A. Pfosser, C. El-Aouni, A. Wuchrer, A. Fritz, F. Globisch, M. Thormann, J. Horstkotte, C. Lebherz, E. Thein, A. Banfi, P. Boekstegers, Cotransfection of vascular endothelial growth factor-A and platelet-derived growth factor-B via recombinant adeno-associated virus resolves chronic ischemic malperfusion role of vessel maturation, J. Am. Coll. Cardiol., 56 (2010) 414-422.

[6] J.P. Veinot, D.A. Gattinger, H. Fliss, Early apoptosis in human myocardial infarcts, Hum. Pathol., 28 (1997) 485-492.

[7] P.W. Thimister, L. Hofstra, I.H. Liem, H.H. Boersma, G. Kemerink, C.P. Reutelingsperger, G.A. Heidendal, In vivo detection of cell death in the area at risk in acute myocardial infarction, J. Nucl. Med., 44 (2003) 391-396.

[8] H.Y. Nam, J. Kim, S. Kim, J.W. Yockman, S.W. Kim, D.A. Bull, Cell penetrating peptide conjugated bioreducible polymer for siRNA delivery, Biomaterials, 32 (2011) 5213-5222.

[9] L.V. Christensen, C.W. Chang, J.W. Yockman, R. Conners, H. Jackson, Z. Zhong, J. Feijen, D.A. Bull, S.W. Kim, Reducible poly(amido ethylenediamine) for hypoxia-inducible VEGF delivery, J. Control. Release, 118 (2007) 254-261.

[10] M. Lee, M. Bikram, S. Oh, D.A. Bull, S.W. Kim, Sp1-dependent regulation of the RTP801 promoter and its application to hypoxia-inducible VEGF plasmid for ischemic disease, Pharm. Res., 21 (2004) 736-741.

[11] M. Lee, J.K. Ryu, S. Piao, M.J. Choi, H.A. Kim, L.W. Zhang, H.Y. Shin, H.I. Jung, I.H. Kim, S.W. Kim, J.K. Suh, Efficient gene expression system using the RTP801 promoter in the corpus cavernosum of high-cholesterol diet-induced erectile dysfunction rats for gene therapy, J. Sex. Med., 5 (2008) 1355-1364.

[12] J.W. Yockman, D. Choi, M.G. Whitten, C.W. Chang, A. Kastenmeier, H. Erickson, A. Albanil, M. Lee, S.W. Kim, D.A. Bull, Polymeric gene delivery of ischemia-inducible

VEGF significantly attenuates infarct size and apoptosis following myocardial infarct, Gene Ther., 16 (2009) 127-135.

[13] S. Kanki, D.E. Jaalouk, S. Lee, A.Y. Yu, J. Gannon, R.T. Lee, Identification of targeting peptides for ischemic myocardium by in vivo phage display, J. Mol. Cell. Cardiol., 50 (2011) 841-848.